Final Technical Report to the

Office of Naval Research

on Contract N00014-86-K-0735

"THE RELATIONSHIP BETWEEN ULTRAVIOLET PHOTON STIMULATED DESORPTION MECHANISMS AND FUNDAMENTAL MATERIALS PROPERTIES"

Principal Investigators:

Richard F. Haglund, Jr. and Norman H. Tolk

Department of Physics and Astronomy and
Center for Atomic and Molecular Physics at Surfaces
Vanderbilt University, Nashville, TN 37235

I. Summary of Scientific Research Goals for the Proposal

The statement of work ~~for ONR contract~~ N00014-86-K-073 involved free-electron-laser-related activities using synchrotron uv sources and frequency up-converted laser light: (1) to measure the *energy dependence* of photon-induced processes of desorption; to vary temperatures of the irradiated samples over a wide range to ascertain the effects of defect mobilities on desorption processes; to use pump-probe techniques to study the time dependence of the energy localization and desorption processes; and to perform kinematically-complete experiments in which all the neutral desorbed species and appropriate level spectroscopy occurs to allow unambiguous identification of the mechanisms. The motivation for the work arose from the need for a clearer understanding of fundamental processes of materials modification and damage in ultraviolet optical materials, particularly with reference to the hoped-for developments in short wavelength free-electron lasers (FELs).

The major objective of the proposal was the elucidation of mechanisms through which bombardment by energetic ultraviolet photon beams over a wide range of energies leads to surface modification, erosion and macroscopic damage. The program emphasis was to be on threshold effects, time structure, interaction mechanisms (both thermal and electronic), and the influence of differing bonding mechanisms on desorption induced in both layers and substrates. By choosing representative model systems to be analyzed using a uniform experimental protocol, we intended to characterize the interactions of photons (over a wide range of photon intensity and energy) with matter in a *generic* way, by categorizing interaction mechanisms and identifying them with particular classes of materials. Such a program would, in turn, have allowed computational modelling for these processes to be put on a more firm physical footing.

Technical Approach to the Proposed Work

The unique expertise of our group lies in the detection and characterization of *neutral* atoms and molecules desorbed from a surface during bombardment by UV photons as well as by electrons and heavy particles. The emphasis on neutral desorbing species, and on the comparison of multiple radiation sources and their effects, constitute the fundamental difference between this work and that of most other researchers in this field, who detect and analyze desorbing ions and usually employ only a single radiation source. Experiments on alkali halide surfaces have demonstrated that the yield of desorbed neutrals is several orders of magnitude larger than that of ions, and that there are important similarities between the electronic mechanisms observed in "sputtering" of these tightly-bound optical materials. Therefore, the study of desorbed neutrals with a variety of radiation sources is essential to a comprehensive understanding of the desorption process itself, as well as of the static and dynamic properties of the surface chemical bond.

The desorption studies we proposed to carry out are concerned with the most basic questions of energy absorption, localization and redirection or decay, and are therefore intimately linked to the specific atomic-scale electronic properties of materials. In considering the detailed dynamics of electronic photon-surface interactions, it is useful to describe electronically-induced desorption as a three-stage process: (1) the initial deposition of energy through creation of a hole, two holes, anexciton or a defect; (2) a fast electronic rearrangement which leaves a surface atom or group of atoms in a spatially and temporally localized repulsive or energetic state; and (3) additional particle-surface interactions (neutralization, Auger transitions, and so on) as the atom, molecule or cluster leaves the surface. In both ESD and PSD experiments on alkali halides, it has been shown that the dominant channels through which energy is absorbed and localized lead to desorption of *neutral* atoms and molecules; hence one must analyze the desorbing neutrals to obtain a picture of the energy balance and the dynamics typical of photon-materials interactions.

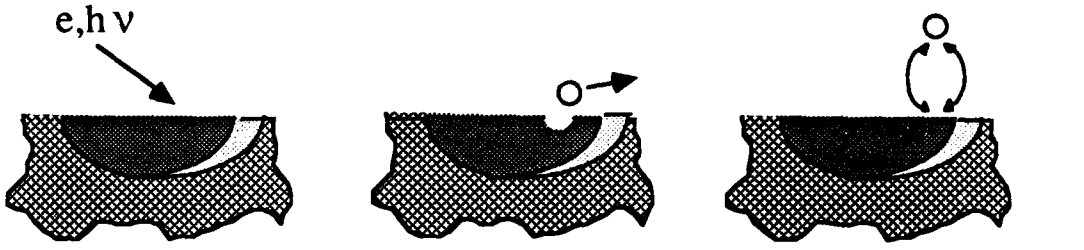

The detailed desorption mechanisms are linked to specific materials properties, because of the influence of material structure and bonding on both the initial absorption and the localization phases, and because of the influence of both surface structure and surface composition on the final-state particle-surface interactions. The differing behaviors of metals and insulators under photon irradiation, for example, clearly arise because in metals the nearly-free electron gas prevents spatial and temporal localization of the incident photon energy, while in insulators there exist a variety of different mechanisms for storing and then re-emitting this electronic energy to produce defects, structural reordering and desorption. Similar contrasts could be drawn between crystalline and amorphous materials, where the orderly localization of electronic charge density in the former and the random localization of electron density in the latter produce quite different radiation responses.

The key issues to be studied involved questions of threshold effects (both in the energy of incoming photons and in the intensity of the incident beam), of specific mechanisms or pathways for redistribution of energy, and of the links between *microscopic* atomic-scale events which occur in conjunction with the energy flow and the *macroscopic* phenomena of large-scale materials modification, surface erosion and damage. The unique experimental approach proposed here has already been enormously productive in increasing our understanding of electronic interactions of photons and electrons with one specific class of materials -- the alkali halides.

Scientific Background and Perspective

The study of Desorption Induced by Electronic Transitions (DIET) by means of electron- and photon-stimulated desorption (ESD/PSD) has emerged in recent years as one of the most fruitful directions in surface chemistry and physics. Interest in stimulated desorption was first aroused in the 1960's with the pioneering work of Menzel, Gomer and Redhead.[1] In the late 1970's, this interest was stimulated by the development of the Knotek-Feibelman desorption model.[2] A link between the angular distribution of desorbing ions and the geometrical properties of the surface chemical bonds predicted by this model was subsequently verified by the experimental and theoretical research of Madey, Yates and their co-workers.[3] This work has made it possible to study both the static and dynamic properties of surface chemical bonds and to contribute significantly to the understanding of technologically-important problems in catalysis, interface formation, corrosion, passivation and surface chemistry in general.

During the years following the work of Knotek and Feibelman, most ESD and PSD studies were dedicated to searching for desorbing ions. However, interest in the field has increasingly focussed on studies of desorbing *neutral* species, by using optical radiation to detect and analyze these species. In 1981, one of us (NHT) in collaboration with others, proposed and implemented a new and efficient method for the detection of *excited* desorbed neutral atoms, by detecting the optical radiation emitted by the desorbing particles as they fly away from the surface.[5,6,7] These

early experiments on alkali atoms desorbed by photon (or electron) irradiation of LiF and NaCl surfaces showed that excited-state desorbed neutrals are *much more abundant* than desorbing ions. The recent use of tunable dye lasers for laser-induced fluorescence detection of the ground-state neutrals desorbing from the alkali halides has shown that the dominant process in stimulated desorption is *ground-state neutral* particle production.[8]

This discovery necessarily changes the perspective required for an understanding of this problem, since no presently available theory correctly describes the desorption of neutrals. While the Knotek-Feibelman theory is correct for ions, it must now be viewed as a special case of a more general treatment of the problem whose outlines are not yet clearly in view. Moreover, the fact that stimulated desorption yields for neutrals are orders of magnitude larger than those for ions means that studies of the *dynamical* processes involved in radiation effects must deal with neutral desorption, since the bulk of the incident energy is clearly redirected to neutral desorption channels. Hence, stimulated desorption must now be re-considered seriously as a contributing factor in technological problems where it formerly was neglected, *e.g.*, in radiation-induced damage in optical materials. In addition, the large yields of neutral adsorbed species -- such as hydrogen -- are also highly significant in a wide variety of industrial and high-technology applications, ranging from semiconductor fabrication to magnetic fusion.

It is now generally accepted that the most abundant products of desorption induced by electronic transitions from the surface of ionic insulators are neutral atoms and molecules, regardless of whether the desorption process is stimulated by energetic electrons or photons. Only a very few results, however, had been published about neutral desorption previously.[9-11] These early experiments suggested the leading role of neutrals in the desorption process. Our initial PSD studies of Li desorbed from LiF demonstrated by direct measurements that the yield of excited neutrals was more than five orders of magnitude greater than the measured yield of desorbed ions.[6] Moreover, the yields of excited-state desorbed neutral hydrogen obtained by looking at the Balmer radiation indicate that this same neutral-desorption phenomenology is relevant to the technologically important case of hydrogen on surfaces.[5] Prior to the initiation of extensive studies at Bell Laboratories and more recently at Vanderbilt, ground-state atomic and molecular neutrals desorbed by electron impact had been studied in only a few cases.[8-11]

Our approach to the detection of desorbed neutrals is based on analysis of the optical radiation which they emit during post-desorption decay. The experimental equipment includes an ultrahigh vacuum chamber, the primary excitation source and an optical detection/analysis system with a monochromator and computer-controlled data processing. For experiments in which neutral excited-state desorption products are observed, only the characteristic atomic line radiation from the excited neutrals enters the focusing optics of the spectrometer. For measurements of ground-state neutral desorption processes, on the other hand, the tunable dye laser is used to identify and characterize particular atomic states of the desorbing atoms by means of laser-induced fluorescence. Through variations in photon collection geometries, it is possible to distinguish the atomic emission line spectra of the desorbed neutrals from the broad-band cathodoluminescence at the substrate. The dependence of desorption yield on the primary-beam intensity, the emission spectral characteristics and several other features (such as correlations with core-hole and valence-band excitation energies) can all be used to help discriminate against such processes as secondary electron excitation of desorbed ground-state neutrals.

These studies of thresholds specific mechanisms for electron- and photon-stimulated desorption are leading to an increasingly comprehensive picture of the dynamics which connect the early, atomic-scale modifications to materials with large-scale materials modification and damage which occur after prolonged or very high-intensity irradiation exposures. For example, it is possible with this new picture of desorption dynamics to understand why short-wavelength

illumination of materials at high intensities appears to produce a mixture of thermal and electronic modifications to the material, and why some materials are damaged much more readily than others.

For an ionically-bonded insulator, such as an alkali halide, in the early stages of irradiation, the substrate is protected by a film of some sort (as yet uncharacterized, but probably rich in hydrocarbons), which acts as a protective overlayer for the substrate. The mechanism by which this film retards desorption is still under active investigation, but it probably occurs because the film does not support the formation of self-trapped excitons, so any electronic excitation produced in the film either results in immediate bond-breaking, releasing the hydrogen and hydroxide observed in our spectra, or else simply a near-surface-bulk luminescence. (Increasing substrate desorption yields are accompanied in our experiments by a decrease in the background luminescence.) As the protective layer is eroded, substrate desorption begins and mobile defects are "gettered" to the interface between the substrate and the film. As more and more free metal begins to accumulate on the surface exposed to the radiation source, plasma generation begins and the agglomerating metal to begin to act as a thermally-absorbing inclusion, which may fracture the material surrounding it. However, even though this phase is the damage is thermal in nature, the facilitating mechanism is in fact electronic.

LIST OF REFERENCES

1. D. Menzel and R. Gomer, J. Chem. Phys. **41**, 3311 (1964). P. A. Redhead, Can. J. Phys. **42**, 886 (1964).
2. M. K. Knotek and P. J. Feibelman, Phys. Rev. Letters **40**, 964 (1978).
3. T. E. Madey and J. T. Yates, Jr., Surface Sci. **63**, 203 (1977).
4. R. Kelly, S. Dzioba, N. H. Tolk, and J. C. Tully, Surface Sci. **102**, 486 (1981).
5. N. H. Tolk et al., Phys. Rev. Letters **46**, 134 (1981).
6. N. H. Tolk et al., Phys. Rev. Lett. **49**, 812 (1982).
7. T. R. Pian et al., Surface Sci. **129**, 539 (1983).
8. N. H. Tolk et al., Nucl. Instr. and Meth. in Physics Research **B2**, 457 (1984).
9. See, for example: T. E. Madey and J. T. Yates, Jr., J. Vac. Sci. Technol. **8**, 525 (1971); D. Menzel, in DESORPTION INDUCED BY ELECTRONIC TRANSITIONS, eds., N. H. Tolk, M. M. Traum, J. C. Tully and T. E. Madey (Springer Verlag, Heidelberg, 1983); P. D. Townsend et al., Radiat. Eff. **30**, 55 (1976); H. Overeinder, M. Szymonski, A. Haring and A. E. deVries, Radiat. Eff. **36**, 63 (1978).
10. P. Feulner, W. Riedl and D. Menzel, Phys. Rev. Letters **50**, 986 (1983).
11. H. Overeinder, R. R. Tol and A. E. deVries, Surf. Sci. **90**, 265 (1979).
12. "Electronically Induced Desorption of Neutral Atoms Observed by Optical Techniques," N. H. Tolk, R. F. Haglund, Jr., M. H. Mendenhall, E.Taglauer, and N. G. Stoffel, Proc. of the Second Int. Workshop on Desorption Induced by Electronic Transitions(DIET-II), (Heidelberg: Springer Verlag, Surface Science Series Vol. 4, 1985), pp. 152-159.
13. N. Stoffel et al., Phys. Rev. B **32**, 6805 (1985).
14. R. F. Haglund, Jr. *et al.*, Nucl. Instrum. Meth. in Phys. Research B, March 1986.

II. Significant Results from the Research Program

The goals for the proposed research program centered around the correlation of threshold effects and specific photon-induced electronic desorption mechanisms with the electronic properties of specific classes of materials. As mentioned above, the experimental evidence supports the key role of *neutral* ground-state and excited-state desorption in DIET processes, particularly with regard to dynamics, energy distribution and localization in the desorption process. These DIET processes are capable ultimately of producing large-scale materials modification and damage in optical materials, and can be initiated by uv photons and electrons produced in the acceleration processes that leads to lasing in the FEL as well as by the FEL output photons. Moreover, they clearly play a key role in the interaction of FEL laser light with materials ranging from crystalline solids in UHV to "natural" materials produced through exposure to normal atmospheric conditions.

From the standpoint of experimental techniques, therefore, the research program we had proposed was logically centered around the following key ideas:

- the use of frequency-doubled dye laser and synchrotron uv sources to study the photon-energy and intensity dependence of DIET processes producing ground-state and excited-state neutral atoms and molecules, with a particular eye toward threshold effects and identification of the participating electronic states;

- the study of desorption yields as a function of the critical parameters such as temperature and pulse-probe time delay, which together with threshold photon energies will allow us to clarify the role played by electronically induced defects; and

- the performance of kinematically complete experiments in which *all* neutral desorbing species are detected and velocity distributions measured, in order to form a complete picture of the relative importance of competing energetic pathways in the excited material.

In accordance with the Itoh taxonomy of materials which display efficient operation of DIET processes, we proposed to carry out these measurements on: (1) a material which forms neither permanent defects nor self-trapped excitons, and so is nominally immune to efficient neutral desorption from purely electronic mechanisms; (2) a material which forms self-trapped excitons, but not permanent defects; and (3) a material which both supports self-trapped excitons and allows these to relax to form permanent electronic defects. The materials to be studied included representatives of each type, and the experimental protocol consists of the three generic types of experiments just mentioned.

The principal research accomplishments for the contract are listed below. Most of them have already been published either in journals or in conference proceedings. Details will be found in the attached copies of the publications and presentations.

Simultaneous Measurement of Several Desorption Channels on LiF

The detailed understanding of the way in which incoming photon energy is absorbed, localized, transformed and dissipated depends crucially on knowing all of the important exit channel particle flux distributions. In the case of PSD on alkali halides, the channels include (in decreasing order of production efficiency): ground-state neutral atoms, excited neutral atoms, secondary electrons and alkali and halogen ions. We have made the first measurements ever carried out in PSD studies on all these channels as a function of photon energy. The target used was LiF, and the photon energies covered the range around the 1s core-hole resonance in Li. One group of typical results is shown in the figure below.

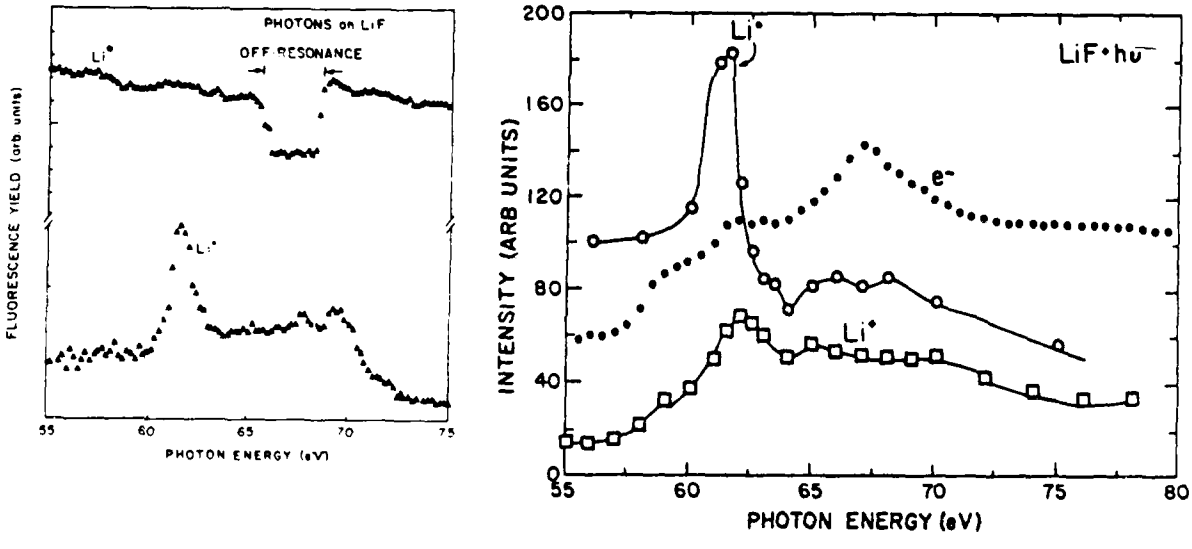

Figure 1. (Left) Yield of ground-state and excited-state Li atoms desorbed by ultraviolet photon irradiation as a function of photon energy. (Right) Yield spectra of excited lithium atoms, lithium ions and secondary electrons as a function of incident ultraviolet photon energy in the vicinity of the 1s core hole energy for LiF. A spectrum of ground-state neutrals desorbed by photons in this same energy range shows virtually no structure.

One of the key questions which has been raised by a number of authors in recent studies of the desorption of excited-state atoms by both photons and electrons is whether or not the desorption of excited-state atoms is purely a secondary process, in which the excited states are created by secondary electron bombardment of desorbed ground-state neutral atoms. These data appear to show plainly that the excited state desorption cannot be entirely due to secondary events, since the excited-state yields do not track secondary electron production. This question is to be examined in detail in a forthcoming publication.

Apart from the question of mechanisms for excited-state desorption, these studies also hint at interesting possibilities for using optical radiation to help quantify secondary electron emission from the surface of insulators -- a difficult measurement under some circumstances because of the photon- and electron-induced damage which occurs during the bombardment producing the secondary electrons. This possibility of using neutral species desorption spectroscopy for surface analysis is one of several interesting features of this work which remain to be explored.

Ultraviolet photon induced metallization of alkali halide surfaces

Rf-linac driven free-electron lasers, with their unique combination of high macropulse and micropulse peak power, high pulse repetition frequency, and trains of ultrashort pulses, deliver photons in uniquely insulting ways to the components of the associated optical systems. For the technology of free-electron lasers, the damage caused by these pulses in the FEL resonator optics is a practical problem of utmost concern, since it is the limiting factor in the optical output of the device and often imposes severe constraints on resonator optimization. Here the materials physics of the photon-matter interaction, particularly for ultraviolet wavelengths, poses questions of great scientific interest and enormous, direct technological relevance.

Studies at Vanderbilt on the ways in which the electronic energy of photons is absorbed, localized, transformed and ultimately dissipated are showing that there are many pathways leading to surface and bulk damage to typical optical materials, such as alkali halides, alkaline earth halides, metal oxides and fused silicas. This is particularly true if the photons are delivered, as is the case with the FEL, on time scales comparable to or shorter than the thermal relaxation times.

Much of the previous work on the interactions of photons with matter has focused on thermal models for the observed effects, because they were, in principle, easy to conceptualize and calculate. But rate constants for processes like optical damage have proven difficult or impossible to calculate because the initial rate-limiting steps are unknown. Indeed, in the picosecond laser regime, it is quite likely that the thermal model must be entirely abandoned because the preconditions for its validity -- namely, the establishment of a local thermodynamic equilibrium -- do not obtain. Electronic processes occur on the time scale of a single vibrational period and under many circumstances are incapable of exciting anything more collective than a single molecular vibration. These concerns underly the critical importance of using bright, tunable, ultrashort probes -- of which the FEL appears to be the most promising -- to study electronic and other non-thermal excitation processes in organic and inorganic materials.

During the past year, we have continued work on studies of photon-induced damage to model wide band-gap optical materials, focusing particularly on modifications to surface composition, surface electronic structure, and loss of surface and near-surface atoms due to atomic and molecular desorption. These studies have included both laser-induced desorption and ultraviolet-photon-stimulated desorption using the newly developed Vanderbilt-SRC partnership beam line at the Aladdin Synchrotron Radiation Center at the University of Wisconsin, Madison.

We have found that even minute changes in surface chemical composition -- whether due to the metallization of the surface stemming from the energetic photon-induced expulsion of the nonmetallic component of a dielectric, or due to the adsorption of small quantities of gases -- can inhibit or entirely close certain desorption channels. In addition, time-resolved studies have provided new insight into the role played by the energetic decay of the self-trapped exciton (STE) as the precursor to desorption events. The STE may be viewed as a phase transition of a photon-created electron-hole pair in which the relevant scale parameter is the effective mass of the hole; the temporary localization of the incident photon energy is made possible by this phase transition in an ordinary Frenkel exciton. The lattice deformation caused by the STE, in turn, provides the kinetic energy needed to expel an atom or atoms from the surface of the material, producing damage on an atomic scale to the host lattice.

These desorption-induced changes in the surface not only change the thermal properties of the surface, but also its electronic properties. These effects have been demonstrated to occur for photon energies below the bulk band-gap energy; hence, the surface metallization following desorption of ground-state non-metallic atoms is expected to be important in pulsed laser irradiation of surfaces, and may even, in the case of ultraviolet lasers, occur via single-photon transitions.

We illustrate this effect with data from a recent experiment on photon-stimulated desorption of LiF, showing the development of a layer of metallic Li on the surface of a pure LiF crystal undergoing ultraviolet photon irradiation in an ultrahigh vacuum environment. The radiation source was the first-order light from the Aladdin synchrotron light source of the University of Wisconsin.

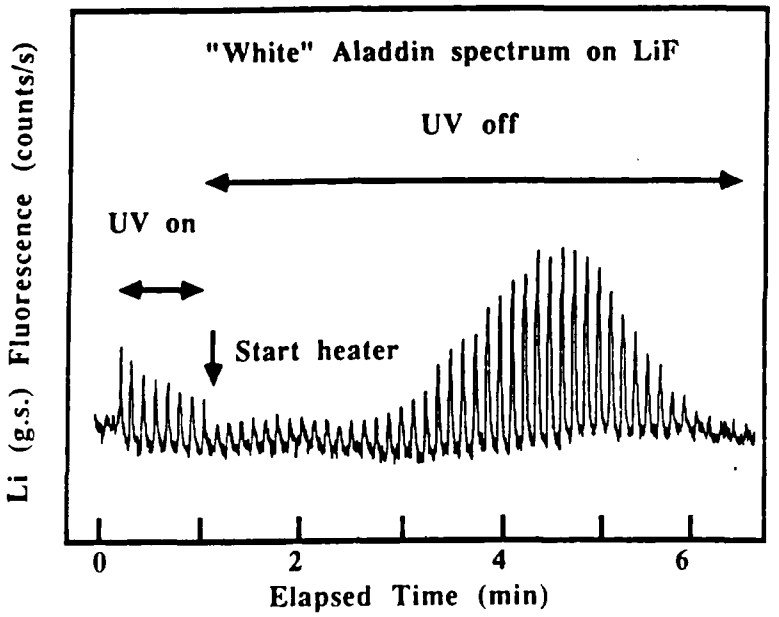

Figure 2. Fluorescence signal from Li^0 desorbed by the "white" ultraviolet photon spectrum from the Aladdin synchrotron light source. At the beginning of the measurement, the LiF crystal is illuminated for about a minute by the uv photons; then the uv irradiation is blocked by a beam stop, and the crystal is heated, while the laser-induced fluorescence signal from desorbing Li^0 is monitored.

The Figure shows the time evolution of the first resonance decay of the desorbed Li^0 excited by light from a tunable dye laser. Each peak in this spectrum represents a scan of the Coherent 599-21 tunable dye laser lasting approximately ten seconds over the first resonance line of the Li atoms at 6707 Å. At the time indicated by the arrow, the synchrotron light was blocked, and the LiF crystal was heated ballistically by turning on the heater block of the sample holder. As the sample temperature increases, the yield of Li^0 increases at first, as metallic Li is desorbed thermally from the surface. As this surface layer of neutral Li is depleted, the laser-induced fluorescence signal gradually dies away. The fact that it does not decay completely is consistent with the long time scales for F-center diffusion seen in previous experiments.

Effects of surface composition changes on excited-state atom desorption

The changes in surface composition inferred from the experiments described above lead to the interesting possibility of using excited-atom desorption as a diagnostic of changes in surface composition in an essentially non-destructive way. In the figure below, we show a composite of the yields of Li* as a function of temperature under white-light irradiation from the Aladdin storage ring at the University of Wisconsin's Synchrotron Radiation Center. These data indicate that there

is an increase of excited-state yield with temperature, probably corresponding to the secondary electron excitation of desorbed ground-state neutral atoms as the thermal desorption of these species increases with temperature.

It should be noted, however, that the Li* yield returns to its original value when a new spot is irradiated, even at temperatures for which the ground-state neutral yield can be shown, from separate measurements, to be negligibly small. Evidently, the Li* yield is extremely sensitive to surface conditions, and may therefore be used as a probe of those conditions as the mechanisms of desorption come to be more fully understood.

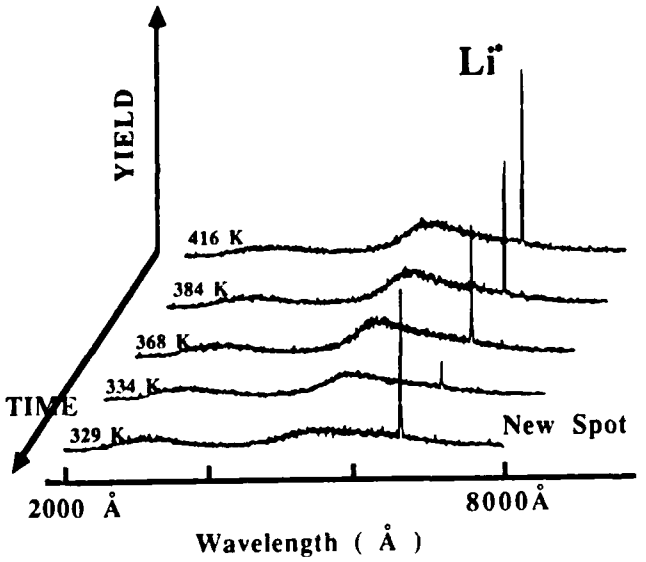

Figure 3. Composite of the desorption yield of Li from the surface of LiF irradiated by the white light spectrum of the Aladdin Synchrotron Light Source. Note the return to a high yield when a new spot is irradiated, even at a relatively low surface temperature.*

Laser-stimulated desorption experiments in pure materials

Up to the present time, ESD and PSD experiments have been conducted in regimes for which the intensities of the irradiating light were During the past year, the first experiments using excimer-pumped dye laser to do wavelength and intensity dependent measurements of these kinds of photon-induced damage studies were begun. The geometry was the same as the standard one used in all of our neutral species desorption experiments.

Pure crystals of KCl were irradiated both by the fundamental 308 nm light from an excimer laser and by the 600 nm output of an excimer-pumped tunable dye laser. Excited states of K were observed using an optical multichannel analyzer, and neutral Cl and K atoms were detected using a mass spectrometer. These preliminary results were encouraging, in that they appeared to show significant neutral species desorption yields even at intensities below the onset of significant laser damage. At present, we are awaiting the imminent arrival of an ultrahigh vacuum chamber which will be dedicated to this type of experiment.

Work will continue in the coming year on laser-stimulated desorption from optical materials of direct interest to the FEL materials problem under the sponsorship of the Vanderbilt Free-Electron Laser Project for Biomedical and Materials Research.

Application of PSD and other studies to laser materials damage issues

The experiments described above -- as well as other work with ion- and electron-stimulated desorption -- are showing that even low-energy electrons, photons and ions can induce significant changes in the surface composition and electronic structure of optical materials. These changes are particularly relevant to questions of damage to intracavity laser optics, whether in ordinary laser cavities or in such technologically demanding applications as ring laser gyroscopes. We have made an initial attempt to summarize the potential effects for intracavity damage in a paper prepared for a symposium on intracavity and extracavity laser optics. (See attached list of publications.)

The fundamental point of view which suggests itself from these experiments is that irradiation by electrons, ions, and the ultraviolet photons present in many laser cavities makes of what began life as a wide band-gap insulator a modified material which, at least in the near-surface bulk, looks much more like a semiconductor or metal. This implies that the laser photons will likely induce radiation damage characteristic of plasma formation (in the case of a metallized surface) or single-photon electron-hole pair formation (in the case of a semiconducting surface). These changes in surface composition, in turn, help to explain how thermal and plasma damage appears to be the final culmination of the process, since the progressive changes in the surface lead to stronger absorption and to direct acceleration of electrons and ions in the electric field of the laser.

We believe that this understanding of the damage process has significant implications for both fundamental and applied aspects of the laser damage question, and will pursue these issues in future research programs.

Theoretical work on surface electronic structure

The proposal noted the current primitive state of desorption theory, and contemplated support for theoretical efforts in this area. Collaborative efforts funded by this program have resulted in a new set of cluster calculations of surface states in the alkali halides using the extended Hückel formalism. The results -- displayed in one of the appended preprints -- appear to indicate the existence of well-defined surface states which could participate in single- or multiple-photon excitations. We intend to search for these states experimentally in future experiments using both the synchrotron light source and our tunable dye laser to clarify the role which these states might play in desorption, particularly of excited-state atoms.

Another study investigated the vibrational properties of chemisorbed hydrogen on the (100) surface of aluminum, using the effective medium theory to treat this highly reactive system.

Purchase and construction of laboratory apparatus

Under this contract, significant expenditures were made for laboratory apparatus appropriate to the research proposed under the contract. These included a portable ultrahigh vacuum chamber which could be used for prototyping experiments at Vanderbilt and for remote experiments at FEL sites; the purchase of a tunable dye laser and doubler that could be used with a large excimer laser supported by another research contract; and a number of items of experimental equipment for data acquisition, including an optical monochromator and a multichannel analyzer. These items were all acquired and used in various portions of the work described above.

III. Publications, Technical Reports and Presentations

Publications in Refereed Journals

R. F. Haglund, Jr., R. G. Albridge, M. H. Mendenhall and N. H. Tolk, "The Role of Electronic Mechanisms in Surface and Near-Surface Radiation Damage," Nuclear Instruments and Methods in Physics Research B, to be published.

R. F. Haglund, Jr., N. H. Tolk, G. M. Loubriel and R. A. Rosenberg, "Threshold Effects and Time Dependence in Electron- and Photon-Stimulated Desorption," Nuclear Instruments and Methods in Physics Research **B18** (1987) 549-554.

Y. Wang, P. Nordlander and N. H. Tolk, "Extended Hückel Theory for Ionic Molecules and Solids: An Application to Alkali Halides," submitted to Physical Review B.

Siqing Wei, Peter Nordlander and Yansen Wang, "Vibrational Properties of H Chemisorbed on Al(100)," manuscript in preparation, to be submitted to Surface Science Letters.

R. F. Haglund, Jr., A. V. Barnes, N. H. Halas, D. A. Ramaker and N. H. Tolk, "Competition between Surface and Near-Surface Defect Formation in the Photon-Stimulated Desorption of Neutral Lithium Atoms," manuscript in preparation; to be submitted to Physical Review B.

Conference Proceedings and Other Technical Reports

R. F. Haglund, Jr., "Laser Intracavity Damage Induced by Ions, Electrons and Ultraviolet Photons," invited paper from OE-LASE 1988, published in Proceedings of the Society of Photo-Optical Instrumentation Engineers, **895** (June 1988).

L. T. Hudson, A. V. Barnes, N. H. Halas, R. F. Haglund, M. H. Mendenhall, P. Nordlander, N. H. Tolk, Y. Wang and R. A. Rosenberg, "Photon-Stimulated Desorption of Excited Hydrogen from KCL," Proceedings of the Third International Workshop on Desorption Induced by Electronic Transitions (DIET III), Shelter Island, NY, May 1987. To be published by Springer Verlag.

N. H. Tolk, R. G. Albridge, A. V. Barnes, R. F. Haglund, Jr., L. T. Hudson, M. H. Mendenhall, D. P. Rujssell, J. Samthein, P. M. Savundararaj and P. W. Wang, "Optical Radiation from Electron, Photon and Heavy Particle Bombardment of Lithium Fluoride and Lithium dosed Surfaces," Proceedings of the Third International Workshop on Desorption Induced by Electronic Transitions (DIET III), Shelter Island, NY, May 1987. To be published by Springer Verlag.

Invited Presentations

R. F. Haglund, Jr., "The Role of Electronic Mechanisms in Surface and Near-Surface Radiation Damage," Fourth International Conference on Radiation Effects in Insulators (REI-IV), Lyons, France, July 6-10, 1987.

R. F. Haglund, Jr., A. V. Barnes, N. Halas, M. H. Mendenhall and N. H. Tolk, "Electronic Transitions in Photon-Stimulated Desorption," Optical Society of America Annual Meeting, Rochester, NY, October 22, 1987. (Presented by R. F. Haglund, Jr.)

R. F. Haglund, Jr., "Damage to Laser Intracavity Optics Induced by Ions, Electrons and Ultraviolet Photons," Symposium on "Laser Optics for Intracavity and Extracavity Applications," O-E LASE '88, Los Angeles, CA, January 1988.

Contributed Presentations

L. T. Hudson, "Photon-Stimulated Desorption of Excited Hydrogen from KCL," Third International Workshop on Desorption Induced by Electronic Transitions (DIET III), Shelter Island, NY, May 1987.

N. H. Tolk, "Optical Radiation from Electron, Photon and Heavy Particle Bombardment of Lithium Fluoride and Lithium dosed Surfaces," Third International Workshop on Desorption Induced by Electronic Transitions (DIET III), Shelter Island, NY, May 1987.

IV. Participants in the Research Program

The ONR Contract has supported the following personnel during the term of the contract:

Richard F. Haglund, Jr., Associate Professor of Physics, Co-Principal Investigator. One month during the summers of 1986 and 1987, ten per cent effort during the academic year 1987-88.

Norman H. Tolk, Professor of Physics, Co-Principal Investigator. One month during the summer of 1986, ten per cent effort during the academic year 1987-88.

Alan V. Barnes, Research Assistant Professor, three months support.

Dwight Paul Russell, Research Associate, nine months support

Wang Yansen, Research Associate (Visiting Professor from Fudan University, Shanghai, People's Republic of China), four months support.

Richard K. Cole, Research Technician, three months support for assistance related to synchrotron radiation studies.

Shirley Roth, Graduate Research Assistant, eighteen months support. Passed Ph.D. Qualifying Examination during term of the assistantship.

Phillip Savundararaj, Graduate Research Assistant, twelve months support. Passed Ph.D. Qualifying Examination during term of assistantship, also received Vanderbilt Dissertation Research Support Award, a special fellowship to provide travel support for thesis-related work.

Wei Siqing, summer Graduate Research Assistant, three months support.

Suresh Kari and David McClure, summer Undergraduate Research Assistants in 1986 and 1987, three months support each.

The contract also provided travel support for synchrotron radiation experiments by a number of other personnel, notably Marcus H. Mendenhall, Assistant Professor of Physics, and Larry T. Hudson, a NASA Graduate Research Fellow, who contributed significantly to the studies of ultraviolet photon- stimulated desorption.

Invited Paper

INTRACAVITY OPTICAL DAMAGE DUE TO ELECTRONS, IONS AND ULTRAVIOLET PHOTONS

Richard F. Haglund, Jr.

Department of Physics and Astronomy and
Center for Atomic and Molecular Physics at Surfaces
Vanderbilt University, Nashville, TN 37235

Abstract

Many of the damage problems experienced by intracavity laser optics, particularly for discharge-pumped and electron-beam-pumped laser systems, arise from the electronic interactions of low-energy electrons, ions and ultraviolet photons with the surface and near-surface regions of the optical material. We shall describe results of recent experiments which display some of the electronic mechanisms involved in these processes, through which incident electronic energy is absorbed, localized, transformed and ultimately dissipated in ways which change the surface composition and electronic structure of model wide bandgap optical materials. We consider discuss recent experimental results on the metallization of dielectric surfaces, the effects of adsorbed overlayers in inhibiting desorption of excited neutral atoms, and the effects of glass processing on response to electron and ion irradiation. We also point out some of the ways in which the changes in the optical surfaces wrought by the low-energy and low-intensity irradiation arising from the laser pumping mechanism can influence thermal, chemical and plasma properties of the surface in ways which alter the surface response to intense laser radiation.

1. Introduction

The low damage resistance of intracavity laser optics is the bane of laser designers and the primordial curse of the optical fabrication houses. Intracavity damage assumes a bewildering variety of forms: thermal stress cracking at the sites of optically absorbing impurities; formation of color centers and other optically active mobile electronic defects; chemical attack of both optical coatings and bare substrate surfaces; erosion, crazing and ablation of the optical surfaces; and high-field laser-induced electric discharges and electron avalanches. In many lasers, the intracavity damage threshold is even lower than that for the extracavity optics, forcing compromises in the laser design that may require costly large-area optics or exotic coatings, lead to suboptimal power system design, and increase the number of elements (and hence the cost and complexity) in master-oscillator power-amplifier trains. The money and effort devoted over the years to engineering development of more reliable and damage-resistant intracavity optics is itself the most eloquent testimonial to the seriousness of the problem.

From the atomic or molecular point of view, the most complex intracavity damage phenomenology is probably to be found in electron-beam-excited and discharge-pumped gas lasers, where laser photons, low-energy ions, excited metastable atoms, ultraviolet light, and electrons all contribute to the problem. The electrons, in particular, may either be primaries from an exciting or controlling electron beam, or secondary electrons created either by electron-atom collisions or in the laser discharge. Moreover, even where the intracavity laser photon intensities are too low to produce non-linear effects (such as self-focusing) or damage through plasma formation, the laser photons may act synergistically with other species to damage intracavity optical surfaces. Thus these laser systems offer a rich area for the study of intracavity optical damage, from which it is possible to draw lessons for laser types, such as those pumped by ultraviolet flashlamps, with less complex damage problems.

In this review, we shall largely ignore the effects of the laser photons, and concentrate primarily on the electronic mechanisms through which those radiation species arising in the excitation cycle of discharge-pumped gas lasers can change the surface composition and electronic structure of model dielectric materials. We shall begin by tring to define the link between the microscopic mechanisms of interest and the macroscopic damage phenomena. We then present the results of recent experiments in our laboratory which show some of the changes in surface composition, structure and radiation response induced by electronic transitions: metallization of the surface under low-energy UV photon bombardment; suppression of excited-state atomic desorption channels by the presence of adsorbed overlayers; and process-dependent response to ion and electron irradiation of fused silica. Finally, we comment briefly on the chemical, thermal and plasma effects facilitated by these changes, and on the additional complications in intracavity damage processes one might expect to be introduced by the laser photons.

2. Relationship between macroscopic damage and microscopic electronic mechanisms

In thinking about the pathways through which electron, ion and photon interactions ultimately lead to intracavity damage, it is useful to have a zeroth order guide to sorting out the most relevant dynamical properties. Here it is assumed that any change which modifies the properties of the optical surface or substrate sufficiently to be detrimental to laser performance is interesting. Among the phenomena of concern are: color-center formation at a density sufficient to increase the bulk absorption; chemical attack which changes the reflectance or absorptance of the optical element; sputtering, etching or erosion which removes material from the surface on a scale comparable to or larger than an optical wavelength; radiation-induced segregation of atomic species which changes the chemical composition of the surface; and migration of defects or impurities, which also may change the surface composition and make it more vulnerable to damaging chemical, plasma and thermal interactions.

Table 1 gives a summary of the various radiation species which can be found in discharge- or electron-beam-pumped lasers, along with their microphysical effects. For the sake of clarity, we point out that we use the word "sputtering" as it has historically been applied, to mean particle emission from surfaces caused by momentum-changing collisions, as in the classical collision cascade model.[1] On the other hand, "desorption" is used here to mean desorption induced by electronic transitions (DIET), where the particle emission is caused by the chain of electronic interactions described in the next section.[2] This usage has greater generality than such terms as "chemical sputtering"[3]

or "electronic sputtering,"[4] since both of these latter phenomena result from transfers of electronic energy, rather than momentum transfer.

Table 1: Sources of Intracavity Damage

Radiation	Energy	Damage Effects
UV photons (Discharge plasma)	5 - 500 eV	Color center formation Desorption Valence-band excitations
X-rays (E-beam *Bremsstrahlung*)	500 - 5000 eV	Color center formation Core-level excitations Secondary electrons
Electrons (Secondary or discharge)	10 - 10^4 eV	Secondary electrons Color center formation Desorption Valence-band excitations
Electrons (from E-beams)	10^4 - 10^5 eV	Sputtering Secondary electrons
Ions	10 - 500 eV	Sputtering Surface Segregation Desorption Secondary electrons
Excited atoms	0 - 50 eV	Sputtering "Hot-atom" reactions

A second set of correlations can be constructed in which the microscopic changes traceable to distinctive physical mechanisms are linked to macroscopically observable changes in optical properties -- such as changes in optical absorption, scatter, or surface figure. These correlations are summarized in Table 2.

Table 2: Macroscopic Optical Effects of Irradiation

Microscopic Radiation Effects	Affected Macroscopic Optical Properties
Color-center formation	Bulk transmittance
Surface segregation	Surface reflectance and scatter Surface chemical reactivity
Defect-induced desorption	Surface thermal properties Optical figure
Sputtering	Surface reflectance and scatter Surface chemical reactivity Optical figure
"Hot atom" interactions	Surface chemical reactivity Optical figure

The experimental evidence shows that electronically induced mobile defects play a special role in surface damage to virtually all optical materials irradiated by low-energy photons, electrons, ions and atoms. The alkali halides and fused silica adduced here as model materials are representative of a large class of optical dielectrics used both as substrates and as optical coatings in which irradiation leads to the formation of self-trapped excitons that relax to form permanent, mobile electronic defects. This class of optical materials includes many metallic oxides, metal fluorides (including the alkaline earth halides), and fused silica.[5] The general features of these results can also be expected to hold even for nominally metallic films and substrates, which under all realistic conditions are completely covered with an oxide overcoat which determines the surface properties. Indeed, it is quite possible that the surface overlayer -- of oxides and whatever other elements, such as hydrogen, that are readily bonded to the surface -- is what really determines the often observed differences between bulk and surface resistance to material modification and damage.

3. Electronic Interactions of Electrons, Ions, Atoms and Photons with Solid Surfaces

It has long been understood that thermal, chemical and plasma damage observed on the surfaces of intracavity laser optics have their origins in electronic interactions of photons, electrons and low-energy atoms, ions and molecules with the optical surfaces -- simply because quantum mechanics teaches us that the primary interaction in this case must be electronic; thermal, chemical and plasma effects are, in a sense, the "trickle down" effects of that primary interaction. However, the tools for isolating the atomic or molecular consequences of those electronic interactions in detail have not been available until quite recently. Recent studies have begun to fill in the details of an integrated picture of the damage process which suggests not only the origins of the damage, but also hints at ways to overcome it. This picture is providing an increasingly detailed and integrated model within which one can account for the effects of differing radiation species, of impurities and overlayers, and particularly of the unique role played by the surface.

When low-energy photons, electrons, ions or neutral atoms interact with atoms in the surface and near-surface layers of dielectric materials, a complex response is set in motion. From the microscopic point of view, it is convenient to characterize this response as consisting of several stages, illustrated schematically in Figure 1 for a surface with adsorbed molecules.

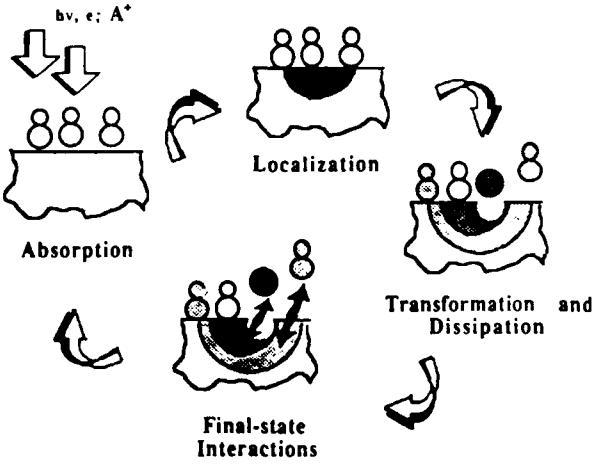

FIGURE 1. Stages in the interaction of photons, electrons and heavy particles with dielectric surfaces.

During the **excitation** stage, which occurs on a time scale of femtoseconds or less, energy from an electron, heavy particle (ion or atom), or photon is absorbed either through the transfer of momentum or *via* an electronic excitation mechanism, generally the creation of electron-hole pairs or the excitation of individual atoms or molecules. A key question is whether or not this excitation occurs in a statistical manner and is thus shared in an equilibrium fashion with a great many surface atoms or adsorbed species. Such a statistical rearrangement of energy is typical of physical (*i.e.*, momentum transferring) sputtering and of photon and electron irradiation of some metals, but not of DIET processes, particularly in dielectrics.

In the **localization** phase, the incident electronic energy is spatially concentrated for a time on the order of 10^{-12} to 10^{-13} s -- roughly the timescale of a vibrational period. In pure metals, of course, this kind of localization is not possible, because energy is dissipated from the initial absorption site by rapid electronic fluctuations on a time scale of order 10^{-16} s. In many dielectrics, the localization occurs because of electrostatic fields which stabilize an electron-hole pair, as in the case of self-trapped excitons.[6]

In the third, or **transformation and dissipation**, stage, the absorbed incident energy is changed from an electronic excitation into forms which we would generally label as "chemical," "kinetic" or "thermal." The transformation from electronic to *kinetic* energy, for example, can occur because the electron-hole pairs distort the crystal lattice, resulting in motion of an atom away from its neighbors to form an interstitial or cause desorption. The transformation that changes electronic to *thermal* energy is electron-phonon coupling, which occurs on a time scale approximately an order of magnitude slower than a vibrational period (10^{-11} to 10^{-12} s). The time scales for dissipation of the incident kinetic energy even in such simple materials as the alkali halides have been measured to be as long as tens of seconds![7]

During the **final-state interaction** phase, depicted in the Figure by a surface atom and an adsorbed molecule desorbing from the surface, particles moving near the surface may also undergo other particle-surface electronic interactions, such as charge exchange or de-excitation. These final-state electronic interactions occur on the femtosecond to picosecond time scale, and change the capacity of the desorbed species and the surface to interact *chemically* with other species in the gas phase near the surface.

One example of this kind of process was proposed independently by Pooley and by Hersh in studies of bulk alkali halides over two decades ago.[8] This mechanism has been shown to be responsible for the desorption of ground-state neutral alkali atoms from the surfaces of alkali halides under both electron and ultraviolet photon irradiation,[9] as well as for the neutral halogens, which were observed much earlier by mass-spectrometric techniques.[10] The Pooley-Hersh model involves a specific electronic excitation leading to preferential and energetic ejection of halogens along the <110> directions. The electronic energy from an incoming photon or electron is localized initially through the creation of a self-trapped exciton, which relaxes in a time on the order of picoseconds to form a V_k center. The V_k center, a self-trapped hole on a transient dihalide molecular ion at the normal site of a single halogen ion, relaxes in a few nanoseconds to form metastable pairs of H-centers (the so-called "crowdion" defects, consisting of singly-ionized dihalide ions on a halogen site) and F-centers (electrons occupying halogen vacancy sites). If formed sufficiently near the surface, the decay of the H center results in energetic desorption of a halogen along the halogen string directions, leaving behind an F center and a defect (halogen interstitial). The F center provides the electron needed for neutralization of the now under-coordinated alkali ion, which then desorbs thermally; the rate-limiting step in the alkali atom desorption is F-center diffusion.[11]

A similar concatenation of events has been shown to operate in other desorption phenomena. For example, in the pioneering work of Menzel and Gomer and of Redhead,[12] the localization of energy on a molecule adsorbed at a metal surface may be long-lasting enough to excite it to an antibonding orbital and lead to molecular desorption. Knotek and Feibelman demonstrated that a localization induced by pairing of holes in maximal valency covalent solids following interatomic Auger decay is responsible for the desorption of oxygen ions from such optical materials as TiO_2.[13] Itoh has recently proposed[14] that laser-induced desorption in semiconductor materials arises from localized holes screened from each other by a dense, laser-excited electron-hole plasma -- the so-called Anderson localization phenomenon.[15] A Pooley-Hersh mechanism has also been demonstrated by Schmid and his coworkers to be responsible for efficient multiphoton laser desorption of alkalis and halogens from KCl and NaCl at intensities well below the single-shot laser damage threshold.[16] In each case, absorption of electronic energy, followed by localization, transformation and dissipation of that electronic energy, precede the chemical, plasma, thermal and desorption effects that are the precursors of macroscopic optical damage.

Moreover, these same electronic processes are observed to occur in amorphous as well as in crystalline materials, because the propensity to absorb and localize electronic energy in a way which allows redistribution of that energy into desorption or localized chemical reaction channels arises not so much from long-range order as from the strongly localized electronic charge distributions characteristic of dielectric materials. Of course, the electronic charge distribution is spatially randomized in amorphous materials, because of the statistical variations in bond angles and bond lengths.[17] Hence, the spatial distribution of electronic defects and the directions in which they can diffuse in amorphous materials will not be the same as in crystalline dielectrics. However, the electronic mechanisms that produce the defects will operate in much the same way, perhaps with slightly lessened efficiency.

4. Experimental Arrangement for Optical Spectroscopy of Radiation-Surface Interactions

The key insight underlying the experimental studies presented below is that desorption from dielectric surfaces is overwhelmingly dominated by the emission of *neutral* ground-state and excited-state atoms and molecules.[9,18,19] Therefore, techniques for detection of neutral atoms and molecules borrowed from optical atomic and molecular spectroscopy are especially valuable additions to the charged- particle spectroscopies typical of many other surface analysis experiments. Details of the experimental method have been presented elsewhere,[20] so that only the essential features of our neutral desorption spectroscopy apparatus and techniques will be highlighted here.

The experimental layout of the experiments is shown schematically in Fig. 2. The sample is mounted on a heated or cooled micromanipulator in an ultrahigh vacuum (UHV) system, at a nominal base pressure of a few times 10^{-10} torr or less. At this pressure, the target surface remains free of adsorbed layers for a period of an hour or more. The surface can be recleaned by heating or sputtering as necessary. Surface analysis techniques routinely employed include ion-scattering spectroscopy (ISS) and detection of surface composition by analysis of neutrals from ionizing impact radiation (SCANIIR).[21]

Radiation incident on the target produces surface and bulk fluorescence, and desorbing atoms and molecules flying away from the surface toward the irradiation source, which in our experiments was either a low-energy, high-current electron gun, a low-energy, mass-selected and highly collimated ion beam from a Colutron electron-impact-ionization source, or the beam from the Aladdin synchrotron storage ring at the University of Wisconsin. De-excitation radiation from neutral atoms leaving the surface of the target material was detected by an optical system arranged to view a small volume (about $5x10^{-5}$ cm^3) out in front of the target. Radiation emitted from this volume along a line orthogonal to the irradiating source beam and parallel to the exposed face of the sample was imaged by a lens system onto the entrance slit of a spectrometer-photomultiplier combination. The optimum volume for observing desorbing species was selected by translating the target with respect to the spectrometer in order to minimize the bulk luminescence signal from the sample.

The photomultiplier output was acquired through standard CAMAC instrumentation modules or a multichannel analyzer (MCA) and stored for off-line analysis in a Macintosh SE computer system which controlled the data acquisition *via* an IEEE-488 CAMAC crate controller. The MCA was particularly useful in obtaining time resolved data on relaxation rates.

In this experimental geometry, desorbing ground-state neutral alkali atoms are illuminated from the rear of the sample by the TEM_{00} (fundamental Gaussian) mode from a single-frequency, actively-stabilized tunable dye laser. Alkali atoms leaving the surface, for example, undergo resonant absorption at the Doppler-shifted frequency appropriate to their rest frame and radiate at the characteristic resonance transitions as they fly away from the sample surface. This radiation is detected by the spectrometer-photomultiplier combination and the results are stored in a computer for off-line analysis. Excited-state neutral alkalis, on the other hand, are detected from their characteristic de-excitation fluorescences lines when the tunable laser is turned off. Desorbing halogen species are not observed in the present experimental set-up, because their resonance lines are in the ultraviolet. However, excited desorbing halogens should, in principle, be observable with a uv spectrometer; ground-state halogens could likewise be observed by using a laser detection technique -- such as resonant multiphoton ionization -- capable of inducing sufficiently energetic transitions out of the ground state.

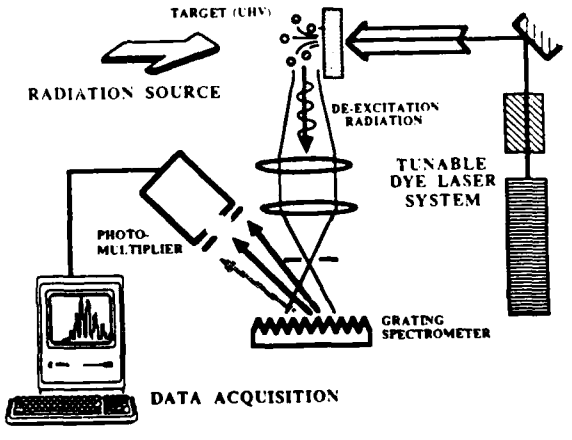

FIGURE 2. Schematic of a radiation-surface interaction experiment using optical spectroscopy to detect desorbing atoms and molecules.

In the geometry shown, this experimental layout permits the measurement of relative yields for different particle species, desorption velocity distributions, and changes in emission characteristics as a function of sample temperature, orientation and surface preparation. Accurate yield measurements for a particular desorbing species, on the other hand, can be made in a Doppler-free geometry, in which the laser is injected perpendicular both to the incident electron or photon beam and to the spectrometer line-of-sight. Desorbed ions and electrons can also be measured by inserting, close to the point of electron or photon impact, an electrostatic analyzer with an exit-plane Channeltron detector. Neutral atoms and molecules can also be detected in such experiments by the use of a sensitive quadrupole mass analyzer. In this way, it is possible to measure essentially all the desorption products relevant to the dynamics.

A sampler of the differences in electronic radiation-surface interaction mechanisms which can be easily detected in this way is shown in Figure 3. Here are displayed the optical spectra from low-energy photon, ion and electron bombardment of an LiF single crystal target.

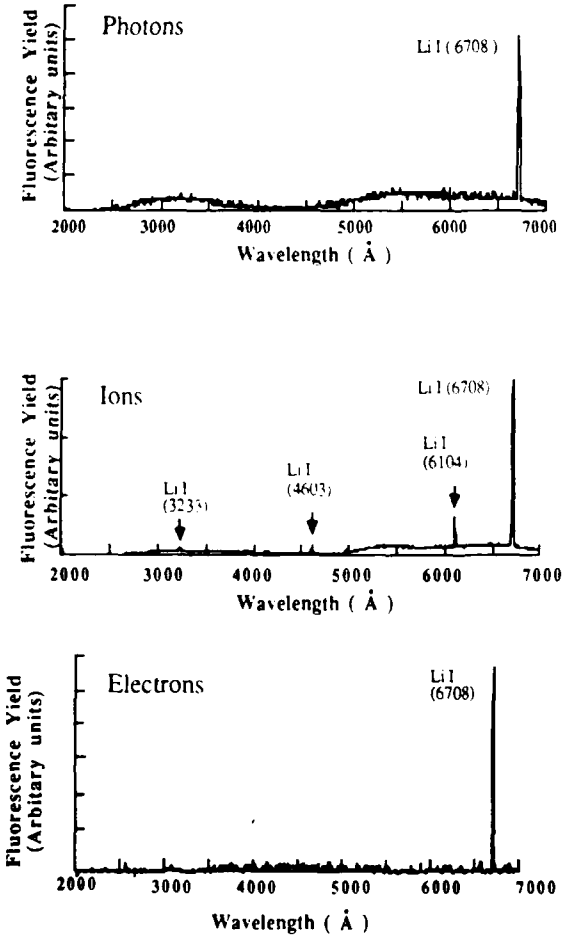

FIGURE 3. Comparison of photon, ion and electron-bombardment-induced optical spectra on LiF.

The variations in these three desorption spectra are characteristic of the differing ways in which energy is absorbed, localized, transformed and dissipated for the three different irradiating species. By comparing desorption effects for variations in the entrance-channel excitations, it is possible to make detailed inferences about the electronic mechanisms that are at work.

5. Metallization of Irradiated Dielectric Surfaces by Ultraviolet Photon Irradiation

Early experience with optics for Nd:YAG and Nd:glass lasers showed the pivotal role played by thermally absorbing platinum inclusions in damaging the laser material. The platinum particles, an artifact of the crucibles in which the laser rods and disks were being fabricated, were explosively heated by preferential absorption of the pulsed laser light at 1.06 μm, and the sudden heating led to thermal fracture of the surrounding host material.[22] While these impurity effects are certainly important in high-power laser cavities, it is interesting that the electronic interactions of photons, electrons and heavy particles can create a metal-rich layer on an optical surface *even in initially pure materials*.

Both electron- and photon-stimulated desorption (ESD/PSD) experiments show that electronically stimulated desorption of *ground-state* neutral alkali atoms from alkali halide crystal surfaces exhibits features consistent with thermal desorption of the alkali metal atoms at a temperature equal to the surface temperature: a Maxwellian distribution of velocities, a yield *vs.* bombarding energy characteristic which shows relatively few structural features at the known locations of alkali core-level energies; and a time dependence consistent with diffusion of F-centers to the surface.[9,11,19] The differences between ESD and PSD results for ground-state alkalis probably reflect either the contrasting energy-deposition profiles or the fact that ESD tends to be a one-step process where PSD can have multi- step effects, including the production of secondary electrons. On the other hand, halogens desorbed from alkali halides under low-energy electron bombardment have suprathermal energies and are emitted preferentially along the halogen "strings" in the crystal. This suggests that the formation and relaxation of V_k centers is a likely mechanism for the ejection of the halogens from the surface and near-surface layers of the bulk. The combined effect of the halogen desorption and the F-center migration is to make the surface alkali-rich and halogen-poor.

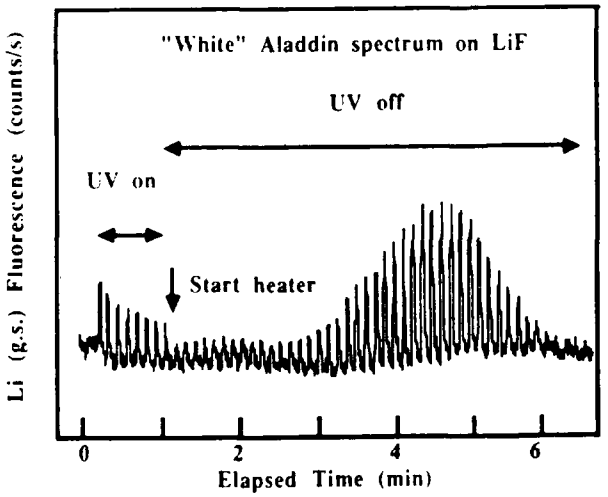

FIGURE 5. Fluorescence signal from Li^0 desorbed by the "white" ultraviolet photon spectrum from the Aladdin synchrotron light source.

The metallization of the surface is important not only because it changes the thermal properties of the surface, but also because it changes its electronic properties, as demonstrated in recent experiments on secondary electron-induced excitation of desorbing neutral atoms in the ground state.[23] It also has been demonstrated to occur for photon energies below the bulk band-gap energy of LiF;[7] hence, the surface metallization following desorption of ground-state alkali atoms is expected to be important in pulsed laser irradiation of surfaces, and may even, in the case of excimer lasers, occur via single-photon transitions. The work of Schmid *et al.* has shown that this mechanism is also operative in multiple-photon laser-stimulated desorption.[16]

We illustrate this effect with two recent experiments on PSD of LiF. The first shows the development of a layer of metallic Li on the surface of a pure LiF crystal undergoing ultraviolet photon irradiation in an ultrahigh vacuum environment. The radiation source was the first-order light from the Aladdin synchrotron light source of the University of Wisconsin.

In Figure 5, we show the time evolution of the first resonance decay of the desorbed Li^0 excited by light from a tunable dye laser in the geometry of Figure 2. Each peak in this spectrum represents a scan of the Coherent 599-21 tunable dye laser lasting approximately ten seconds over the first resonance line of the Li atoms at 6707 Å. At the time indicated by the arrow, the synchrotron light was blocked, and the LiF crystal was heated ballistically by turning on the heater block of the sample holder. As the sample temperature increases, the yield of Li^0 increases at first, as metallic Li is desorbed thermally from the surface. As this surface layer of neutral Li is depleted, the laser-induced fluorescence signal gradually dies away. The fact that it does not decay completely is consistent with the long time scales for F-center diffusion seen in previous experiments.[7]

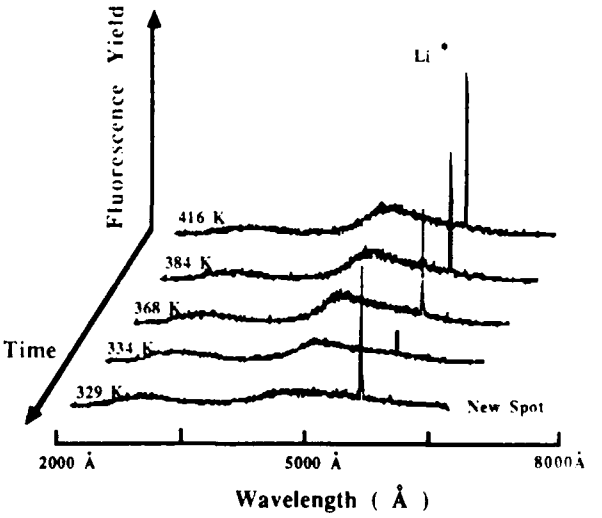

FIGURE 6. Fluorescence spectra showing desorbed Li^* as a function of temperature. The temperature was decreasing as a function of time. The final spectrum is taken at a previously unirradiated spot on the LiF single-crystal target.

A similar hysteresis effect resulting from thermal cycling is shown in the desorption of Li^*, the second most numerous product of electronically-induced desorption in alkali halides. In Fig. 6, we show a composite photon-stimulated desorption (PSD) spectrum of the yields of Li^* as a function of temperature under white-light irradiation from the Aladdin storage ring University of Wisconsin Synchrotron Radiation Center. These data indicate an increase of yield with temperature, although the rate of increase appears to be less than that observed for the ground-state yield. Curiously, a similar measurement of Na^* desorbed by photon irradiation from NaCl shows precisely the opposite behavior.[24]

The resolution of this apparently contradictory behavior may lie in the fact that the data of Figure 6 were obtained at incident photon flux levels significantly (perhaps a factor of 100) in excess of those available for the measurements of Ref. 24. In the foremost spectrum in Fig. 6, it is apparent that the yield returns to its former value when a new spot is irradiated. Since the near-surface bulk luminescence retains its general shape and yield for all the spectra, we can infer that the absorption of the incident energy in the near-surface bulk is not much affected by surface radiation damage; what is changed is the surface, which is known to be the source of the excited Li atoms. Thus it is likely that the surface damage to the LiF was more extensive than earlier NaCl results -- with an attendant change in the temperature dependence of the excited alkali atom desorption.

Incidentally, these measurements also suggest that studies of excited-neutral species may be a sensitive probe of surface composition and electronic structure once the mechanisms of desorption are well understood. Since most typical surface analytical tools, such as low-energy electron diffraction (LEED) and secondary ion mass spectrometry (SIMS), damage dielectric substrates even during the analytical process, the great sensitivity of the optical techniques employed here may yield significant advantages.

7. Changes in Radiation-Surface Interaction Effects from Adsorbed Surface Layers

Surface overlayers play a critical role in desorption and other radiation effects at surfaces, whether the layers are artifacts of surface preparation, are deliberately introduced, or are created by diffusion from the subsurface bulk. These overlayers can saturate dangling bonds influence surface composition and chemistry, modify surface geometric or electronic structure, and provide a non-vacuum interface which getters defects and impurities from the bulk. In the experiments described below, we have observed that surface overlayers may, when irradiated, form molecular states not accessible either in gas phase or bulk solids, thus opening new channels of chemical activity not predictable from three-dimensional experience. Moreover, these overlayers exhibit a dynamical response to incident electronic energy which differs from bulk or gas-phase responses, thus providing an energy reservoir or alternate decay channel for the incident energy. As indicated particularly by experiments in hydrogen adsorption, this may allow the overlayer to inhibit desorption of certain species, perhaps even to act as a protective layer, for the substrate.

In a number of experiments going back a decade or more, it has been found that low-energy electrons, heavy particles (atoms or ions) and photons incident on a number of alkali halide surfaces produce two distinguishable optical signals: a broad-band bulk luminescence, and line radiation from excited atomic and molecular species originating both in the nominal substrate surface and in the overlayer.[18,25] The bulk luminescence signal, a superposition of separately identifiable bands tens of nanometers wide, arises from the decay of electrons excited into the conduction band to lower-lying defect states ("trap states") whose energies lie within the bulk band gap. The bulk luminescence is relatively structureless, and varies only a little from one material to another. Its amplitude is, however, a strong function of the sample preparation; it can be considerably reduced, for instance, by heating.[26]

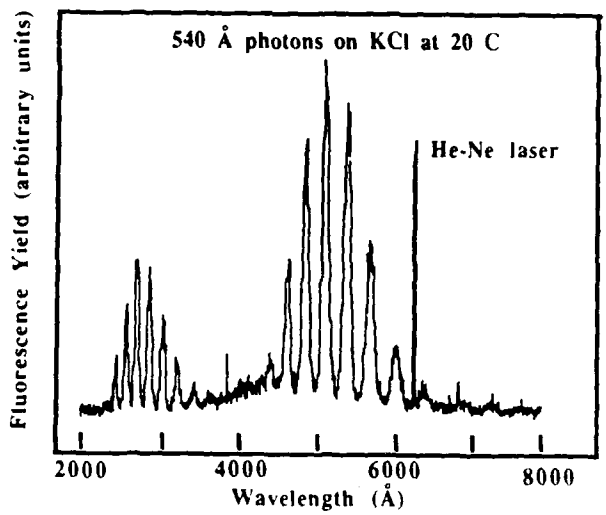

FIGURE 7. Spectrum of CN^- vibrational band radiation observed under photon bombardment of KCl. The fundamental band is in the ultraviolet; the second-order spectrum of the grating appears in the visible. Note the He-Ne laser line for calibration.

One feature of the spectrum which does change from material to material is a molecular band system in the ultraviolet, shown in Fig. 7. This striking radiation signature has been observed in a number of experiments with electron, ion, and photon bombardment of alkali halides,[18, 25] including, most recently, excitation by the white-light spectrum of the Aladdin synchrotron light source.[27] The spacing of the bands in this system is approximately 0.25 eV, which is characteristic of the most strongly bound diatomic molecules and molecular ions, such as H_2^-, CO, CN^- and NO^+.

The most frequently nominated candidate for the source of the radiation has been CN^-, because it is a pseudo-halide,[28] has a size consistent with the Cl^- ion in a normal alkali halide lattice, and because the bands match expectations for the $A(^3\Pi) \rightarrow X(^1\Sigma)$ transition in CN^-. (The long lifetime of the transition argues in favor of its being emission from the lowest triplet state to a singlet ground-state; however, arguments can be adduced in favor of either a $^3\Pi$ or a $^3\Sigma$ initial state in this case. A definitive identification of the upper level would require determination of the symmetry of the excited state.) However, some experimental observations -- notably, the growth in intensity of the bands as the sample is dosed with water vapor[26] -- are not consistent with a simple picture of CN^- substitutional impurities. Moreover, it remains unclear whether the bands originate from species *in* or *near* the surface, and whether or not the sources of the radiation are localized; previously there has been speculation that the CN^- might be bound at the surface as a hindered rotor. Also, the threshhold energy required to initiate the radiation is exceptionally low: synchrotron radiation experiments show that the CN^- radiation can be excited with ultraviolet photons as low as 7 eV.

Time-resolved measurements of this radiation have revealed a number of interesting properties relating to the role of the molecular luminescence in the dynamics of desorption from the underlying substrate. This is illustrated in Fig. 8, where the behavior of the bulk fluorescence is contrasted with that of the CN^-. The KCl sample was irradiated with a pulsed electron beam at low energy (200 eV), while the output of the spectrometer detecting the radiation was fed into a multichannel analyzer. The bulk fluorescence turns on and off synchronously with the electron pulse (to within the 10-μs time resolution of the multichannel anlyzer), while the CN^- radiation is astonishingly long-lived, with a lifetime of ~ 80 ms. This means that the incident electronic energy is "stored" as it strikes the surface, then released for a long period of time after the radiation source is turned off, probably because the upper state in the radiative decay sequence is formed through a forbidden triplet-singlet transition.

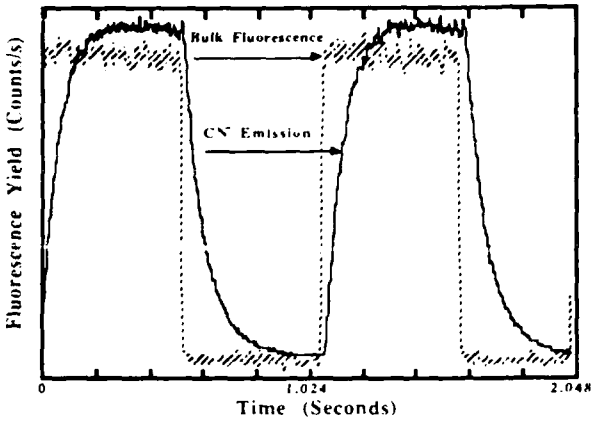

FIGURE 8. Time dependence of the fluorescence associated with the CN^- bands (solid curves) and with the bulk fluorescence (cross-hatched curves).

There is evidence that the presence of these bands is correlated with the absence of excited-state radiation from substrate atoms -- thus showing that the CN^- radiation acts as a kind of reservoir for the incident electronic energy, competing with excited-state desorption for the available energy. Whether or not this indicates the presence of a "protective overlayer," barring surface erosion through desorption of ground-state neutrals as well, remains to be established.

In excitation functions looking at the CN^- radiation as a function of ultraviolet photon energy,[27] there is a sharp and very intense peak at 7 eV in addition to a broad emission band (with significant superimposed fine structure) which develops at synchrotron photon energies above 12 eV. The 7 eV peak is a barely resolved doublet, and matches the position of a transition known from molecular computations. However, this particular transition cannot be studied in gas phase, because it is above the autoionization limit; it is also impossible to see the transition in the bulk, because electron-phonon coupling to the crystal lattice quenches the excitation before a radiative transition occurs. From the fundamental scientific point of view, this result is intriguing because it suggest the possibility for a kind of two-dimensional matrix isolation spectroscopy, in which the binding energy effects of the surface are just sufficient to depress (othewise unobservable) high-lying excited states below the conduction band. From the point of view of intracavity optical damage, it means that there are also surface states of adsorbates differing from those found in the gas phase which may have significant effects on surface chemistry, either because of providing new energy states or storing the incident photon or electron energy for periods of time long enough for chemical reactions to occur which might otherwise be forbidden.

The notion of a reservoir of surface electronic states which preferentially absorb incident electronic energy is clearly an interesting one, especially if the energy is released "harmlessly" through radiatiave transitions instead of through desorption. We have found that the physisorption of hydrogen on KCl is correlated with the disappearance of excited-state potassium atoms desorbed from the clean KCl surface at room temperature, as shown in Fig. 9; the potassium doublet at 766-770 nm disappears from the spectrum with the addition of a partial pressure of H_2 amounting to only $2 \cdot 10^{-8}$ torr. (The small size of the K^* peak results from the relatively inefficient desorption of ground-state neutrals from the surface at this temperature, as in Fig. 4. The surface was maintained at room temperature in order to prevent thermal desorption of the weakly adsorbed layer of hydrogen.) This shows that hydrogen has inhibited the otherwise efficient electron-stimulated desorption of excited potassium atoms from the substrate, and thus effectively closed a particular electronic mechanism for energy absorption, transformation and dissipation, presumably through the alteration of the surface electronic structure.

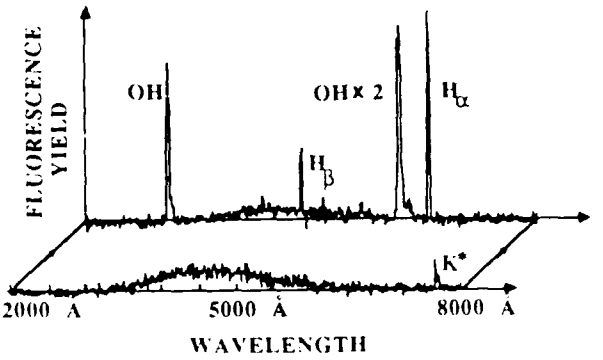

FIGURE 9. Fluorescence yield from atoms and molecules desorbed by electron bombardment from KCl for a clean surface (foreground spectrum) and for a surface dosed with hydrogen. The K^* line disappears in the hydrogen-dosing measurement.

Whether or not the hydrogen might be functioning as a kind of "protective barrier" against macroscopic erosion can only be conjectured for now, since simultaneous measurements of the desorbing ground-state potassium atoms -- which should be by far the more numerous species -- have not yet been undertaken. In any case, other measurements made with hydrogen on KCl indicate that the physisorbed hydrogen dissociates to form strong surface bonds, and this "chemical" interaction has a strong effect on the electronic channels available for electron-induced desorption.[29]

Both of these examples illustrate the importance of surface overlayers not only in influencing surface chemistry, but also in controlling the flow of energy deposited by electrons, ions and photons in the surface and near-surface bulk regions of dielectrics. The CN^- radiation, for example, appears to be a result of a mechanism for storing incident energy for long periods of time and then releasing it through non-desorptive channels. In contrast to the bulk luminescence, the incoming energy appears to be localized on a particular molecular species, and to be exceedingly long-lived (on the time scale of typical molecular excitation lifetimes) -- but the initial excitation does not give rise to the localized distortion of the surface lattice that could produce desorption.

7. Process-dependent Response of Fused Silicas to Low-Energy Electron and Ion Bombardment

Fused silica is to glasses what the alkali halides are to wide bandgap dielectric solids: a much-studied model material which can be prepared with some reproducibility. Wide variations in damage thresholds reported in the literature for various fused silicas suggest that process chemistry may have a significant impact on the response of the material to low-energy ionizing radiation. In the experiments summarized here, we used optical techniques to characterize two particular radiation damage effects -- atomic desorption and radiation-induced luminescence -- occurring in damaged regions within 20 nm of irradiated surfaces. The correlation between damage phenomenology and OH content suggests that electronic damage processes can be strongly influenced by surprisingly small impurity concentrations.

In our experiments, an electron or ion beam (see Figure 2) was incident along the surface normal of clean, optically transparent silica samples maintained under ultrahigh vacuum (nominal base pressure 10^{-9} Torr) at room temperature. Fluorescence decay signals from the desorbing ground-state and excited-state atoms were detected by a spectrometer and photomultiplier. Where the focal volume intersected the sample surface, luminescent emission from the irradiated volume was detected. The normal beam current of 1 μA corresponds to a flux of about 5×10^{13} particles/cm^2 -- about 0.01 ions/surface site/s, with a beam cross-sectional area of approximately 0.13 cm^2. No special precautions were taken against sample charging; however, the intensity of the bulk luminescence remained essentially constant over a period of two hours, indicating negligible Coulomb repulsion on the incoming ions from charge accumulation in the samples. This lack of charging is indeed puzzling; it appears that the electric field induced by the deposited ions must reach equilibrium within a short time after the start of irradiation.

Four different kinds of high-purity silica glasses have been used as model materials in our radiation-damage studies: Spectrosil, Spectrosil-WF, Suprasil-1 and Suprasil W-1. These glasses can be conveniently categorized into two subgroups based on method of preparation and principal impurity content.

Table 3. Synthetic Silica Characteristics

Sample Material	Preparation (Glass Type)	OH (ppm)	Cl (ppm)
Spectrosil	Flame hydrolysis	200	50
Suprasil-1	(Type III)	1200	130-180
Spectrosil WF	Plasma-CVD	< 2	180
Suprasil-W1	(Type IV)	< 5	230-280

Optically polished silica discs approximately 30 mm in diameter and 1 mm thick, were supplied by Thermal American Fused Quartz Company. The disks may have had a residual modified surface layer from the polishing process which has been reported to affect various surface properties.[30] Our samples were cut to shape with a diamond blade, chemically cleaned by acetone, methanol and deionized water, etched in hydrofluoric acid, and then washed again in deionized water and air dryed. Samples were subsequently handled with clean tweezers. This cleaning procedure appears to yield a reproducible surface with minimum contamination. A single HF etch removes about 150 Å of the surface; of course, the ion bombardment in the experiment provides continuous sputter cleaning of the irradiated area.

In these studies, as in electron- and ion-bombardment studies of the alkali halides, we have observed two principal generic features in the optical spectra from the near-surface regions of ion- and electron-irradiated silicas: atomic emission lines from desorbing species, and bulk luminescence. In general, the former are indicative of damage through desorption [surface erosion] processes, while the latter result from radiative decay of electronic excitations stemming from electron-hole pair production, exciton formation, and so on. Thus the two processes can be studied to ascertain the relative efficiency of competing energy-absorption and -dissipation mechanisms in the irradiated materials, to look for changes in the damage mechanisms, and to make spectroscopic identifications of the electronic states involved.

In one set of experiments, we compared the near-surface damage susceptibility of the four silica samples by bombarding them with argon, nitrogen and hydrogen ions while monitoring the optical emissions from excited atoms ejected from the surface and near surface region. These optical emissions typically consist of broad maxima, identified with the bulk luminescence, punctuated by sharp peaks corresponding to characteristic emission lines of excited atoms leaving the surface region. The wavelength scale of the spectrometer was calibrated from Hg emission lines.The relative yields of substrate and impurity atoms are obtained by integration of the emission lines; Figures 10 and 11 show spectra from the four glasses bombarded by Ar^+ ions at an incident energy of 9 keV. Comparison of the total optical yields going into bulk fluorescence *vis á vis* emission lines are one possible indicator of the total energy diverted into non-desorptive channels.

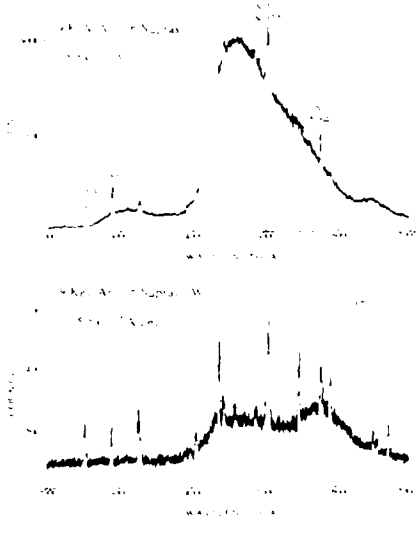

FIGURE 10. Optical fluorescence yields (in counts•s^{-1}) as a function of wavelength for Suprasil (top of figure) and for Suprasil-W1 (bottom of figure) bombarded by 9-keV Ar ions at a current density of 9×10^{-6} A•cm^{-2}. Some of the excited Si emission lines are identified.

Inspection of the figure will show that the total yields are about an order of magnitude larger for the irradiated Suprasil 1. Of perhaps greater interest is the fact that relatively more yield is in the line radiation compared to the bulk fluorescence for the ion-bombarded Suprasil W1. Another clear signature of electronic processes at work is the enormous variation in the shape of the bulk fluorescence spectrum in the two cases; since the luminescence is believed to come from de-excitation of shallow traps in the glass, this variation is an indication that the reduced OH content in the Suprasil W1 has a huge impact on the formation and de-excitation of those trap states.

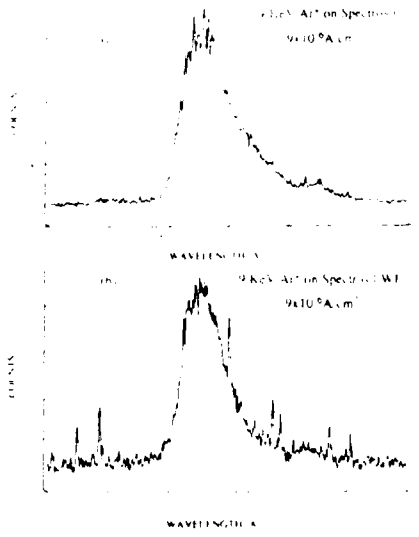

FIGURE 11. Optical fluorescence yields (in counts•s^{-1}) as a function of wavelength for Spectrosil (top of figure) and Spectrosil-WF (bottom of figure) bombarded by 9-keV Ar ions at a current density of 9x10^{-6} A•cm^{-2}.

In the case of Ar^+ irradiated Spectrosil and Spectrosil-WF, the overall difference in yields between the OH-rich and OH-poor silicas is only about a factor of 3, and the change in the shape of the bulk fluorescence is less pronounced. However, the Si and other line radiation is clearly more prominent, relative to the bulk fluorescence amplitude, for the irradiated Spectrosil-WF. The collision-cascade model of heavy-particle sputtering -- which should be valid for incident particles in this energy range -- offers no explanation for such dramatic changes from one glass sample to another where the only difference in the glasses is the impurity concentrations. Such effects cry out instead for an interpretation based on *electronic* bond-breaking mechanisms.[31]

A critical point here is that the excited silicon atoms *may* not be the dominant desorbing species. In experiments involving alkali halides which exhibit a generically similar desorption mechanism, the dominant desorption channel involves ground state neutral atoms and molecules.[19] Nevertheless, excited state neutral desorption is generally correlated with the desorption of ground state neutrals, and their appearance in the spectrum signals the onset of at least one form of surface damage, which typically has an efficiency of a few *per cent* in alkali halides.

To compare the radiation damage induced by a combination of collision cascade and electronic transitions with desorption attributable purely to electronic mechanisms, we also bombarded the surfaces of the Spectrosil (S) and Spectrosil-WF (SWF) samples by low-energy electrons. Figure 12 shows a typical spectrum of SWF sample irradiated by 320 eV electrons at normal incidence, using the same experimental arrangement described for the ion bombardment experiments. The electron current was maintained at approximately 1.0 μA/cm^2 on both samples. Four luminescence bands, located near 290 nm, 450 nm, 560 nm and 640 nm, appear during the electron irradiation of both S and SWF at room temperature. The integrated intensity of the 450 nm (2.7 eV) bulk luminescence band on S (see Figure 12) was invariably smaller than that from SWF. An important spectral feature from the ion experiments was conspicuous by its absence here: in most cases, we observed no sharp emission lines from desorbing excited atoms or ions for either of these silicas.[32]

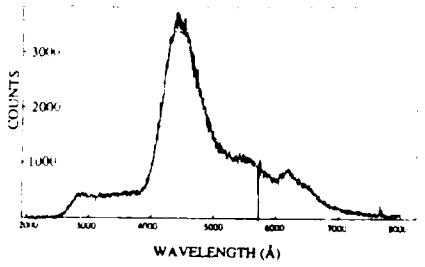

FIGURE 12. Fluorescence spectrum (counts•s^{-1}) observed for a Spectrosil sample irradiated by 320-eV electrons at normal incidence.

For the electron-irradiated samples, we measured the temporal decay time τ of the different fluorescence bands by setting the spectrometer to the center of one band, chopping the electron beam, and monitoring, with a multichannel analyzer connected to the photo-multiplier of the spectrometer, the decay of the luminescence signal after the electron beam was turned off. Figure 13 shows the lifetime measurements for the 290 nm and 450 nm bands; τ (450 nm) = 20 ms, while τ (290) < 10 μs, this being the lower limit of the dwell time for the multichannel analyzer. Measured decay times for the fluorescence signals at 560 and 640 nm were likewise less than 10 μs.

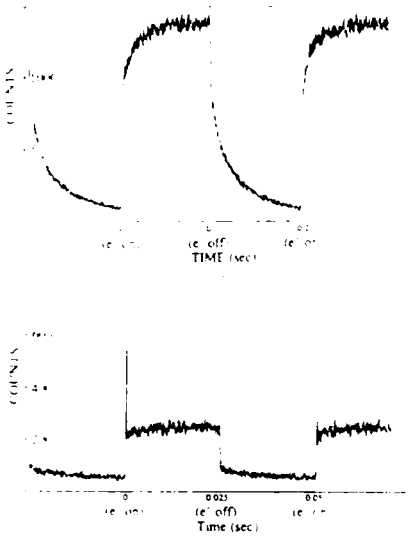

FIGURE 13. Fluorescence decay signals plotted as a function of time for beam-off-beam-on measurements of electron-irradiated Spectrosil. The upper spectrum, with a decay time on the order of 20 ms, is measured at 450 nm (see Fig. 12), while the lower curve is the fluorescence decay of the 290 nm band.

To correlate the optical observations with the large body of previous work identifying point electronic defects induced by ion and electron irradiation, electron paramagnetic resonance (EPR) measurements were carried out on irradiated samples at X band frequencies, using an IBM-Bruker spectrometer. The EPR spectrum of the irradiated samples shows a characteristic peak for the E_1' center (a singly-charged oxygen vacancy in the glass network), but with a lineshape broadened by defect-defect or dipole-dipole interactions.[33] The measured signal strength for the E' center implies large densities even for low ion and electron energies; near the surface, this defect is likely to produce under-coordinated Si atoms in much the same way that Pooley- Hersh desorption of halogens *via* the focused collision sequence leads to undercoordinated surface alkali atoms in irradiated alkali halides.

8. Thermal, Chemical and Plasma Effects on Intracavity Optical Surfaces

The experiments described in the preceding sections indicate that even low-energy electrons, photons and ions can induce significant changes in the surface composition and electronic structure of optical materials typical of those employed in laser cavities. In fact, for intracavity optical elements in gas lasers, the energies of these irradiating species are such that the primary energy deposition occurs in a thin layer (less than 30 - 50 nm) near the surface, and hence a significant coupling to the surface atomic or molecular layers. These compositional and structural changes, whether induced by momentum-changing collisions or electronic transitions, change the thermal, optical and chemical properties of intracavity optical surfaces. When laser photons are combined with intracavity radiation species, there are significant additional effects, some linear and some probably noniinear or even synergistic. We now consider in a qualitative way some of the consequences for intracavity damage processes.

In alkali halides, surface irradiation leads to ejection of the halogen component and subsequent enrichment of the metallic component at the surface. This metallization of the surface, which apparently occurs in many dielectrics and proceeds *via* the creation of mobile, permanent electronic defects, modifies both the thermal and optical properties. Alkali ions at the surface of an alkali halide undergoing electron or photon bombardment, for example, are replaced by neutral alkali atoms unless the temperature is high enough to produce thermal desorption. Because the atoms are more likely to be bound to each other by weak Van der Waals forces than to ionic partners in the lattice, it is quite likely that there is some "islanding" of metal on the surface, leading to changes in thermal conductivity of the surface layers and to changes in the surface absorption spectrum. In fused silica, on the other hand, the measured increases in the E' center concentration suggest a loss of oxygen in the near-surface material and a consequent enrichment in silicon. As in the case of the alkali halides, these changes inevitably lead to modifications of surface optical absorption and of surface thermal conductivity.

Thus intracavity irradiation by electrons, ultra-violet photons and heavy particles process makes of what initially had been a good optical dielectric a modified material which, at least in the surface presented to future irradiation, more nearly resembles a semiconductor or even a metal. This implies, in particular, that radiation damage by laser photons will more likely proceed either through the formation of electron-hole pairs (in the case of a semi-conductor-like surface), or through the excitation and acceleration of free electrons and ions by intense laser fields.

Of what consequence is the metallization? Calculations have shown that even a monolayer of alkali atoms is sufficient to create most of the essential features of the metallic state, including an appropriate band structure.[34] Thus we may expect that the thermal properties of the irradiated surface quickly cease to resemble the bulk material and rapidly begin to assume the characteristics of the metal. It has long been suspected, and recent work in laser-induced optical damage has confirmed, that the thermodynamic properties of thin films are an important diagnostic for susceptibility to damage.[35] Also, recent work on pulsed laser damage in metals suggests that a variety of mechanisms, such as has been called "hydrodynamic sputtering," operate for lasers incident on metals but not on their oxides.[36]

Chemical effects which would be observable at radiation-damaged surfaces include reactive etching -- a synergistic effect which occurs when reactive ions are present with electrons or photons[37]; laser-induced surface chemistry, including laser-induced or laser-enhanced adsorption, catalysis and etching[38, 39]; "hot atom" chemistry which uses the kinetic energy of slow atoms and ions to get over Langmuir-Hinshelwood barriers that inhibit certain kinds of chemical reactions[40]; and modification of by electronic mechanisms leading to changes in the surface chemical properties or the creation of new molecular species which cannot exist in the bulk or gas phase. The defect-induced desorption processes which modify the thermal properties of the surface also change its chemical properties. Thus, in the laser environment typical of many gas lasers, especially excimers with their mixtures of fluorine, noble-gas ions and residual oxygen, this change makes the surfaces more prone to chemical attack. In addition, the diffusion of electronic defects such as F-centers to the surface -- which in pure alkali halides is apparently the rate-limiting step in electron- and photon- stimulated desorption of neutral alkali atoms[11] -- can also lead to recombination reactions with surface adsorbates.[38]

Plasma effects in intracavity optical damage occur primarily as a result of or in connection with laser photons. In one sense, of course, laser photons are no different than other photons in their electronic interactions with surfaces. When a laser photon interacts with a surface or near-surface atom, the same generic kinds of energy absorption, localization, transformation and dissipation occur in all optical materials. But significant effects arise from the enormous photon fluxes typical of lasers in general and high-power pulsed lasers in particular, and from the temporal coherence and spectral purity inherent in the laser. These unique features of laser light have both physical and chemical consequences, particularly when combined with the effects of the low-intensity but longer-lasting irradiation from intracavity electrons, photons, ions or atoms.

The physics of surface damage with laser photons depends strongly on whether or not one is dealing with a nearly metallic, a semiconducting, or dielectric surface. In the case of a metal, a single monolayer of metal atoms -- say, Li atoms on the surface of LiF -- has an areal density of about 10^{15} atoms$\cdot$cm^{-2}. Suppose now that one has a pulsed laser with an intracavity irradiance of order 10^4 W$\cdot$cm^{-2}, not a particularly impressive intensity. Treating the laser as a plane wave, one finds that this irradiance is accompanied by an electric field of some 2 kV$\cdot$cm^{-1}, quite adequate to impart significant energies to the free electrons in the metallic monolayer and produce significant electron damage, including desorption. In the case of the semi-conductor, the deposition of a few hundred mJ$\cdot$cm^{-2} of visible light has been calculated to produce a carrier-concentration of order 10^{-3} cm^{-3} in the absorption depth of Si,[41] and the electron-phonon collision rate is high enough to achieve rapid thermalization to the lattice. For a dielectric, on the other hand, the deposition of the laser light may create a dense electron-hole plasma where the screening lengths are sufficient to allow the so-called "Anderson localization" to occur, allowing electronic energy to be localized long enough to cause desorption and damage by yet another mechanism.[14, 15] In all of these cases, the laser-induced damage is based on some catastrophic breakdown in the integrity of the material, this time one which is caused by radiation-induced changes in the material rather than by deficiencies in the manufacturing process.[42]

In a recent review of lasers in materials processing -- an environment similar in many respects to that found in laser cavities -- Osgood has pointed out[39] that lasers play a number of different roles in the chemistry at interfaces: because of their spectral purity laser photons have a high degree of specificity in the chemical reactions they can induce; particularly, in the light of pulsed-laser multiphoton excitation, lasers are excellent catalyzers of excited-atom-surface reactions; and laser-induced chemical reactions may proceed at substantially higher rates than nominally identical reactions on undifferentiated, "planar" surfaces under conventional conditions. The degree of chemical reactivity and specificity are also dependent on the laser intensity in a way which is still not well understood. Further progress in this area almost certainly depends on continued microscopic physical and chemical studies that will elucidate specific mechanisms and pin down reaction rates.

Moreover, although we have made a sort of artificial separation here for purposes of discussion, the laser in fact mixes "chemical" and "physical" processes in a unique way because of the way the laser can alter the solid-state properties of the material with which the laser interacts. For example, Schafer and Lyon observed an enhanced thermal oxidation rate in Si which they attribute partly to strong local heating of the Si substrate by the laser and partly to electronic excitation of the Si-SiO_2 interface; this latter step could come about by transfer of an electron from the conduction band of the Si into the conduction band of the SiO_2.[43] In that sense the laser-induced chemistry would depend on the detailed band structure at an evolving interface -- a complicated chemical physics problem indeed! However, once the unifying role of electronic excitation mechanisms has been recognized, even this kind of problem can be reduced to more manageable details, for precisely such interesting electronic transfers are also seen in low-energy ion-surface reactions at energies typical of ions in laser cavities.[44]

9. Summary and Conclusions

In a sense, the focus on electronic mechanisms in intracavity optical damage only reinforces the impression of enormous complexity associated with this problem, a complexity which has been only too well known to the optical design and fabrication community for many years. On the other hand, the concept of electronic transitions as the fundamental damage mechanism is also unifying and simplifying, since it leads both to the correct fundamental physics of the damage process(es) and to the crucial emphasis on the damage process as a question of the *dynamical* interaction of radiation and matter, rather than the *static* properties of materials -- this latter being the trap into which one easily falls by considering everything from a thermal, equilibrium perspective. It also appears to be the one perspective that can encompass such diverse elements as changes in surface structure and composition due to irradiation, the effects of overlayers and adsorbate, and processing-related changes in radiation response.

In the foregoing discussion, we have largely concentrated on the damage process in pure materials in ultrahigh vacuum, since that allows one to be maximally specific about the conditions of the irradiated surface. It is clear that, in the real world of laser cavities, this picture must be modified to include gas-surface and plasma-surface interactions, once again with an emphasis on the dynamical rather than the static equilibrium which must be considered when the interaction times are comparable to the characteristic time scales of electron-phonon, electron-plasmon and electron-electron collisions. Experimental evidence is clearly accumulating in support of the idea that it is possible to influence the ways in which the energy of incident radiation is absorbed, localized, transformed and dissipated by an optical material. The fact that these dynamical pathways share certain generic features in a large class of optical materials -- namely, those which form self-trapped excitons that relax to permanent, mobile defects -- means, it would appear, that continued, detailed study of simple model materials is likely to produce new insights which are not only interesting from the standpoint of fundamental physics, but which are also likely to produce practical guidance for laser optical design, processing and fabrication.

Acknowledgements

It is a pleasure to acknowledge the contributions of many colleagues to the gathering and interpretation of the experimental data reviewed here. These include Profs. Royal Albridge, Donald Kinser, Marcus Mendenhall, Joel Tellinghuisen, Norman Tolk and Robert Weeks of Vanderbilt University; Drs. Peter Nordlander and Paul Wang, also of Vanderbilt; Drs. Gerhard Betz and Wolfgang Husinsky, and Messrs. Bernhard Strehl and Johannes Sarnthein of the Institute for General Physics, Technical University of Vienna; and Dr. Richard Rosenberg of the Synchrotron Radiation Center at the University of Wisconsin. Graduate student participants included Patrick Bunton, Larry Hudson, Homyar Mogul, Shirley Oyog-Roth and Phillip Savundararaj of Vanderbilt University.

Portions of this work were supported by the Office of Naval Research (Contract Number N00014-86-K-0735), the Air Force Office of Scientific Research (Contract Numbers 86-0150 and F49620-86-C-0125), Sandia National Laboratories (Contracts 65-2377 and 53-6681), and the Acurex Corporation (Contract RC-6331). Travel support for the collaboration with the Technical University of Vienna came from the National Science Foundation (Grant Number INT-8512674).

References

1. P. Sigmund, "Theory of sputtering I. Sputtering yield of amorphous and polycrystalline targets," Phys. Rev. **184** (1969) 383.

2. An overview of current thinking about DIET processes and mechanisms can be found in two recent conference proceedings: and *Desorption Induced by Electronic Transitions, DIET II*, eds. W. Brenig and D. Menzel (Springer-Verlag, Berlin, 1985).

3. M. A. Loudiana, A. Schmid, J. T. Dickinson and E. J. Ashley, "The chemical sputtering of silica by Ar^+ ions and XeF_2," Surf. Sci. **141** (1984) 409.

4. J. E. Rothenberg and R. Kelly, "Laser sputtering II: the mechanism of the sputtering of Al_2O_3," Nucl. Instrum. Meth. in Phys. Research **B1**, 291 (1984).

5. N. Itoh and T. Nakayama, "Electronic excitation mechanism of sputtering and track formation," Nucl. Instrum. Meth. in Phys. Res. **B13** (1986) 487.

6. K. S. Song, A. M. Stoneham and A. H. Harker, "Electronic structure of the self-trapped exciton in alkali fluorides and chlorides," J. Phys. C.: Solid State Phys. **8**, 1125 (1975). D. R. Jennison and D. Emin, "Strain-induced localization and electronically stimulated desorption and dissociation," Phys. Rev. Lett. **51**, 1390 (1983).

7. R. F. Haglund, Jr., N. H. Tolk, G. M. Loubriel and R. A. Rosenberg, "Thresholds and time-dependence of electron- and photon-stimulated desorption in alkali halides," Nucl. Instrum. Meth. in Phys. Research B **18**, 549-554 (1987).

8. D. Pooley, "[110] anion replacement sequences in alkali halides and their relation to F-centre production by electron-hole recombination," Proc. Phys. Soc. London **87**, 245 (1966), and H. N. Hersh, "Proposed excitonic mechanism of color-center formation in alkali halides," Phys. Rev. **148**, 928 (1966).

9. N. G. Stoffel *et al.*, "Photon-stimulated desorption of neutral sodium from alkali halides observed by laser-induced fluorescence," Phys. Rev. **B32** (1985) 6805.

10. M. Syzmonski, "On the model of the electron sputtering process of alkali halides," Rad. Effects **52** (1980) 9.

11. T. A. Green, G. M. Loubriel, P. M. Richards, N. H. Tolk and R. F. Haglund, Jr., "Time dependence of desorbed ground-state lithium atoms following electron-beam irradiation of lithium fluoride," Phys. Rev. B **35**, 781 (1987).

12. D. Menzel and R. Gomer, "Desorption from metal surfaces by low-energy electrons," J. Chem. Phys. **41** (1964) 3311. P. A. Redhead, "Interaction of slow electrons with chemisorbed oxygen," Can. J. Phys. **42** (1964) 886.

13. M. L. Knotek and P. J. Feibelman, "Ion desorption by core-hole Auger decay," Phys. Rev. Lett. **40** (1978) 964.

14. N. Itoh, T. Nakayama and T. A. Tombrello, "Electronic-excitation mechanism in sputtering induced by high density electronic excitation," Phys. Lett. **108A**, 480 (1985).

15. P. W. Anderson, "Model for electronic structure of amorphous semiconductors," Phys. Rev. Lett. **34**, 953 (1975).

16. A. Schmid, P. Braunlich and P. K. Rol, "Multiphoton-induced directional emission of halogen atoms from alkali halides," Phys. Rev. Lett. **35** (1975) 1382.

17. Richard Zallen, *The Physics of Amorphous Solids*, pp 10-16, John Wiley and Sons, New York, (1983).

18. N. H. Tolk *et al.*, "Optical radiation from electron-stimulated desorption of excited particles," Phys. Rev. Lett. **46** (1981) 134, and "Optical radiation from photon-stimulated desorption of excited atoms," Phys. Rev. Lett. **49** (1982) 812.

19. R. F. Haglund, Jr. *et al.*, "Mechanisms of Electron- and Photon-Stimulated Desorption in Alkali Halides," Nucl. Instrum. Meth. in Phys. Research **B13**, 525 (1986).

20. N. H. Tolk *et al.*, "Neutral atom desorption observed by optical techniques," in *Desorption Induced by Electronic Transitions, DIET II* (see Ref. 2).

21. C. W. White, N. H. Tolk and D. L. Simms, "Surface composition by analysis of neutral and ion impact radiation," in *Characterization of Solid Surfaces*, eds. P. F. Kane and G. B. Larrabee, p. 641, Plenum, NY (1974).

22. N. Bloembergen, "Role of cracks, pores, and absorbing inclusions on laser induced damage threshold at surfaces of transparent dielectrics," Appl. Opt. **12**, 661 (1973).

23. P. Avouris, R. V. Walkup and A. Ghosh, "Excited-atom production by electron bombardment of alkali halides," Phys. Rev. Lett. **57** (1986) 2227.

24. E. Taglauer *et al.*, "Temperature dependence of photon-stimulated desorption of ground-state and excited-state Na from NaCl," Surf. Sci. **169** (1986) 267.

25. D. Cherry *et al.*, "Broadband luminescence from particle bombardment of alkali halides," Nucl. Instrum. Meth. in Phys. Research **B13**, 533 (1986).

26. W. A. Metz and E. W. Thomas, "Formation of CN^- radicals by ion implantation," Nucl. Instrum. and Meth. **194**, 505 (1982).

27. M. H. Mendenhall *et al.*, "Ultraviolet spectroscopy of CN^- in alkali halides: dynamics of the metastable triplet state," submitted to Chem. Phys. Lett.

28. For a sample of recent work in this area, see R. C. Spitzer, W. P. Ambrose and A. J. Sievers, "Observation of persistent ir spectral hole burning in the vibrational spectrum of CN^- in KBr," Phys. Rev. B **34**, 7307 (1986).

29. L. T. Hudson, "Photon-stimulated desorption of excited hydrogen from KCl," *Desorption induced by Electronic Transitions (DIET III)*, ed. M. L. Knotek, to be published.

30. D. J. King and M. J. Downs, "Ellipsometry applied to films on solid substrates," Surface Sci., **16**, 137 (1969)

31. For a discussion of the electronic regime in collisional sputtering, see *Sputtering by Particle Bombardment I*, ed. R. Behrisch, Springer, Heidelberg, 1981.

32. P.W.Wang *et al.*, "Luminescence from electron irradiation of synthetic silicas," in *Desorption induced by Electronic Transitions (DIET-III)*, to be published.

33. D. L. Griscom, "E' center in glassy SiO_2," Phys Rev. **B20**, 1823 (1979) (Springer-Verlag, Berlin, 1985),

34. E. Wimmer, "All-electron local density functional study of metallic monolayers I: alkali metals," J. Phys. F: Met. Phys. **13**, 2313 (1983).

35. For an introduction to the special laser-damage problems of coatings and thin layers, see R. M. Wood, *Laser Damage in Optical Materials*, Ch. 3, Adam-Hilger, Briston, 1986.

36. R. Kelly and J. E. Rothenburg, "Laser sputtering III: the mechanism of the sputtering of metals at low energy densities," Nucl. Instrum. Meth. in Phys. Research **B7/8** (1985) 755.

37. A broad sample of interesting work in this area is in the proceedings of the 1986 Symposium on Sputtering, in Nucl. Instrum. Meth. in Phys. Research **B18** (1987).

38. T. J. Chuang, "Laser-Induced Gas Surface Interactions, Surf. Sci. Reports **3** (1983) 1.

39. R. M. Osgood, "Laser Microchemistry and its Application to Electron-Device Fabrication," Ann. Rev. Phys. Chem **34**, 77 (1983)

40. H. Kang, T. R. Schuler and J. Wayne Rabelais, "Kinetic Energy dependence of molecular and dissociative reactions of CO^+ with a Ni(111) surface in the range 3-20 eV," Chem. Phys. Lett. **128**, 348 (1986).

41. W. L. Brown, "Transient laser-induced processes in semiconductors," in *Laser and Electron Beam Processing of Materials*, Eds. C. W. White and P. S. Pearcy, p. 20, Academic Press, New York (1980).

42. A model for catastrophic laser damage based on surface effects is sketched in R. F. Haglund, Jr. and N. H. Tolk, "Experimental studies of photon-surface interaction dynamics in the alkali halides, Proc. SPIE **690** 9 (1986).

43. S. A. Schafer and S. A. Lyon, "Wavelength dependence of laser-enhanced oxidation of silicon," J. Vacuum Sci. Technol. **21**, 422 (1981)

44. G. Betz *et al.*, "On the velocity dependence of excited sputtered atoms sputtered from metals and oxides," submitted to Phys. Rev. Lett.

Nuclear Instruments and Methods in Physics Research B18 (1987) 549 - 554
North Holland, Amsterdam

THRESHOLD EFFECTS AND TIME DEPENDENCE IN ELECTRON- AND PHOTON-STIMULATED DESORPTION *

Richard F. HAGLUND Jr and Norman H. TOLK

Department of Physics and Astronomy, Vanderbilt University, Nashville, TN 37235, USA

G.M. LOUBRIEL

Sandia National Laboratories, Albuquerque, NM 87185, USA

Richard A. ROSENBERG

Synchrotron Radiation Center, University of Wisconsin, Madison, WI 53706, USA

The use of optical techniques to study the dynamics of neutral alkali emission from alkali halides in electron- and photon-stimulated desorption (ESD, PSD) has produced significant new insights into the ways in which incident electronic energy is converted into kinetic energy of desorbing neutral atoms. In this paper, we show that the threshold for efficient PSD of Li from LiF lies below the band-gap energy, lower than those obtained from earlier ESD threshold measurements on NaCl. Time-resolved measurements of ground-state and excited-state Li desorption from LiF under both electron and photon irradiation exhibit a clear distinction between the spatial and physical origins of these two desorption products. The data suggest a possible identification of excited-state neutral desorption with surface-specific processes; on the other hand, a *defect-diffusion model* for ground-state desorption is more consistent with the data than are earlier thermal drift models. We also discuss briefly the implications of this work for technological problems as diverse as high-power laser optical damage and the production of intense lithium ion beams for fusion applications.

1. Introduction and motivation

Recent experiments in electron- and photon-stimulated desorption (ESD/PSD) on pure alkali halide crystals have confirmed early conjectures [1,2] of the dominant role played by self-trapped excitons and the migration of permanent defects to the surface in electronically stimulated desorption of ground-state neutral alkalis [3,4]. However, the wealth of detailed dynamical information in these new experiments has also revealed a rich phenomenology, with a correspondingly greater opportunity to separate ESD/PSD mechanisms belonging to various entrance and exit channels in desorption induced by electronic transitions (DIET). In particular, careful study of the mechanism(s) for ESD and PSD of excited-state alkali atoms now seems to differentiate quite clearly between surface and near-surface-bulk processes.

We have recently completed a series of ESD/PSD measurements – primarily in LiF – which have outlined in startling relief certain previously undiscovered features of the desorption process. These measurements have shown that ground-state and excited-state neutral yields dominate both ion and electron yields by orders of magnitude at electron and photon energies in the vicinity of the first core exciton peak. However, threshold measurements have shown that the onsets for efficient neutral alkali desorption occur at very low photon and electron energies, quite possibly within reach even of tunable lasers. This opens the way not only to new techniques for studying particularly the resonant excitation of certain modes, but also has significant implications for radiation damage effects in the wide-band-gap dielectrics typical of optical materials for short-wavelength, high-power laser systems.

The time-dependent measurements, on the other hand, have shown a dramatic difference in the behaviour of the ESD/PSD yields of ground-state and excited-state alkali neutrals as a function of time following irradiation. The experimental data have also proven to be stringent tests for model calculation of defect diffusion from the near-surface bulk following irradiation. In particular, it has been possible to correctly describe within this model the effects of the differing energy-deposition profiles of electrons and photons on

* Research performed at Vanderbilt University was partially supported by the Sandia National Laboratories under contract 65-2377. Portions of the work reported here were also performed at the Sandia National Laboratories which is supported by the U.S. Department of Energy under Contract Number DE-AC04-76DP00789.

0168-583X/87/$03.50 © Elsevier Science Publishers B.V.
(North-Holland Physics Publishing Division)

ground-state neutral alkali desorption. These time-dependent measurements have significant implications for the production of intense Li ions beams for particle-beam fusion systems, as we shall discuss briefly in section 5 below.

2. Experimental layout and procedures

Details of the experimental method have been presented elsewhere [5], so that only the essential features of our neutral desorption spectroscopy apparatus and technique will be highlighted here. The layout of the ESD/PSD experiments is shown schematically in fig. 1. The sample – a cleaved, single-crystal alkali halide – was mounted on a heated precision micromanipulator in an ultrahigh vacuum (UHV) system, at a nominal base pressure of $3-4 \times 10^{-10}$ Torr. Radiation incident on the target produces desorption products emerging toward the irradiation source, which in our experiments was either a low-energy, high-current electron gun or the beam from the Tantalus synchrotron storage ring at the University of Wisconsin. Deexcitation radiation from neutral atoms leaving the surface of the target material was detected by an optical system arranged to view a small volume (about 5×10^{-5} cm^3) out in front of the target. Radiation emitted from this volume along a line orthogonal to the irradiating source beam and parallel to the exposed face of the sample was imaged by a lens system onto the entrance slit of a spectrometer–photomultiplier combination. The optimum observation volume was selected by manipulating the target to minimize background from the bulk luminescence of the sample.

In this experimental geometry, desorbing ground-state neutral alkali atoms (M^0) are illuminated from the rear of the sample by the TEM_{00} (fundamental Gaussian) mode from a single-frequency, actively-stabilized tunable dye laser. Alkali atoms leaving the surface undergo resonant absorption at the Doppler-shifted frequency appropriate to their rest frame and radiate at the characteristic first resonance transition (3p to 2s) as they fly away from the sample surface. This radiation is detected by the spectrometer–photomultiplier combination and the results are stored in a PDP-11/73 computer for off-line analysis. Excited-state neutral alkalis (M^*), on the other hand, are detected from their characteristic deexcitation fluorescences lines when the tunable laser is turned off. Desorbing halogen species (X^0, X^*, X^+) are not observed in the present experimental setup.

In the geometry shown, this experimental layout permits the measurement of comparative yields for different particle species, desorption velocity distributions, and changes in emission characteristics as a function of sample temperature, orientation and surface preparation. Accurate yield measurements for a particular desorbing species, on the other hand, can be made in a Doppler-free geometry, in which the laser is injected perpendicular both to the incident electron or photon beam and to the spectrometer line-of-sight. Desorbed ions and electrons can also be measured by inserting, close to the point of electron or photon impact, an electrostatic analyzer with an exit-plane Channeltron detector. In this way, it is possible to measure essentially all the desorption products of interest and to ascertain their relative importance in the dynamics of DIET processes.

3. ESD/PSD threshold measurements in alkali halides

As Townsend pointed out in his pioneering papers on ESD from alkali halides [1], if the creation of a

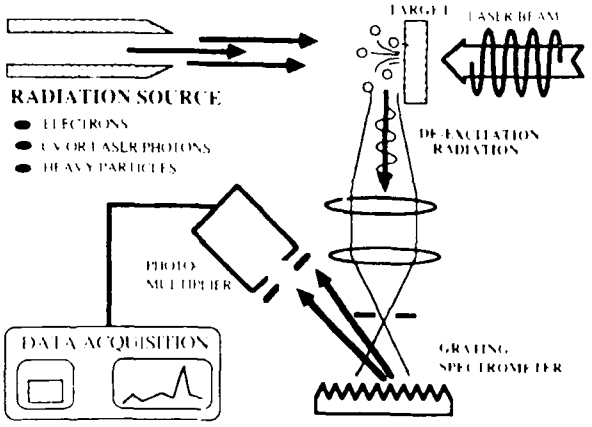

Fig. 1. Schematic of electron- and photon-stimulated desorption experiments using optical spectroscopy to identify desorbing neutral ground- and excited-state alkali atoms.

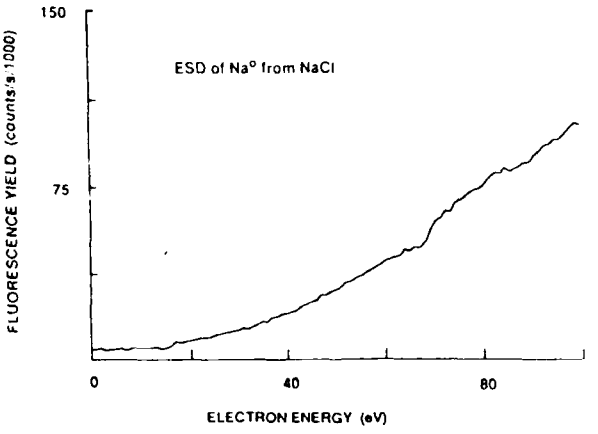

Fig. 2. Desorption yield as a function of energy for ground-state (Na^0) sodium atoms desorbed from a single-crystal (100) NaCl surface.

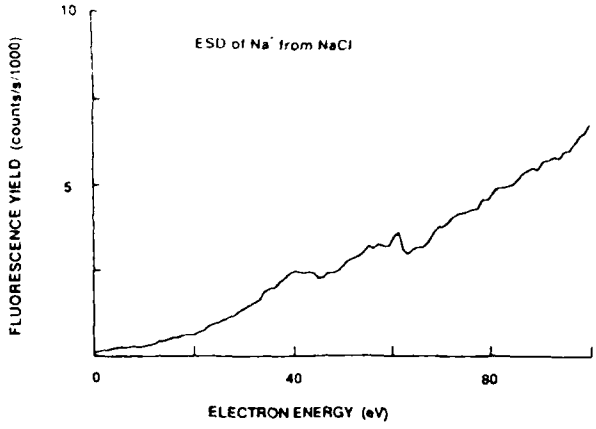

Fig. 3. Desorption yield as a function of energy for excited-state sodium (Na^*) desorbing from a single-crystal (100) NaCl surface.

self-trapped exciton is the first step in electronically stimulated desorption, one needs only the energy required to create the exciton on the dihalide molecule $(X_2)^*$ to initiate the process. However, nearly all measurements of the stimulated desorption process to date have relied on electrons or photons of significantly higher energies than the few electron volts mandated by this requirement. Moreover, until the development of the sensitive optical techniques necessary for tracking neutral desorption, it was not necessarily easy to look for the onset of desorption yields.

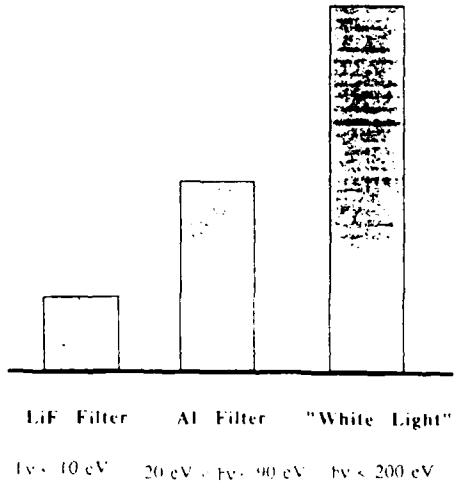

Fig. 4. Relative yields of ground-state lithium (Li^0) desorbed from LiF for photons in the indicated energy bins. The "white spectrum" of the Tantalus synchrotron light source extends to approximately 200 eV for the toroidal grating monochromator.

We have recently measured the thresholds for ESD of Na^0 and Na^* from NaCl, and for PSD of Li^0 from LiF and found them indeed to be very low in energy. The low-energy electron gun (0–100 eV) used for the threshold measurements produced several microamperes of current even at the lowest measured energies while maintaining a reasonably focused beam. Target charging problems were avoided in these measurements because they were made at temperatures high enough both to thermally desorb neutrals and to produce thermionic emission of excess electrons.

The threshold measurements made on NaCl are illustrated in figs. 2 and 3. It is clear from both figures that the onset of significant neutral desorption is certainly not more than 10–15 eV for both ground-state neutrals and for excited-state atoms. The curves in both cases are relatively featureless, although the desorption yield for Na^* does show some minor structure at energies corresponding to the Na core-hole excitation energies. As pointed out in ref. [3], this is apparently a quite general property of DIET processes in the alkali halides, arising from the relatively low mobility of defects produced by core excitations compared to those arising from valence band holes.

The PSD threshold measurements of desorbing Li^0 from LiF were made with filters to ascertain the relative yields in different regions of the incident UV photon spectrum. As shown in the bar graph representation in fig. 4, the three spectral bins were from 0 to 13.3 eV (LiF filter), from 20 to 90 eV (Al filter), and from 0 to 200 eV (full zeroth order spectrum transmitted through the toroidal grating monochromator (TGM) used in this set of measurements). The relative yields shown in fig. 4 for the Al and LiF filters were calibrated by the convolution of the raw yield with a trapezoidal-rule integration of the measured spectral response of a gold photodiode to the light transmitted through of the TGM [6].

There is some uncertainty about the upper-end cutoff of photon energies transmitted through the LiF filter, since it showed signs of significant radiation damage (color centers) which would have lowered the cutoff below the nominal value given by the bandgap energy. However, it is evident that approximately 25% of the total Li^0 yield is produced by photons from the lowest energy bin. The low value of this neutral emission threshold is consistent with results obtained by Schmid et al. almost a decade ago using four-photon excitation from a pulsed ruby laser [7]. This is not surprising, since the DIET mechanism producing ground-state neutrals will be valid for excitation pulses which are long compared to the energy localization time required to produce the defect. Recent anecdotal evidence in the subpicosecond laser community suggests that at ultrashort time scales, the threshold for photon-induced desorption, both in photon energy and in local photon intensity, may well be different.

4. Time-resolved ESP / PSD of ground- and excited-state alkalis

Time-resolved measurements of defect-induced desorption by Overeijnder et al. [8] using velocity selector techniques showed that the ground-state neutral alkalis desorbed from NaCl, RbI and RbBr by electron bombardment at 540 eV were produced with a time delay less than 0.0001 s following irradiation. However, it was possible with this technique only to identify prompt (nonthermal) and delayed (thermal) halogen and alkali emissions. Our recent measurements have had sufficiently greater time resolution to resolve the distinctive differences between the temporal behavior of the laser-induced fluorescence yield from neutral ground-state alkalis, and the fluorescence decay of excited-state alkali atoms desorbed at comparable electron bombarding energies.

This is fortunate because, from the beginning, optical spectroscopy of excited-state neutrals showed features differing sharply from the results of studies on ground-state neutral desorption. Measurements of relative ESD yields of Li from LiF as a function of temperature, for example, showed that the excited-state neutrals had a sharply lower temperature threshold for desorption and had a distinctly non-thermal behavior [4], while the ground-state neutrals exhibited an Arrhenius-like desorption characteristic as a function of temperature and a characteristic Maxwellian velocity distribution at the temperature of the sample surface [9]. Measurements of excited-state fluorescence yields as a function of distance from the sample surface for ESD of Na from NaCl have generally been consistent with a kinetic energy of several eV [4]. All of these data, together with other experimental results on desorbing neutral hydrogen, indicate that the difference in mechanisms between M^0 and M^* from alkali halide crystals should provide key insights into the nature of the dynamics underlying DIET processes.

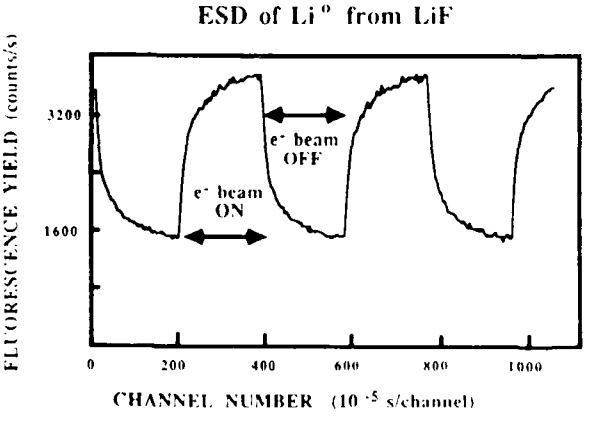

Fig. 5. Time-resolved yield of ground-state neutral Li atoms desorbed from LiF by electron irradiation at 200 eV, at a sample temperature of 400°C. The time scale is 10^{-5} s/channel.

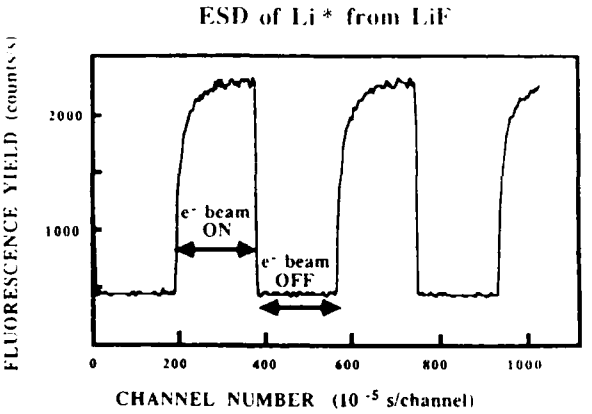

Fig. 6. Time-resolved yield of excited-state neutral Li atoms desorbed by electron irradiation of LiF under the same energy and temperature conditions as the data of fig. 5.

We have now completed a series of measurements which indicate unequivocally that one of the differences between ground-state and excited-state neutral alkali desorption is that the former results from a combination of surface and near-surface-bulk excitations mediated by diffusion of electronic defects from the near-surface bulk – whereas the latter appears to be produced at the crystal surface. This fact is significant not only for what it reveals about DIET processes, but also as an indicator of the power of neutral species desorption spectroscopy as an analytical tool. However, it should be noted that the question of surface excitations in excited-state desorption cannot now be regarded as settled; there is evidence that the characteristics of excited-state neutrals desorbed under ESD are influenced by electron energy, electron-beam current, sample temperature and previous history of the sample.

Figs. 5 and 6 display the results of ESD experiments on LiF which contrast the desorption characteristics of Li^0 and Li^* for the same electron-gun and temperature parameters. In this case, the temperature of the LiF surface was maintained at 400°C, and the gun was chopped at a rate of a few kHz. The laser-induced-fluorescence (LIF) yield was measured for the ground-state Li, and then the laser was turned off to measure the yields of Li^*. In fig. 5, the LIF yield for Li^0 is shown as a function of time for a pair of electron gun pulses. The yield climbs sharply at first, and then shows a gradual saturation as the contribution from near-surface bulk layers increases. When the electron gun is turned off, the LIF yield is observed to drop sharply at first, and then fall quite slowly until the next electron-gun pulse is turned on. In fig. 6, on the other hand, the behavior of the Li^* yield on the leading edge of the incident elec-

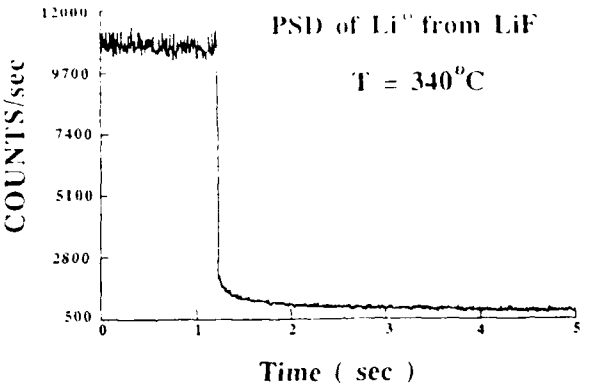

Fig. 7. Time-resolved desorption yield of Li^0 from LiF under irradiation by the "white spectrum" from a synchrotron light source, following shutting off the beam.

tron pulse is the same as that for Li^0, while the trailing-edge behavior shows that the Li^* turns off instantaneously when the exciting source is removed. Indeed, a measurement of this trailing edge of the Li^* fluorescence pulse with the best time resolution possible with our multichannel analyzer (10^{-7} s) showed that the yield decreases from 0.9 to 0.1 of its maximum value within 0.1 μs. This means that while the *source* of Li for excited-state Li is the same as that for the ground state Li, the excitation *mechanism* yielding Li^* is distinctively different. The ground-state data are well described by a diffusion model based on realistic electron-energy depostion profiles [10,11]; preliminary indications are that such a model will be appropriate for describing ground-state PSD of alkalis from alkali halides as well.

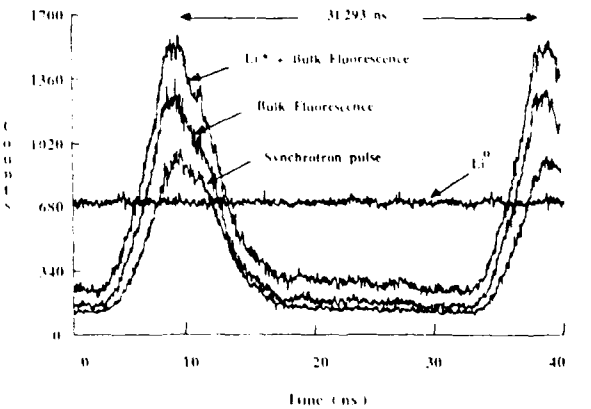

Fig. 8. Desorption yield of Li^* as a function of time, shown together with the measured fluorescence yield from the Tantalus beam itself, the measured yield with the laser background and Tantalus beam only, and the yield with sample, laser and exciting UV beam. The straight line is the long tail of the Li^0 fluorescence yield.

Similar behavior is observed for PSD of Li^0 and Li^*, as shown in figs. 7 and 8. In fig. 7, we display the results of PSD experiments using the full, "white light" spectrum of the Tantalus storage ring to produce desorption in a LiF crystal. The incident light source was "chopped" by inserting a beam stop at the entrance to the TGM ahead of the UHV chamber, consuming approximately a millisecond. As in the case of the ESD measurements of the Li^0 yield from LiF, there is a long decay of the LiF signal, indicating (see below) that there is a contribution to the ground-state neutral yield from near-surface bulk of the crystal. In this case, however, the decay constant is a matter of seconds, rather than milliseconds; we believe this is a result of the deeper energy deposition profile of the UV photons when compared with the electrons. The yield of excited-state Li once again shows a significant difference from the Li^0, but in this case the length of the exciting photon pulse is also significantly different: Here we have used the 5.6 ns pulse of the Tantalus storage ring itself to provide a fast excitation source for Li^*. The fluorescence signal from the photomultiplier (see fig. 1) was in this case fed into a time-to-amplitude converter (TAC), allowing a measurement to be made on a ns time scale, stored in a multichannel analyzer, and then dumped to a computer. Fig. 8 shows the superposition of four distinct signals: that from the synchrotron pulse itself, that from the synchrotron pulse plus background luminescence, that from both of these sources plus the desorbed Li^*, and, finally, that from the ground-state-neutral fluorescence decay. The excited-state Li signal appears to be turning on and off – with a response time of less than 1 ns – in synchronism with the exciting ultraviolet light pulse.

This may be evidence for a direct surface electronic excitation leading to desorption. Indeed, recent preliminary results for very short electron pulses have produced similar results on a microsecond time scale – without the contribution from near-surface Li produced by diffusion from the bulk. However, the critical point is, once again, that the time-resolved measurement indicates no such short-time-scale behavior in the ground-state neutral yield, indicating that the process creating ground-state neutrals is clearly distinct from that producing the Li^*. While it is possible to produce Li^* from gas-phase excitation of desorbed Li^0 under certain circumstances [12], we believe that those particular conditions are not obtained in the present experiments.

5. Discussion and conclusions

Defect-induced desorption produced by formation of a self-trapped exciton, relaxation to a permanent defect and migration of that defect to the surface of a large-band-gap insulator is now a firmly established concept

in the radiation damage community. However, this concept is also interesting from a fundamental point of view because it represents the limiting case of an exciton so strongly coupled to (in more modern parlance "dressed by") neighboring phonons that it is immobile, and therefore has to decay by giving up its energy in a manner which is highly localized in space and time. Desorption – induced by the initial electronic transition – is one such possible event. In the case of ground-state neutral alkali desorption in the alkali halides, this electronic excitation mechanism affects only the halogen sublattice directly, but does so with great efficiency and can even be calculated with reasonable accuracy.

In the case of excited-state neutral alkali desorption, on the other hand, no such simple explanation has yet been found. One reason may well be that a surface exciton is not so easily self-trapped, so that its energy does not remain localized following the turning off of the irradiating electron or photon pulse. The assumption that the fundamental mechanism for excited-state neutral desorption was linked to the 1s core exciton in Li was based on the similarity between optical absorption measurements and the structure of PSD measurements of Li^0 [13]. This same general excitonic structure has also been observed in PSD yields of Li^+ from LiF and, in preliminary measurements, for electrons produced in the PSD process. It is likely that further detailed measurements of desorbing halogens will be necessary to fully map out the kinetics of the excited-state DIET mechanisms.

The technological implications of this line of research are manifold and interesting. In a general way, LiF is an ideal model material for studies of the generic class of materials in which electron- and photon-stimulated desorption produces self-trapped excitons which relax to form permanent defects. This category of materials includes many of the wide-bandgap dielectrics used as optical coatings and optical substrate materials [14]. Here, the threshold measurements have an obvious application to the problem of surface damage induced by high-power, short-wavelength laser pulses. The present results show that the electronc mechansim for laser-induced damage in transparent dielectrics is obviously no intrinsically a multiphoton process. Therefore, the idea that macroscopic damage can originate with DIET processes – suitably modified to take account of the role of surface overlayers [15] – is clearly a viable one.

Another more specific application centers on the use of lithium-loaded dielectrics to serve as anode materials in high-current alkali ion sources for particle-beam fusion applications. From the time-dependent measurements presented here, it seems clear that high yields can be produced by very short pulses provided that some conditioning occurs to produce the required free-metal overlayer at the surface. Indeed, recent preliminary measurements at even shorter pulse lengths (as short as 10 μs) show that ground-state neutral desorption can occur efficiently for short excitations, indicating the possibility of a very rapid, surface-specific process. Further work on even shorter excitation pulses – of both electrons and photons – would thus seem to be a fruitful area for further study.

It is a pleasure to thank the staff of the Synchrotron Radiation Center, University of Wisconsin, for their expert help in providing UV photons and technical assistance in the PSD experiments.

References

[1] P.D. Townsend, R. Browning, D.J. Garlant, J.C. Kelly, A. Mahjoobi, A.M. Michael and M. Saidoh, Radiat. Eff. 30 (1976) 55; F. Agullo-Lopez and P.D. Townsend, Phys. Status Solidi B97 (1980) 9.

[2] M. Szymonski, Radiat. Eff. 52 (1980) 9.

[3] N.G. Stoffel, R. Riedel, E. Colavita, G. Margaritondo, R.F. Haglund, E. Taglauer and N.H. Tolk, Phys. Rev. B32 (1985) 6805.

[4] For results on Li desorbed by ESD from LiF, see R.F. Haglund Jr et al., Nucl. Instr. and Meth. B13 (1986) 525. For analogous (and in some respects antithetical) experimental results for Na desorbed by ESD from NaCl, see M. Szymonski et al., Desorption Induced by Electronic Transitions (DIET-II), eds., W. Brenig and D. Menzel (Springer, Heidelberg, 1985) pp. 160–168.

[5] N.H. Tolk, R.F. Haglund, Jr., M.H. Mendenhall and E. Taglauer, Desorption Induced by Electronic Transitions (DIET-II), eds., W. Brenig and D. Menzel (Springer, Heidelberg, 1985) pp. 152–159.

[6] C.E. Olsen, University of Wisconsin Synchrotron Radiation Center TGM Instruction Manual.

[7] A. Schmid, P. Bräunlich and P.K. Rol, Phys. Rev. Lett. 35 (1975) 1382, see also N.L. Boling, P. Bräunlich, A. Schmid and P. Kelly, Appl. Phys. Lett. 27 (1975) 191.

[8] H. Overeijnder, R.R. Tol and A.E. De Vries, Surf. Sci. 90 (1979) 265.

[9] N.H. Tolk et al., Nucl. Instr. and Meth. B2 (1984) 457.

[10] G.M. Loubriel et al., Phys. Rev. Lett. 57 (1986) 1781.

[11] T.A. Green, G.M. Loubriel, P.A. Richards, N.H. Tolk and R.F. Haglund Jr, Phys. Rev. B, to be published.

[12] Z. Postawa, J. Rutkowski and M. Szymonski, these Proceedings (Symposium on Sputtering, 1986) Nucl. Instr. and Meth. B18 (1987) 574.

[13] N.H. Tolk, M.M. Traum, J.S. Kraus, T.R. Pian and W.E. Collins, Phys. Rev. Lett. 49 (1982) 812.

[14] N. Itoh and T. Nakayama, Nucl. Instr. and Meth. B13 (1986) 487.

[15] R.F. Haglund Jr and N.H. Tolk, Proc. 3rd Topical Conf. on Coherent Short-Wavelength Generation and Applications (Am. Inst. of Physics, New York, 1986) in press.

Paper presented at the Fourth International Conference on Radiation Effects in Insulators (REI-4)
Universite Claude Bernard, Lyons, France -- July 6 - 10, 1987

To be published in Nuclear Instruments and Methods in Physics Research B

ELECTRONIC TRANSITIONS IN SURFACE AND NEAR-SURFACE RADIATION EFFECTS*

R. F. Haglund, Jr., M. H. Mendenhall and N. H. Tolk
Department of Physics and Astronomy and
Center for Atomic and Molecular Physics at Surfaces
Vanderbilt University, Nashville, TN 37235 USA

G. Betz and W. Husinsky
Institut für Allgemeine Physik,Technische Universität, A-1040 Vienna, Austria

ABSTRACT

Studies of surface effects arising from electron, heavy particle or photon irradiation of dielectric surfaces are increasingly focusing on the electronic interactions by which energy is absorbed, localized, and transformed or transferred prior to the ultimate dissipation of the incident energy -- through, for example, ejection of atoms or molecules from the dielectric. Recent experiments in our laboratories illustrate the varied roles played by electronic transitions in determining the flow of electronic energy during the bombardment of dielectric surfaces by photons, electrons and heavy particles. Specific examples include: the effects of surface overlayers and adsorbed hydrogen in retarding substrate desorption; substrate-temperature- and energy-resolved studies of photon-stimulated desorption from alkali halides; and electronic level-hybridization effects in the sputtering of metal oxides by argon ions. These simple model systems are a critical testing ground for studying the mechanisms of surface radiation damage in more complex materials because of the wealth of information available about their electronic and geometric structure, and because the character and modes of formation of their permanent electronic defects are well understood.

---

* Supported in part by the Office of Naval Research (Contract Number N00014-86-K-0735), the Air Force Office of Scientific Research (Contract Numbers 86-0150 and F49620-86-C-0125), Sandia National Laboratories (Contracts 65-2377 and 53-6681), Acurex Corporation (Contract RC-6331), and the National Science Foundation (Grant Number INT-8512674).

1. Introduction

The phenomenology of radiation effects at dielectric surfaces exhibits a remarkable richness and complexity, ranging from luminescence to desorption of individual atoms or molecules, and on to rapid, efficient etching of large surface areas and macroscopic track formation. Scientifically, surface radiation effects in dielectrics are interesting because the large band-gap of these materials creates many channels through which incident energy can be absorbed, localized and transformed into the kinetic energy necessary to break a bond in a solid lattice or network. In technology, dielectric surface damage plays a critical role in such diverse areas as microelectronics fabrication and reliability, damage to high-power laser optical elements, and the development of optical elements for high-power tunable ultraviolet and X-ray light sources.

Studies of desorption, ablation, erosion and etching induced by energetic photons, electrons and heavy particles are increasingly emphasizing the microscopic details of the *electronic* mechanisms responsible for these phenomena. This concern for electronic rather than thermal mechanisms is particularly appropriate for dielectrics, because electronic features play significant roles in virtually all radiation effects, including those accompanying low-energy sputtered particles moving adiabatically with respect to electronic velocities in the solid; low-energy (primary or secondary) electrons or ultraviolet photons which are absorbed in thin layers near the surface; and laser photons for which the broken spatial symmetry at the surface allows non-linear or resonant interactions which are forbidden in the bulk. Moreover, in many instances -- as in intracavity optical damage in gas lasers or reactive ion etching -- simultaneous irradiation by photons and/or electrons and/or heavy particles produces synergistic effects which cannot be explained as a linear superposition of individual processes. Hence, a detailed understanding of the available electronic channels through which energy can be absorbed, localized, transformed and dissipated is a *sine qua*

non for understanding the immense variety of radiation effects.

Conversely, the need for identifying the specific material characteristics that play the decisive roles in enhancing or inhibiting damage is pushing us beyond older models of desorption (or sputtering), particularly at low energies, because it is becoming increasingly apparent that energy is often *not* shared in a statistical (thermal or collisional) way among all the atoms in the zone where energy is deposited. This makes it necessary to move beyond pictures of equipartition of energy among competing degrees of freedom, to a more sophisticated picture in which the flow of energy into and out of the surface is tracked within the framework of models which are faithful both to the fundamental interaction physics of particles or photons with the surface, and to the electronic properties of those materials.

In particle-, electron- and photon-induced radiation damage, electronic mechanisms are manifested in several generically distinct ways, including: excitation of electrons into the conduction band and excitation of atomic and molecular species on and near the surface; creation of bound electron-hole pairs, possibly with subsequent relaxation into permanent electronic defects and atomic/molecular excitations in surface overlayers; competition between "direct" desorption and desorption following diffusion of radiation-induced defects to the surface; and effects of the energy-level structure of a particle-surface system on the internal quantum states of desorbed particles. In this review, we shall illustrate these general considerations with several examples.

- optical radiation from electron- and photon-irradiated surface overlayers;
- photon-stimulated desorption of alkali metals from alkali halides; and
- velocity distributions of excited metal atoms sputtered from a metal and its oxide.

The emphasis in the experiments is on measurements of quantum states of desorbed particles, including their temporal evolution, with the ultimate goal of inferring the details of the potentials

which give rise to the observed states.

2. Experimental apparatus and procedure

The key insight underlying the dynamical studies presented here is that desorption from dielectric surfaces is overwhelmingly dominated by the emission of *neutral* ground-state and excited-state atoms and molecules. Therefore, the techniques of gas-phase atomic and molecular optical spectroscopy are the critical tools, rather than the charged-particle spectroscopies typical of surface analysis experiments. Details of the experimental method have been presented elsewhere [1, 2], so that only the essential features of our neutral desorption spectroscopy apparatus and techniques will be highlighted here.

The experimental layout of the ESD/PSD experiments is shown schematically in Fig. 1. The sample -- typically a cleaved, single-crystal alkali halide -- is mounted on a heated micromanipulator in an ultrahigh vacuum (UHV) system, at a nominal base pressure of a few times $1C^{-10}$ torr. Radiation incident on the target produces desorption products emerging toward the irradiation source, which in our experiments was either a low-energy, high-current electron gun or the beam from the Aladdin synchrotron storage ring at the Undiversity of Wisconsin. De-excitation radiation from neutral atoms leaving the surface of the target material was detected by an optical system arranged to view a small volume (about $5x10^{-5}$ cm^3) out in front of the target. Radiation emitted from this volume along a line orthogonal to the irradiating source beam and parallel to the exposed face of the sample was imaged by a lens system onto the entrance slit of a spectrometer-photomultiplier combination. The optimum observation volume was selected by manipulating the target to minimize background from the bulk luminescence of the sample.

In this experimental geometry, desorbing ground-state neutral alkali atoms are illuminated from the rear of the sample by the TEM_{00} (fundamental Gaussian) mode from a single-frequency,

actively-stabilized tunable dye laser. Alkali atoms leaving the surface undergo resonant absorption at the Doppler-shifted frequency appropriate to their rest frame and radiate at the characteristic first resonance transition (3p to 2s) as they fly away from the sample surface. This radiation is detected by the spectrometer-photomultiplier combination and the results are stored in a computer for off-line analysis. Excited-state neutral alkalis, on the other hand, are detected from their characteristic de-excitation fluorescences lines when the tunable laser is turned off. Desorbing halogen species are not observed in the present experimental set-up, because their resonance lines are in the ultraviolet. However, excited desorbing halogens should, in principle, be observable with a uv spectrometer; ground-state halogens could likewise be observed by using a laser detection technique -- such as resonant multiphoton ionization -- capable of inducing sufficiently energetic transitions out of the ground state.

In the geometry shown, this experimental layout permits the measurement of relative yields for different particle species, desorption velocity distributions, and changes in emission characteristics as a function of sample temperature, orientation and surface preparation. Accurate yield measurements for a particular desorbing species, on the other hand, can be made in a Doppler-free geometry, in which the laser is injected perpendicular both to the incident electron or photon beam and to the spectrometer line-of-sight. Desorbed ions and electrons can also be measured by inserting, close to the point of electron or photon impact, an electrostatic analyzer with an exit-plane Channeltron detector. In this way, it is possible to measure essentially all the desorption products relevant to the dynamics.

In the sputtering experiments described in Section 5, the geometry is similar, but the spectrometer views the desorbing particles at an angle to the surface normal in order to measure their velocity distribution. Connecting the observed laser-induced fluorescence with the velocity distribution requires the choice of a model for the sputtering process, in order to deconvolute the

contributions of excited-state radiation from atoms traveling in different directions; in this case, we assume the validity of the collision cascade and calculate the velocity distribution for a given spectrometer angle using the Thompson formula. That this is a reasonable choice has been shown in a great many experiments, provided the direct knock-on contribution remains insignificant -- which requires using the incident sputtering beam at near-normal incidence.

3. EXPERIMENTS: luminescence and desorption from surface overlayers

Surface overlayers play a critical role in understanding desorption phenomena at surfaces, whether they are artifacts of surface preparation, are deliberately introduced or are created by diffusion from the subsurface bulk. These overlayers can saturate dangling bonds, influence surface composition and chemistry, modify surface geometric or electronic structure, and provide a non-vacuum interface which getters defects and impurities from the bulk. In the experiments described below, we shall discuss results suggesting that surface overlayers may also inhibit desorption, thus acting as an energy reservoir, or even a protective medium, for the substrate.

Experimentally, it is found that low-energy electrons, heavy particles (atoms or ions) and photons incident on dielectric surfaces produce two readily distinguishable optical signals: a broad-band bulk luminescence, and line radiation from excited atomic and molecular species originating both in the nominal substrate surface and in the overlayer. The bulk luminescence, which is frequently considered as a superposition of separately identifiable bands tens of nanometers wide, arises from the decay of electrons excited into the conduction band to lower-lying defect states ("trap states") whose energies lie within the bulk band gap. The bulk luminescence is relatively structureless, and varies only a little from one material to another. Its amplitude is, however, a strong function of the sample preparation; it can be considerably reduced, for instance,

by heating.

One feature of the spectrum in which does change from material to material is a molecular band system in the ultraviolet, shown in Fig. 3. This striking radiation signature has been observed in a number of experiments with electron, ion, and photon bombardment of alkali halides [4-7], including excitation by the white-light spectrum of the Aladdin synchrotron light source [5]. The spacing of the bands in this system is approximately 0.25 eV, which is characteristic of the most strongly bound diatomic molecules and molecular ions, such as H_2^-, CO, CN^- and NO^+.

The most frequently nominated candidate for the source of the radiation has been CN^-, because it is a pseudo-halide [5,6], has a size consistent with the Cl^- ion in a normal alkali halide lattice, and because the bands match expectations for the $A(^3\Pi) \text{--} X(^1\Sigma)$ transition in CN^-. (The long lifetime of the transition argues in favor of its being emission from the lowest triplet state to a singlet ground-state; however, arguments can be adduced in favor of either a $^3\Pi$ or a $^3\Sigma$ initial state in this case. A definitive identification of the upper level would require determination of the symmetry of the excited state.) However, some experimental observations -- notably, the growth in intensity of the bands as the sample is dosed with water vapor [6] -- are not consistent with a simple picture of CN^- substitutional impurities. Moreover, it remains unclear whether the bands originate from species *in* or *near* the surface, and whether or not the sources of the radiation are localized; previously there has been speculation that the CN^- might be bound at the surface as a hindered rotor. Also, the threshhold energy required to initiate the radiation is exceptionally low: synchrotron radiation experiments show that the CN^- radiation can be excited with 8.5 eV ultraviolet photons. These issues are a matter of continuing investigation [7].

Time-resolved measurements of this radiation have revealed a number of interesting properties relating to the role of the molecular luminescence in the dynamics of desorption from the underlying substrate. This is illustrated in Fig. 4, where the behavior of the bulk fluorescence is

contrasted with that of the CN^-. The KCl sample was irradiated with a pulsed electron beam at low energy (200 eV), while the output of the spectrometer detecting the radiation was fed into a multichannel analyzer. The bulk fluorescence turns on and off synchronously with the electron pulse (to within the 10-μs time resolution of the multichannel anlyzer), while the CN^- radiation is astonishingly long-lived, with a lifetime of ~ 80 ms. This means that the incident electronic energy is "stored" as it strikes the surface, then released for a long period of time after the radiation source is turned off, probably because it arises from a forbidden triplet-singlet transition leading to the formation of the upper state.

There is evidence that the presence of these bands is correlated with the absence of excited-state radiation from substrate atoms -- thus showing that the CN^- radiation acts as a kind of reservoir for the incident electronic energy, competing with excited-state desorption for the available energy. Whether or not this indicates the presence of a "protective overlayer" barring surface erosion through desorption remains to be established.

However, the notion of a surface reservoir of electronic states which preferentially absorb incident electronic energy is clearly an interesting one, for both scientific and technological reasons. We have found that the physisorption of hydrogen on KCl is correlated with the disappearance of excited-state potassium atoms desorbed from the clean KCl surface at room temperature, as shown in Fig. 5; the potassium peak at 680.6 nm disappears from the spectrum with the addition of a partial pressure of H_2 amounting to only $2 \cdot 10^{-8}$ torr. This shows that hydrogen has inhibited the otherwise efficient electron-stimulated desorption of excited potassium atoms from the substrate, and thus effectively closed a particular electronic mechanism for energy absorption, transformation adn dissipation, presumably through the alteration of the surface electronic structure. Whether or not the hydrogen might be functioning as a kind of "protective barrier" against macroscopic erosion can only be conjectured for now, since simultaneous measurements of the desorbing ground-state

potassium atoms -- which should be by far the more numerous species -- have not yet been undertaken. In any case, other measurements made with hydrogen on KCl indicate that the physisorbed hydrogen dissociates to form strong surface bonds, and this "chemical" interaction has a strong effect on the electronic channels available for electron-induced desorption.

Both of these examples illustrate the importance of surface overlayers not only in influencing surface chemistry, but also in controlling the flow of energy deposited by electrons, ions and photons in the surface and near-surface bulk regions of dielectrics. The CN^- radiation, for example, appears to be a result of a mechanism for storing incident energy for long periods of time and then releasing it through non-desorptive channels. In contrast to the bulk luminescence, the incoming energy appears to be localized on a particular molecular species, and to be exceedingly long-lived (on the time scale of typical molecular excitation lifetimes) -- but the initial excitation does not give rise to the localized distortion of the surface lattice that could produce desorption.

4. EXPERIMENTS: Surface effects in photon-stimulated desorption

A large number of experiments conducted over some two decades [8, 9] has shown that the electron- and photon-stimulated desorption (ESD/PSD) of halogen atoms from alkali halides is a result of the formation of mobile H centers (the so-called "crowdion," neutral halogen atoms compressed into interstices along the <110> crystal directions). Systematic studies of alkali metal atoms desorbed by photon irradiation of sodium halides showed that the velocity distributions of the ground-state alkalis were Maxwellian with a temperature equal to that of the surface [10], leading to the conclusion that the desorption of the alkalis was essentially a thermal process. However, more recent ESD studies [11] of Li^0 desorbed from LiF have shown that at high temperatures, the rate-limiting time scale in the ESD process is that of F-center diffusion from the

near-surface bulk to the surface.

Experiments in both the electron- and photon-stimulated desorption of excited and ground-state neutral alkalis from alkali halides showed that, where the ground state neutral alkalis are desorbed thermally, following the diffusion of radiation-induced F-center to the surface, the excited states exhibited a more complex behavior [12, 13]. In recent experiments using synchrotron radiation, we have measured the behavior of the desorbed excited-state lithium atoms in the vicinity of the 1s core exciton . In Fig. 5, yields of both the desorbed ground-state (Li^0) and excited-state (Li^*) atoms are shown as a function of incident photon energy. The clear signature of an electronic excitation mechanism is the large resonant yield of Li* shown. Such a large yield could, of course, be evidence of the excitation of *gas-phase* Li^0 already desorbed from the surface but not yet outside the collection solid angle of the spectrometer (see Fig. 1), as has already been proposed as a mechanism for creating Na* by electron bombardment of NaCl [14]. However, recent measurements in which Li^0, Li*, Li^+ and secondary-electron yields were measured *simultaneously* as a function of photon energy in this region show no corresponding rise in secondary-electron production in the vicinity of the core exciton, and the secondary electron spectrum is too soft in energy to account for the observed increase in fluorescence yield [15]. The virtually instantaneous desorption of the Li^* compared to the slow, diffusion-dominated desorption of Li^0 indicates that a specific electronic mechanism -- a core-hole excitation, in this case -- is directly correlated with the desorption phenomenon.

A further indication that the yield of excited alkalis is, to a significant degree, influenced by electronic excitation mechanisms and surface electronic structure rather than thermally-driven processes, such as diffusion, comes from studies of excited atom yields as a function of temperature. In an earlier experiment, photon-stimulated desorption of Na* was measured as a function of temperature [16], and there were indications that the yield of Na* *decreased* with temperature, while the yield of Na^0 *increased*. Corresponding measurements in

electron-stimulated desorption of Li* from LiF showed that Li* emission yields remained essentially constant throughout a temperature range in which the yield of Li^0 increased from zero to its saturation value [12].

However, the opposite trend as a function of substrate temperature has been measured as well. In Fig. 7, we show a composite of the yields of Li* as a function of temperature under white-light irradiation from the Aladdin storage ring University of Wisconsin Synchrotron Radiation Center. These data were obtained at incident flux levels significantly (perhaps a factor of 100) in excess of those available for the measurements of Ref. [14]. They indicate an increase of yield with temperature, although the rate of increase appears to be less than that observed for the ground-state yield.

The resolution of this apparently contradictory behavior may lie, perhaps, in the foremost spectrum in Fig. 7, which shows that the yield returns to its former value when a new spot is irradiated. Since the near-surface bulk luminescence retains its general shape and yield for all the spectra, we can infer that the absorption of the incident energy in the near-surface bulk is not much affected by surface radiation damage. But the Li* yield is evidently extremely sensitive to surface conditions, and it is difficult to imagine a thermally activated process with that degree of sensitivity unless it involves the interaction of thermally-driven defects with the surface. The measurements of Ref. [14] were taken using the Tantalus storage ring as the ultraviolet photon source, while those shown above were measured on Aladdin -- a source with both significantly higher brightness and a higher endpoint energy than the photon flux from Tantalus. The fact that opposing trends in excited atom yields can be observed in experiments differing only in the state of the surface suggests that excited-neutral species desorption may be a sensitive probe of surface composition and electronic structure once the mechanisms of desorption are understood.

5. EXPERIMENT: final-state particle-surface interactions in sputtering

The collision-cascade theory of sputtering [17] has been applied with significant success to the prediction of yields and energy distributions of substrate atoms desorbed by energetic ions from both metals and insulators [18]. However, the study of more detailed dynamical characteristics of desorbed excited atoms -- such as their velocity distributions -- has remained an active and even controversial field of inquiry, because the statistical distributions of excited states predicted by the cascade model fail to agree with experimental data. Resonant tunneling models [19] by themselves also apparently do not give a complete picture. We have found in recent experiments that the electronic properties of the sputtered solid can have significant effects on velocity distributions, and may hold the key to a more complete understanding of internal quantum states of desorbed excited atoms. Indeed, these recent results suggest that neither the simple resonant tunneling model nor the static bulk band theory is adequate to explain the distribution of excited states of particles sputtered from either metals or dielectrics.

The final states of atoms sputtered from a solid surface may be determined in several different ways: (1) through the time evolution of hybridized particle-surface states created in the interaction of (internal) collision products with the surface; (2) through charge-exchange processes (such as Auger decay and tunneling) in the final (external) interaction with the surface; (3) from the inflight decay of molecules created in pre-dissociative states *via* collisions with surface atoms; and (4) through secondary electron impact on desorbed ground-state atoms and molecules. In all of these processes, it is assumed that the relevant quantum numbers are to be found from an examination of the band structure of the sputtered solid (modified as appropriate at the surface) and the electronic structure of the desorbed atom. However, both the band structure and the atomic structure are modified spatially and temporally *in a dynamical way* by the interaction, and it is necessary to consider those modifications to the *static* picture if we are to understand the sputtering process.

The model we have in mind is sketched in Fig. 7; to simplify matters, we deal only with the first resonance level of the desorbing atom. For an atom desorbed from the surface, we are dealing with a bond-breaking process made possible by collisional processes, and we assume in general that the desorbing particle exists as an ion inside the solid. As is well known, the atoms escaping from the surface have energies which are typically much less than the Bohr velocity (corresponding to an energy of a few electron volts), so we can assume that the adiabatic condition is satisfied. In our experiments, where the velocity distributions of only the excited atoms are observed, the changes in velocity distribution from metal to oxide can only be interpreted as arising from loss of flux in the excited-atom exit channel; since we have no information about other desorbing species, we can only guess at the most likely mechanism(s).

Now two separate kinds of experimental observations need to be reconciled: First, the yield of sputtered excited neutral atoms always appears to increase in comparing desorption (sputtering) from a metal to desorption from its corresponding oxide; in the present work, changes of factors of two to ten in the total intensity of the observed atomic emission line were observed. Second, the velocities and the velocity distribution of the desorbing particle appears to be strongly influenced by the ability to lose excitation through resonant tunneling. That is, the flux of excited *slow* atoms can be reduced by tunneling deexcitation (or resonant neutralization), thus preferentially preserving the fast excited neutrals. As we shall show, even a consistent, qualitative treatment of this process requires an understanding of the dynamical relationships between atomic or ionic levels and the solid state electronic structure.

It has been known for a long time that the flux of excited sputtered atoms increases from a metal to its corresponding oxide. The classic picture of resonance tunneling [20] used to explain this effect assumed that, if the excited atomic level were in the unoccupied region of states above the metal Fermi level, resonance ionization would occur due to tunneling into an unoccupied

metallic electron state -- thus preferentially removing an electron from slow-moving atoms near the surface. In the case of the oxide, on the other hand, it was assumed that no such tunneling would be possible since the excited atomic state would lie in the forbidden band gap of the oxide, permitting the excited atoms to survive long enough to escape from the surface. Such a picture would support both a broadening of the velocity distribution of excited atoms sputtered from a metal, and the increased yield in excited states for sputtering from the corresponding oxide.

Our recent experiments on Al and Al_2O_3, however, show precisely the opposite result: the yield of Al^* is higher from the oxide, but the velocity distribution for the oxide is *broader* than that observed for Al^* desorbed from the metal surface, indicating a preferential destruction of slower moving excited Al atoms for the oxide, rather than for the metal where resonant tunneling should be easier. This suggests that the simple resonant-tunneling model, which explains both the change in yield and the change in velocity distribution as manifestations of the same mechanism, is inadequate. We suggest that, in fact, the higher excited-state yield on oxides may reflect nothing more complicated than the fact that sputtering from insulators and from metals takes place on a time scale of a vibrational period, 10^{-13}-10^{-12} s. On this time scale, there are some 10^3 electronic fluctuations in the neighborhood of a given atom desorbing from a metal, giving many possible deexcitation interactions for the excited desorbing atom. For at atom desorbed from an insulator, on the other hand, the desorption lifetime is comparable with the significantly slower hopping rate for electrons in an insulator, and hence the possibility of deexcitation for any given atom is less.

If electronic tunneling is a significant contributor to the differences in desorption between metals and oxides, however, the measured velocity distributions will also be very sensitive not only to the velocity with which the excited atoms leave the surface, but also to the relative positions of the excited atomic level and the Fermi surface. If there are surface states in the band gap of the oxide -- well-known to be the case in aluminum oxide -- those states represent available channels

for the excited electron to tunnel into; if, in addition, the excited atomic level is depressed with respect to the Fermi surface of the metal, the number of accessible tunneling states will also be reduced. Thus, the velocity distribution of sputtered excited atoms will be sensitive not simply to the perpendicular velocity of escape from the surface [19] -- which is determined by the properties of the collision cascade in the cases we have studied -- but also to the relative positions of the excited level *vis a vis* the Fermi surface of the metal and any band-gap states in the oxide. We are continuing the investigation of these phenomena by comparing a variety of metals and their oxides in order to determine how differing band structures and the presence or absence of surface states affects the velocity distributions.

6. Conclusions

Both the material surface and the near-surface bulk play significant roles, particularly in low-energy radiation effects in dielectrics. The surface, with its exposed network of bonds, respects the fragile, reactive interface which acts to influence the transfer of energy from external sources and the rates at which substrate atoms and molecules can be ejected, as well as providing the final-state interactions determining the asymptotic quantum states of the ejecta. The properties of this "nominal" surface can be strongly influenced by (deliberately or unintentionally) adsorbed layers, even to the point, as will become apparent, of retarding desorption from the nominal surface. The subsurface atomic layers contribute as well, by generating the band structure of the material and thus determining the channels through which electronic excitation or de-excitation can occur. Also, radiation-induced changes in surface composition can influence on desorption dynamics, overcoming even the effects of radiation-induced defects migrating from the near-surface bulk. In the long run, understanding the mechanisms of surface and near-surface radiation damage will require a more or less complete description of all of these effects.

From the point of view of surface dynamics, the problem of desorption and other radiation effects in insulators may be characterized as a series of differentiated steps, each one of which has a more or less well-known microscopic (*i.e.*, atomic scale) character. There is an *initial state* of the system, consisting of the probing particles or photons in known energy, momentum and internal quantum states, and a well-characterized surface with a given set of energy bands and constituents. The radiation effects begin with an *interaction* phase, described by the microscopic physics of the probe-surface interaction; this interaction may be a photon-electron interaction, creating excited states of atoms or molecules, or electron-hole pairs; for incident heavy particles, it may be a collision cascade, producing a shower of particles internal to the solid, jarred loose by the momentum transferred by an energetic ion. In any case, this interaction is likely to be much better known and understood than the phases of *localization*, *transformation*, and *dissipation*, during which the initial electronic energy deposited by the probes is converted into electronic energy of desorbing particles, localized electronic defects and restructured surface and subsurface bonds. The final state is once again composed of desorbing particles and a well-characterized surface, either or both of which may be be different states than the initial state of the system. The challenge to the experimenter consists in elucidating the localization, transformation and dissipation mechanisms in such a way as to account for the observed yields and, one hopes, to provide information on the microscopic potentials responsible for the observed interaction products.

In recent years, methods of atomic and molecular spectroscopy -- such as laser-induced fluorescence and other optical techniques -- have been employed with increasing success to determine the quantum states of desorbing or sputtered particles. However, these particles are only part of the final state of the system, of course; thus, the next stage in fully characterizing the dynamical processes involved in radiation effects is perhaps dependent more on an enhanced understanding of the initial and final states of the insulator surface than any other single experimental variable. For example, understanding the structural and compositional evolution of an

alkali halide surface undergoing ultraviolet photon bombardment is vital to resolving the nature of the precursor steps in photon-stimulated desorption, because knowing whether the surface is stoichiometric or metal-enriched determines the kinds of surface excitations or surface states which may be present, as well as the nature of the solid lattice or network whose distortion results in the ejection of a particle.

This knowledge of the composition and structure of the surface is not easily obtained for insulators, since typical surface analytic tools -- such as low-energy electron diffraction and secondary ion mass spectroscopy -- work well for metals and even semiconductors, but are known to cause radiation damage in dielectrics. However, studies of desorption dynamics are themselves hinting at ways in which desorption provides spectroscopic clues about the state of the surface. In addition, a continuing focus on the *electronic* mechanisms of particle-, electron- and photon-surface interactions will make it possible to use the specific clues available from solid-state physics about the initial and final states of the surface and near-surface regions of differing materials. As long as one treats the irradiated material as an undifferentiated aggregation of particles characterized by thermal or collisional properties, it is not possible to use the more differentiated electronic characteristics -- such as band structure -- to help solve the dynamical problem by selectively emphasizing certain reaction pathways. Experiments emphasizing the electronic mechanisms involved in desorption and other radiation effects in insulators are thus both part of the problem and, very likely, a key ingredient in the solution.

ACKNOWLEDGEMENTS

It is a pleasure to acknowledge our debt to colleagues who participated in many of the experiments reported here, including: Royal G. Albridge, Alan V. Barnes and Dwight P. Russell

of Vanderbilt, and Richard A. Rosenberg of the Synchrotron Radiation Center of the University of Wisconsin. We also thank Joel Tellinghuisen, of the Vanderbilt University Department of Chemistry, for sharing his spectroscopic insights about the CN^- vibrational bands and for a thoughtful reading of the manuscript.

REFERENCES

[1] N. H. Tolk, R. F. Haglund, Jr., M. H. Mendenhall and E. Taglauer, DESORPTION INDUCED BY ELECTRONIC TRANSITIONS (DIET-II), eds. W. Brenig and D. Menzel (Heidelberg: Springer, 1985) pp. 152-159.

[2] W. Husinsky, G. Betz, I. Girgis, Phys. Rev. Lett. **50** (1983) 1689.

[3] M. L. Yu, D. Grischkowski, A. C. Balant, Phys. Rev. Lett **48** (1982) 472.

[4] A. I. Bazhin, E. O. Rausch and E. W. Thomas, J. Chem. Phys. **65** (1976) 3897. W. A. Metz and E. W. Thomas, Nucl. Instrum. and Meth. **194** (1982) 505. E. von der Heyden and F. Fischer, Phys. Stat. Sol. **69** (1975) 63. N. H. Tolk, L. C. Feldman, J. S. Kraus, R. J. Morris, M. M. Traum and J. C. Tully, Phys. Rev. Lett. **46** (1981) 134.

[5] D. Cherry *et al.*, Nucl. Instrum. and Meth. in Phys. Res. **B13** (1986) 533.

[6] T.-K. Ha and G. Zumofen, Molec. Phys. **40** (1980) 445. J. Berkowitz, W. A. Chupka and T. A. Walter, J. Chem. Phys. **50** (1969) 1497.

[7] J. Tellinghuisen, A. V. Barnes, R. F. Haglund, Jr., L. T. Hudson, M. H. Mendenhall, D. P. Russell and N. H. Tolk, submitted to Phys. Rev. Lett.

[8] Some important references for electron-stimulated desorption of halogens are in: P. D. Townsend, R. Browning, D. J. Garlant, J. C. Kelly, A. Mahjoobi, A. M. Michael and M. Saidoh, Radiat. Effects **30** (1976) 55; F. Agullo-Lopez and P. D. Townsend, Phys. Stat. Sol. B **97** (1980) 9. H. Overeijnder, R. R. Tol and A. E. DeVries, Surf. Sci. **90** (1979) 265. M. Syzmonski, Rad. Effects **52** (1980) 9.

[9] Multiphoton laser-induced desorption of chlorine from NaCl has been treated by A. Schmid, P. Bräunlich and P. K. Rol, Phys. Rev. Lett. **35** (1975) 1382. See also N. L. Boling, P. Bräunlich, A. Schmid and P. Kelly, Appl. Phys. Lett. **27** (1975) 191.

[10] N. G. Stoffel, R. Riedel, E. Colavita, G. Margaritondo, R. F. Haglund, E. Taglauer and N. H. Tolk, Phys. Rev. B **32** (1985) 6805.

[11] G. M. Loubriel *et al.*, Phys. Rev. Lett. **57** (1986) 1781. T. A. Green, G. M. Loubriel, P. M. Richards, N. H. Tolk and R. F. Haglund, Jr., Phys. Rev. B **35** (1987) 781.

[12] R. F. Haglund, Jr. *et al.*, Nucl. Instrum. and Meth. in Phys. Res. **B13** (1986) 525.

[13] R. F. Haglund, Jr. and N. H. Tolk, Proc. SPIE **690** (1986) 9.

[14] P. Avouris, R. V. Walkup and A. Ghosh, Phys. Rev. Lett.

[15] R. F. Haglund, Jr., A. V. Barnes, M. H. Mendenhall, and N. H. Tolk, submitted to Phys. Rev. Lett.

[16] E. Taglauer *et al.*, Surf. Sci. **169** (1986) 267.

[17] P. Sigmund, Phys. Rev. **184** (1969) 383.

[18] T. A. Tombrello, Nucl. Instrum. Meth. in Phys. Res. **B2** (1984) 555.

[19] M. L. Yu and N. D. Lang, Phys. Rev. Lett. **50** (1983) 127.

[20] C. W. White, N. H. Tolk and D. L. Simms, CHARACTERIZATION OF SOLID SURFACES, eds. P. F. Kane and G. B. Larrabee (New York: Plenum, 1974) p. 641.

FIGURE CAPTIONS

1. Schematic of experimental apparatus for measuring the properties of neutral atoms and molecules desorbed from solid surfaces by electron, ion or photon impact. Radiation from the desorbed particles is detected in a spectrometer arranged to view them in flight from the surface; the tunable laser is used to induce fluorescence in selected ground-state species.

2. Broadband luminescence in the form of molecular vibrational bands observed during photon bombardment of a single crystal of KCl in ultrahigh vacuum; the source is the first-order light from the Aladdin synchrotron light source. The ultraviolet light spectrum in the region between 230 and 300 nm is the fundamental; the visible bands come from the second order of the diffraction grating in the spectrometer. Note the He-Ne laser line used for wavelength calibration at 632.8 nm.

3. Comparison of the time dependence of the radiation from the vibrational bands opf CN^- (measured lifetime 80 ms) and from the bulk luminescence created by electron bombardment of KCl ("instantaneous" decay on this time scale). The long lifetime of the CN^- radiation is characteristic of a triplet-singlet transition.

4. Optical emission spectra of excited atoms emitted from the surface of clean KCl and from KCl in a low ambient pressure of hydrogen gas, under low-energy electron bombardment. Note the disappearance of the excited potassium line when the hydrogen is admitted to the ultrahigh vacuum chamber. The KCl sample was at room temperature, so the hydrogen is presumed to be weakly physisorbed.

5. Comparison of ground-state with excited-state lithium atom yield from the photon-irradiated surface of LiF, measured as a function of bombarding photon energy. The "off-resonance" points were taken by shifting the tunable dye laser (see Fig. 1) off the first resonance line of the lithium atoms at 670.7 nm.

6. Temperature dependence of the radiation from excited-state lithium atoms desorbed from the surface of LiF under ultraviolet photon irradiation. Note that the final (foremost) spectrum is taken with the photon beam striking a previously unirradiated spot on the crystal surface, but is taken at virtually the same temperature as the spectrum just preceding it.

7. Schematic energy-level diagram showing the relative positions of (from left) the density of states in a metal; the spectrum of a two-level atom as a function of distance from the metal; and the spectrum of bands and surface states in a metal oxide. Note the shifting and broadening of the atomic levels very close to the metal surface, which may have the effect either of raising the excited level E_1 above the Fermi surface (case (a), typical of transition metals) or of lowering it below the Fermi level (case (b), as calculations show to be the situation for the 4s level of Al, for example). The existence and the spectrum of the surface states for the oxide is extremely sensitive to the type of material and the condition of the surface.

8. Measured Doppler-shifted laser-induced emission spectra for excited Al atoms sputtered from the surfaces of clean Al and aluminum oxide, as indicated. The emission line shown is the first resonance line. The hollow-cathode lamp spectrum gives a calibration for thermal velocity atoms. Velocity distributions are inferred by convoluting the emission spectra with the Thompson form of the sputtered atom energy distribution.

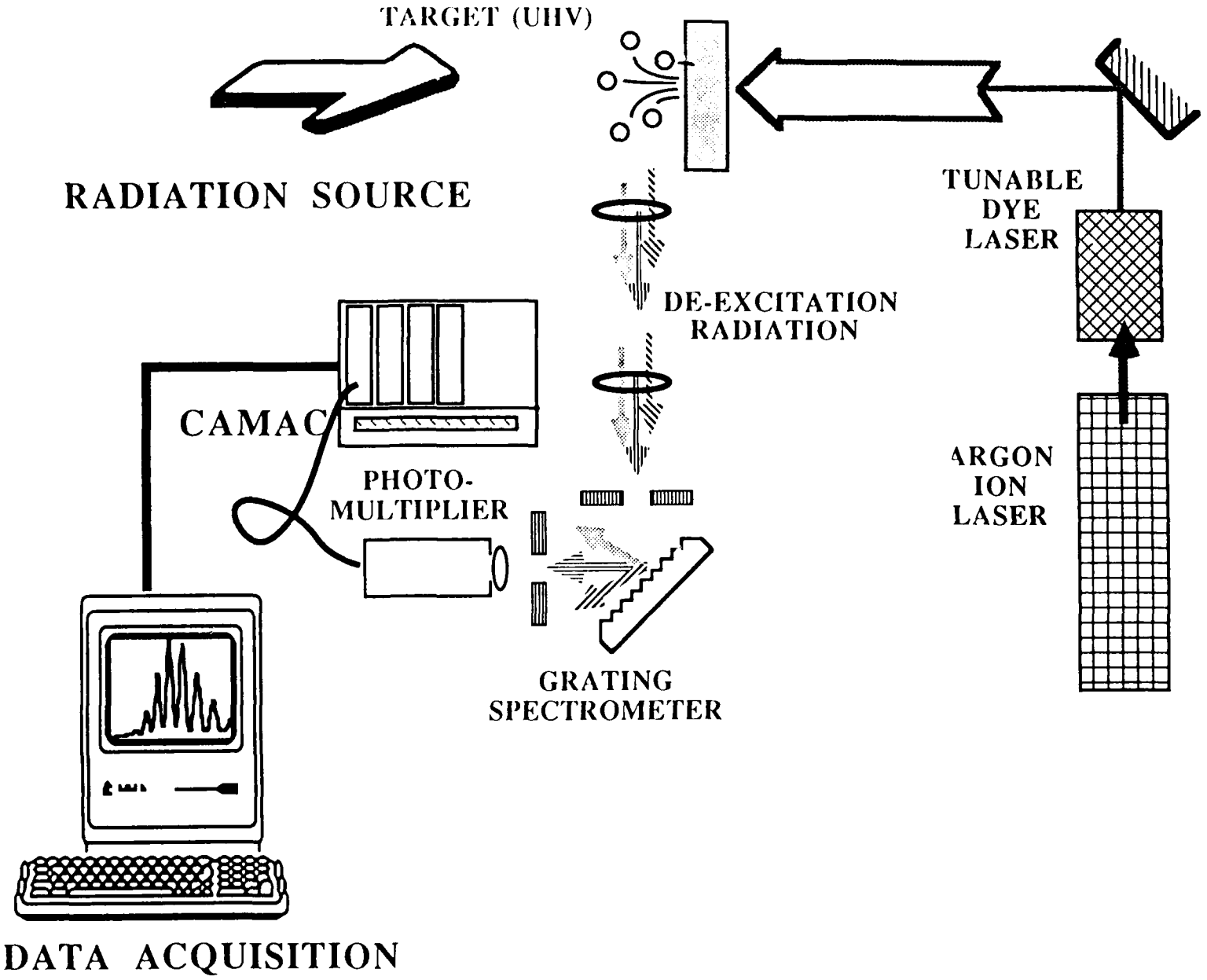
TARGET (UHV)
RADIATION SOURCE
TUNABLE
DYE
LASER
DE-EXCITATION
RADIATION
CAMAC
PHOTO-
MULTIPLIER
ARGON
ION
LASER
GRATING
SPECTROMETER
DATA ACQUISITION

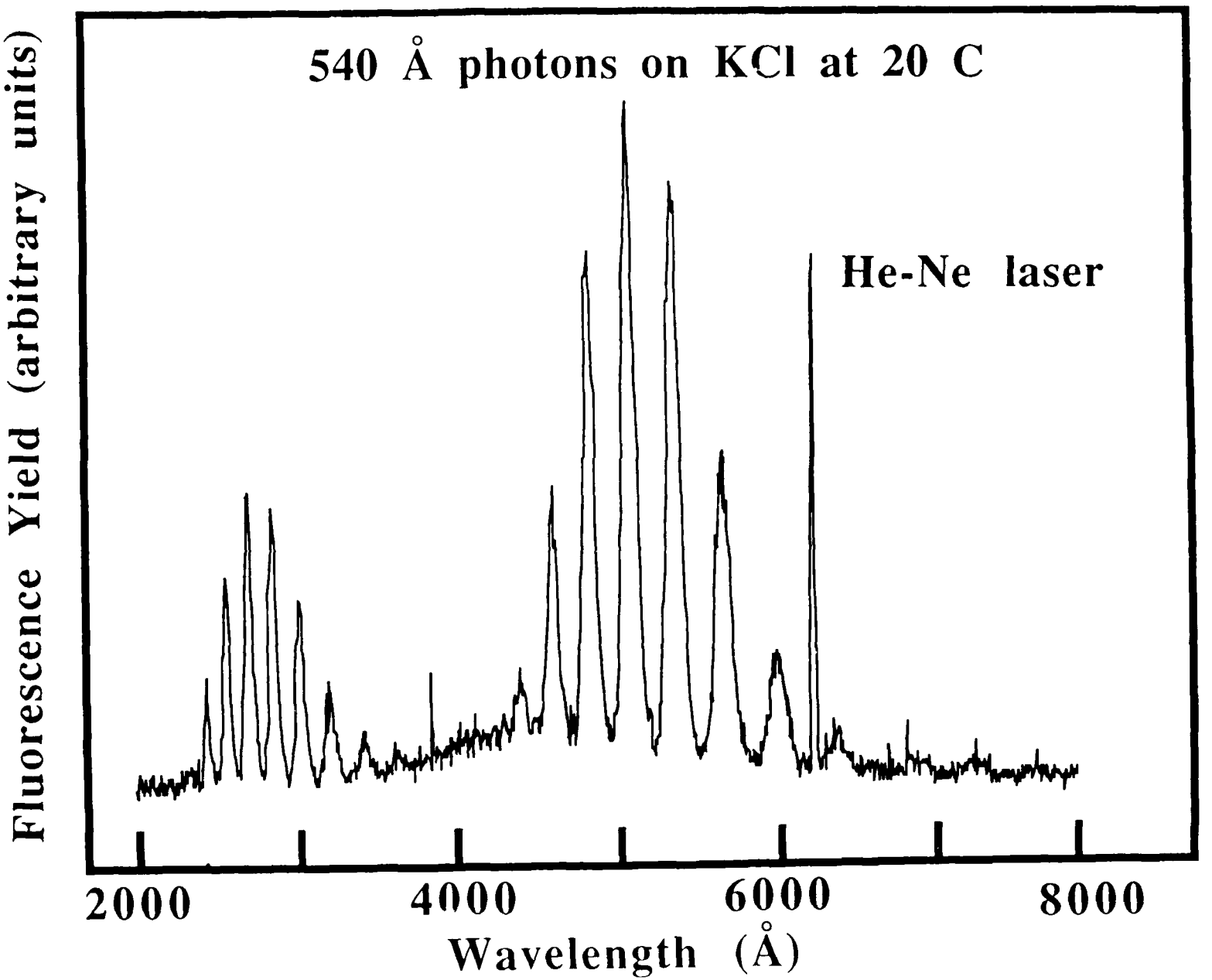
540 Å photons on KCl at 20 C
He-Ne laser
Fluorescence Yield (arbitrary units)
2000
4000
6000
8000
Wavelength (Å)

FIGURE 2

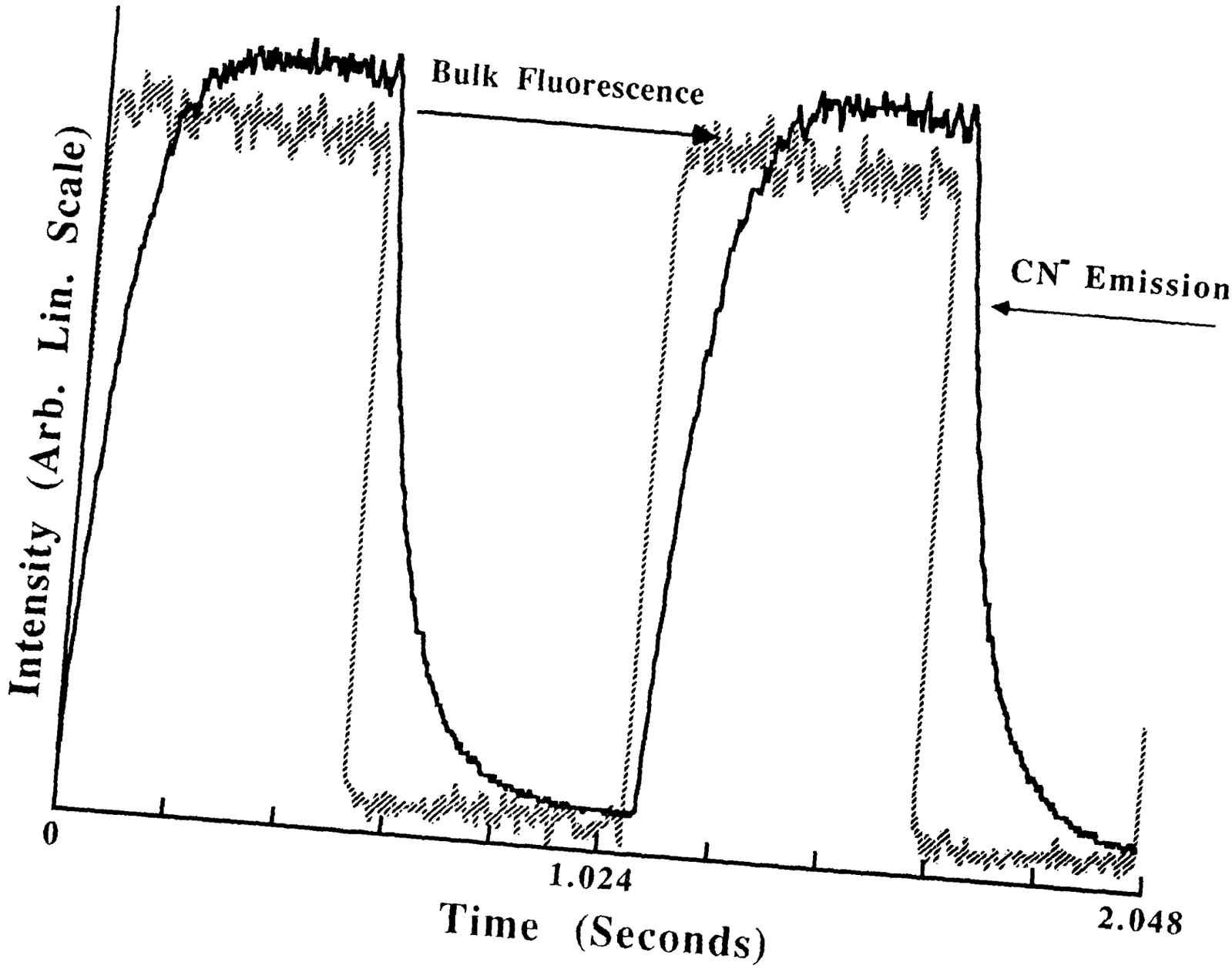
Bulk Fluorescence
CN⁻ Emission
Intensity (Arb. Lin. Scale)
0
1.024
2.048
Time (Seconds)

FIGURE 3

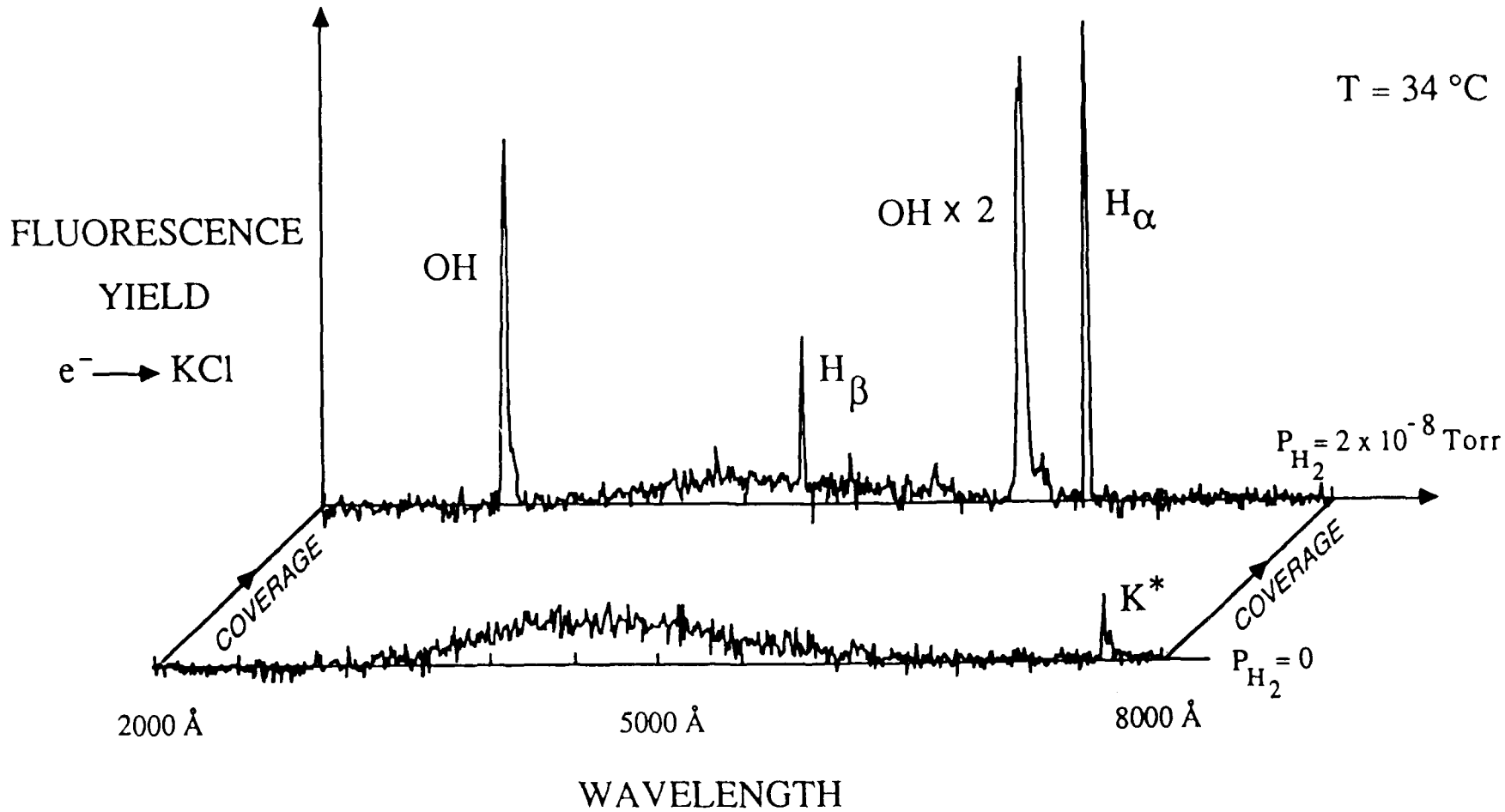
T = 34 °C
FLUORESCENCE
YIELD
e⁻ → KCl
OH
OH x 2
Hα
Hβ
P H2 = 2 x 10-8 Torr
COVERAGE
K*
COVERAGE
P H2 = 0
2000 Å
5000 Å
8000 Å
WAVELENGTH

FIGURE 4

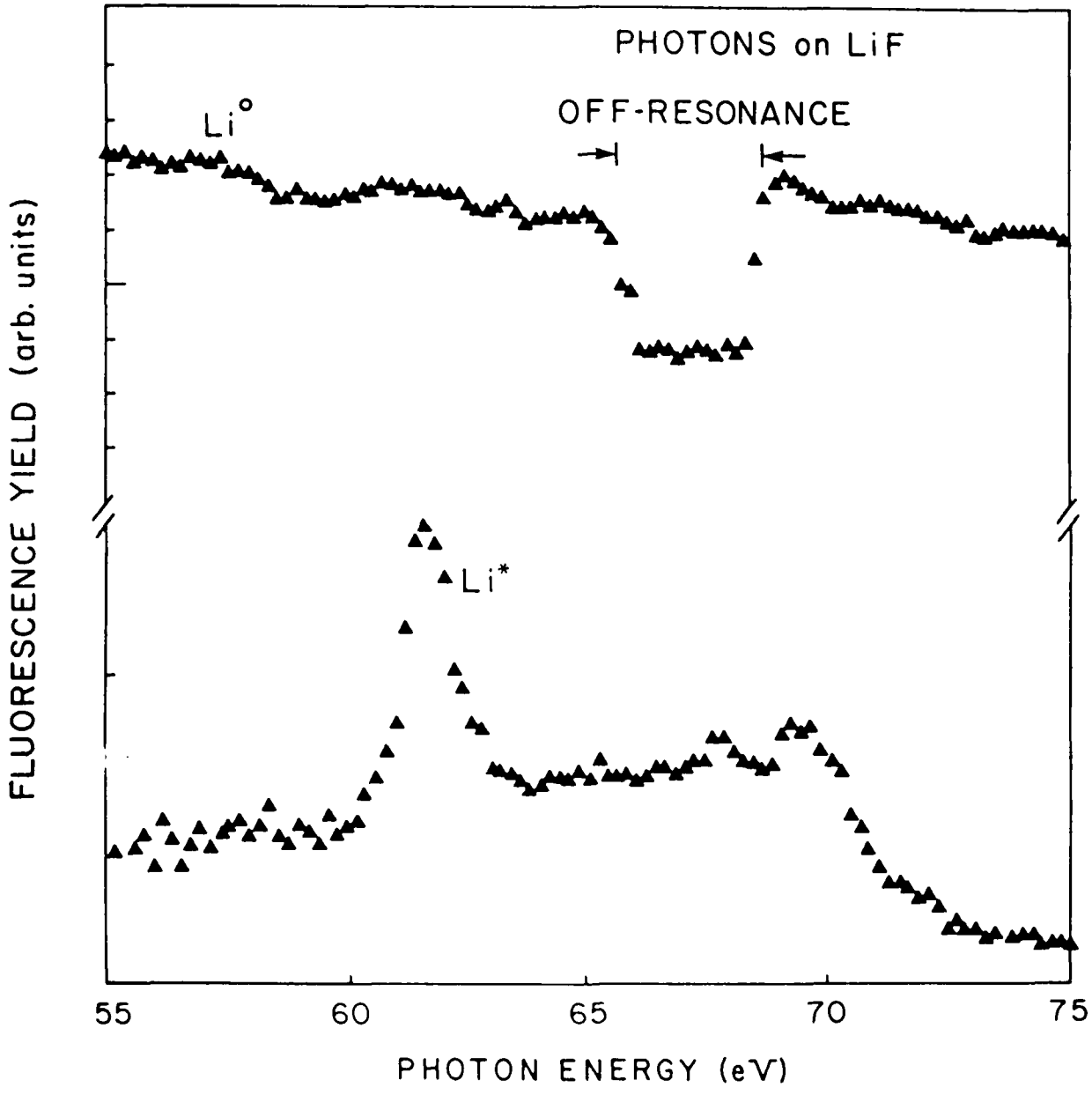
PHOTONS on LiF
OFF-RESONANCE
Li°
Li*
FLUORESCENCE YIELD (arb. units)
55
60
65
70
75
PHOTON ENERGY (eV)

FIGURE 5

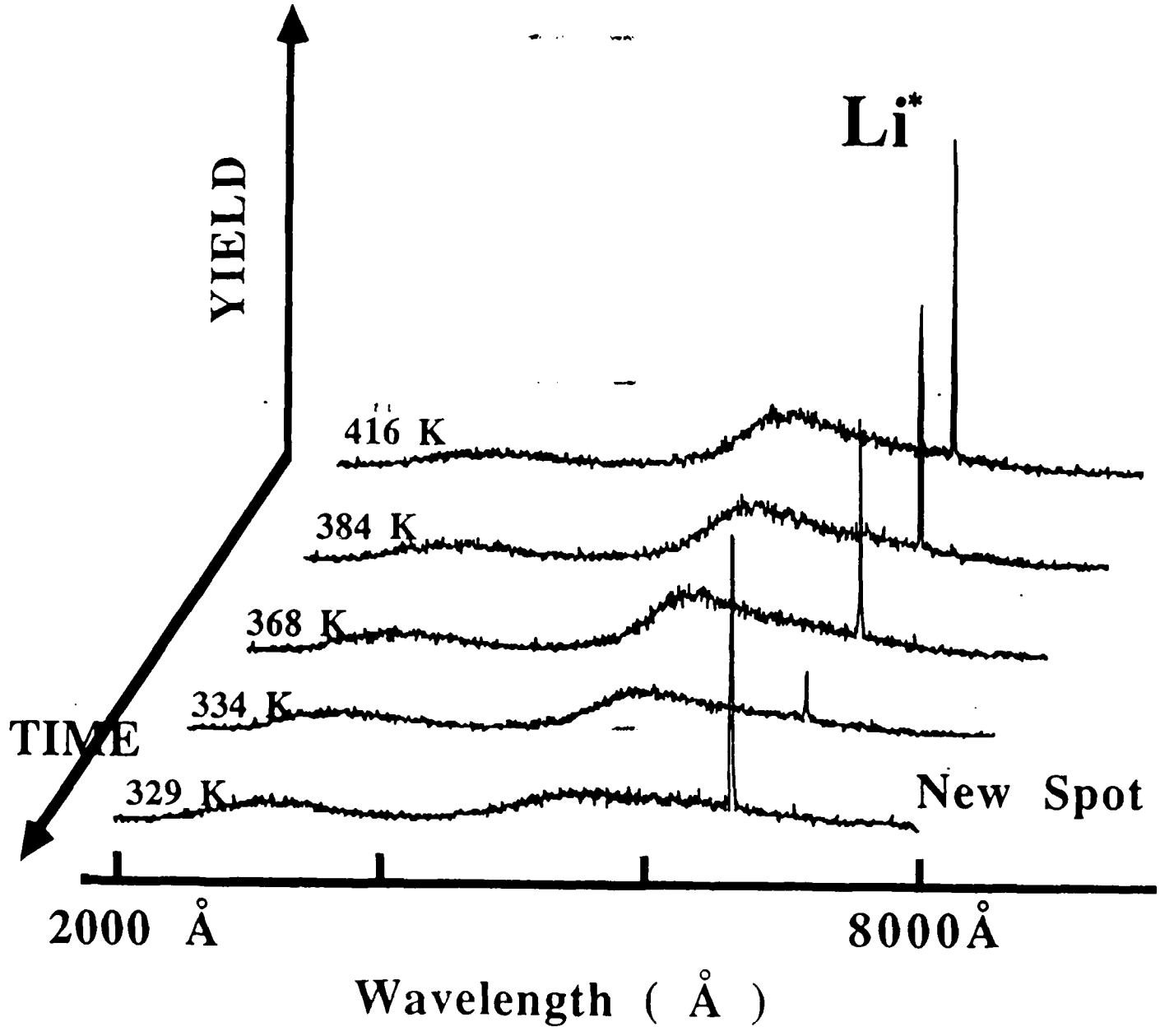
Li*
YIELD
416 K
384 K
368 K
334 K
329 K
TIME
New Spot
2000 Å
8000Å
Wavelength (Å)

FIGURE 6

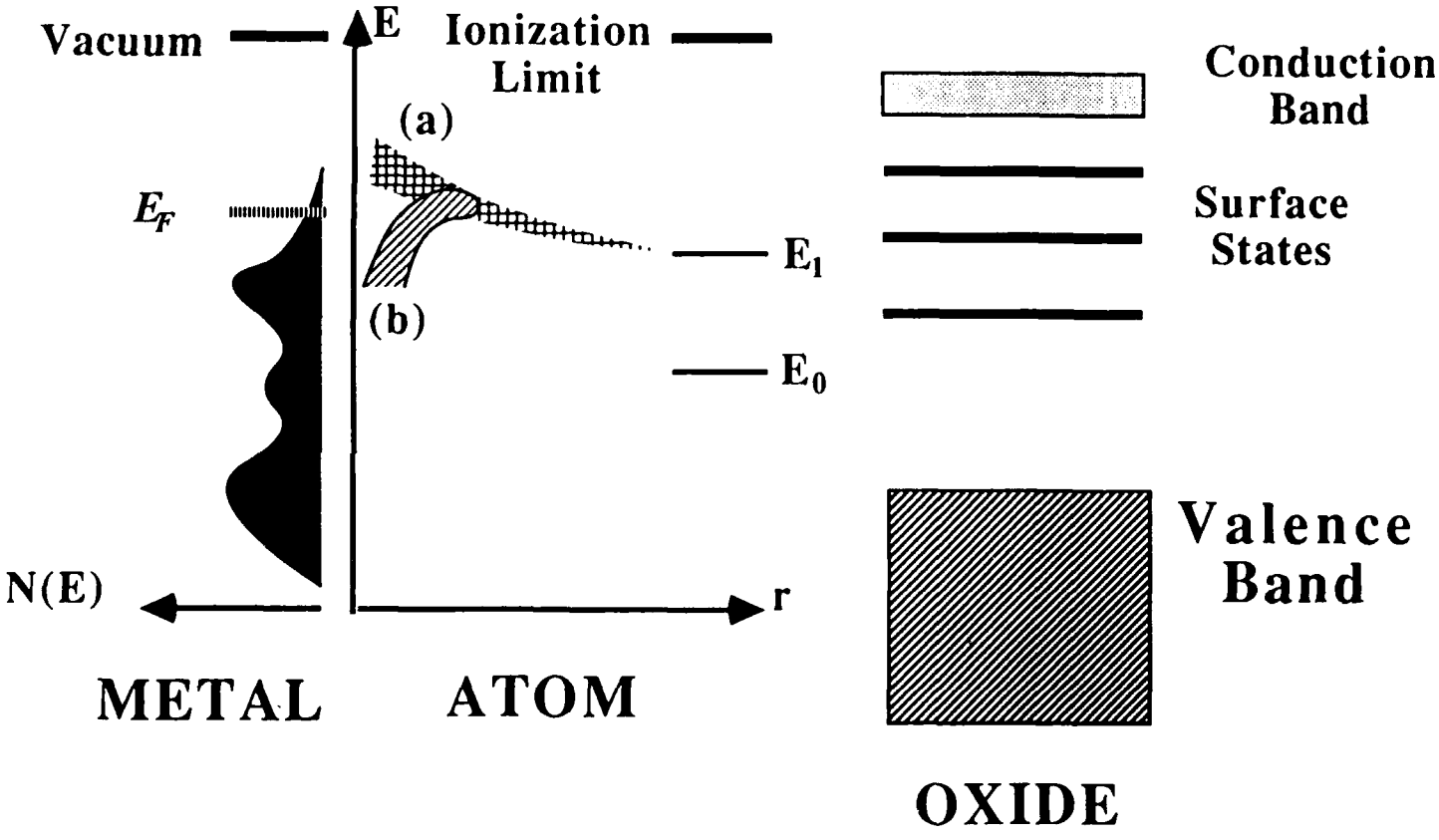
Vacuum
E
Ionization Limit
(a)
E_F
E_1
(b)
E_0
N(E)
r
METAL
ATOM
Conduction Band
Surface States
Valence Band
OXIDE

FIGURE 7

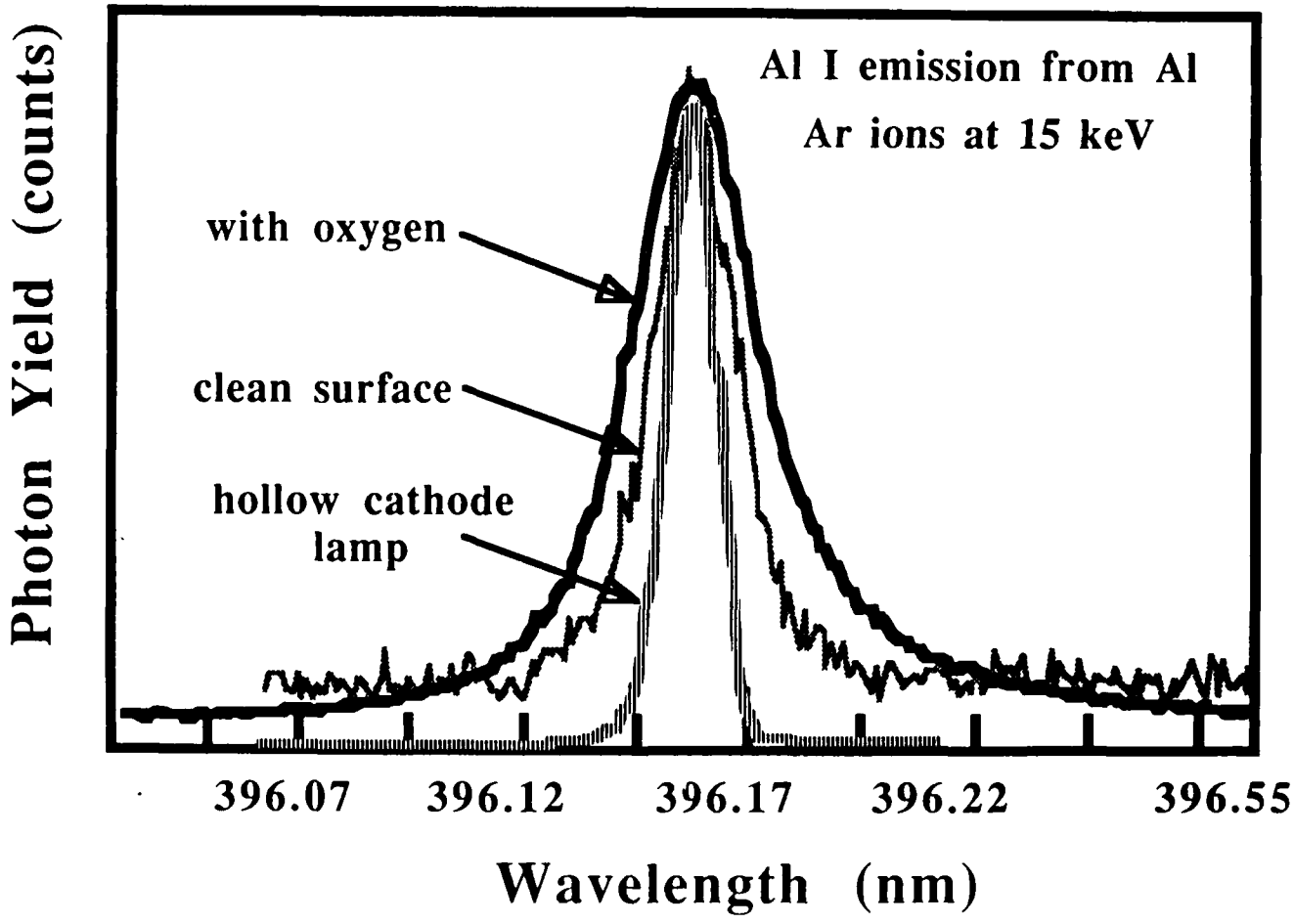
Al I emission from Al
Ar ions at 15 keV
with oxygen
clean surface
hollow cathode
lamp
Photon Yield (counts)
396.07
396.12
396.17
396.22
396.55
Wavelength (nm)

FIGURE 8

Extended Huckel theory for ionic molecules and solids, an application to alkali halides

Yansen Wang*, Peter Nordlander and Norman H. Tolk

The Center for Atomic and Molecular Physics at Surfaces,

Department of Physics and Astronomy

Vanderbilt University, Nashville, TN 37235

Abstract

We present a simple method to incorporate electrostatic forces into the Extended Huckel scheme, thereby extending its range of application to ionic systems. A series of applications to alkali halide molecules and clusters show the importance of including the Madelung energy in such calculations. The amount of charge transfer, the position of the valence levels and the bandgap are found to depend on the inclusion of the electrostatic potential. The calculated bulk and surface electronic structure compares well with experimental findings.

* Permanent address: Department of Nuclear Science, Fudan University, Shanghai, People's Republic of China

1. Introduction

The study of ionic crystals plays an important role in physics. Both from the technological applications of these materials as insulators and from their role as prototype systems for elucidating various physical phenomena. The physical properties of ionic crystals, dominated to a large extent by the electrostatic Madelung potential and the interatomic interaction potentials as well as the crystal fields, can be reasonably well described by purely electrostatic potentials which are relatively easy to model. This fact has stimulated a large number of theoretical and experimental studies. Recently, interest in studying such insulators have been intensified since they have been shown to exhibit a large number of interesting desorption and sputtering phenomena[1]. This is also the stimulation for the present work. Our intention is to develop a formalism whereby a qualitative understanding of how the electronic structure of alkali halides are influenced by *surface defects* and *impurities* in the bulk and on the surface. In this first paper we will present the elements of the method and illustrate its accuracy by an application to alkali halide molecules and large alkali halide clusters.

Central to the understanding of the properties of matter is a knowledge of the electronic structure. Numerous methods have been developed to calculate the electronic structure of crystals. Among the methods one can distinguish ab-initio methods and empirical methods. In the ab-initio methods, the Schrodinger equation is solved with basically no other input than the atomic number of the atoms that constitute the solid. Such calculations are however very extensive and their applications to low symmetry situations such as surfaces or impurities result in very time consuming and complicated calculations. In the so-called empirical methods, one introduces certain parameters and then attempts to model the crystal in terms of these parameters. The justification for the empirical methods can come from agreement with experiment or after ab-initio methods have been applied to similar systems so that a comparison can be made.

There exists in the literature several calculations of the electron structure of the alkali halides. The bandstructure for perfectly periodic alkali halides have been calculated[2-5] and compared favourably with experimental photoemission results.[5-9] Applications to systems with defects, such as surfaces and impurities are very rare. The electronic structure arising from such defects can be strongly modified compared to the bulk bandstructure.[10]

In order to properly model the system one need to incorporate both the extended nature of a solid and the local nature of the *defect*. It is the conflict between those two aspects of a defect in a solid that complicates the description. Furthermore, in the desorption of alkali halides it has been shown that the mobility of certain defects such as F-centers play a crucial role for the yield of particles.[11] In describing a diffusing defect or atom it is crucial to include the surrounding lattice relaxation. To properly estimate the diffusion barriers it is therefore necessary to minimize the total energy over a multi-dimensional coordinate space involving the coordinates of the lattice atoms as well as the diffusing particle. It would be impossible presently to undertake such calculations using ab-initio methods. Instead we propose an empirical method based on the Extended Huckel Theory (EHT) introduced originally by Hoffman.[12]

The EHT method has been used extensively to study both molecules and solids. In particular for covalent and metallic systems the method has been shown to provide quite accurate results. It was pointed out earlier that the EHT method fails to adequately describe ionic molecules due to the neglect of electrostatic forces.[13] Earlier attempts to solved this problem involved the introduction of extra parameters.[14]

In the present paper we suggest a very simple method of incorporating Madelung forces into the EHT scheme. The Madelung forces are calculated within the scheme and no extra parameters are needed. While still an empirical method, the application to alkali halides in the present paper shows that a large number of experimental results can be simultaneously reproduced with only one single parameter. This fact justifies the use of the EHT for ionic molecules and crystals and in our opinion gives sufficient credibility to the method to apply it to situations where there is insufficient experimental information.

In the next section the EHT will be briefly reviewed *and the proposed theoretical improvements elaborated*. Section 3. is divided in two parts. In section 3.1 we show how an application to diatomic molecules and subsequent comparison with experimental results allows the single parameter in the model to be unambiguously determined. We are able to reproduce experimentally obtained equilibrium properties such as the binding energy, the bond length and the vibration frequencies. In section 3.2 we perform calculations of a NaCl clusters of different sizes. We calculate the local and the total density of states. An application to a series of different clusters show good cluster size convergence and that both the bulk and the surface electronic structure can be extracted. Our calculated bandgap and widths of the valence band for the bulk crystal compares well with experimental photoemission results. In section 4. we discuss the implications of our calculation on the interpretation of recent ESD experiments on NaCl.

2. Theory

Extended Huckel theory was proposed as a semiempirical method to obtain reasonable electronic structure for molecules.[12] The idea behind the method is to approximate the self-consistent Hartree-Fock matrix with a simplified one-electron Hamiltonian[15] that contains certain atomic parameters, such as ionization potentials. Subsequent sophistication of the method has taken into account the effects of charge transfer on the ionisation potentials with the requirement that the calculations had to be made self-consistent in the charge transfers.[16]

In EHT the total wave function is expanded in terms of basis functions

$$\psi_i = \sum_p C_{i,p}\chi_p \qquad (1)$$

A LCAO basis set with Slater type orbitals

$$\chi_p = A r^{n-1} e^{-\zeta r} Y_{lm}(\theta,\phi) \qquad (2)$$

is used in the present calculations. The values of the parameters are listed in table 1. The coefficients $C_{i,p}$ satisfies the secular equation

$$\sum_q (h_{pq} - \varepsilon_j S_{pq}) C_{jq} = 0, \; j=1,2 \ldots\ldots; \; p=1,2 \ \ldots\ldots \tag{3}$$

and the energies can straightforwardly be obtained from the determinantal equation

$$\| h_{pq} - \varepsilon S_{pq} \| = 0 \tag{4}$$

The matrix element of the Hamiltonian h_{pq} and the overlap S_{pq} are given by

$$h_{pq} = \int d^3 r \, \chi_p^* \, H \, \chi_q$$

$$S_{pq} = \int d^3 r \, \chi_p^* \chi_q \tag{5}$$

In EHT the fundamental assumption is that the matrix elements of the Hamiltonian can be approximated as

$$H_{pp} = I_p$$

$$H_{pq} = -K_{pq} \frac{I_p + I_q}{2} S_{pq} \tag{6}$$

where the nondiagonal elements are approximated using the Wolfsberg-Helmholtz formula,[17] and I_p is the ionisation potential of the atomic orbital p. The factor K_{pq} entering the nondiagonal part of the Hamiltonian is the only free parameter that enters the EHT scheme. Usually K_{pq} is given a value of 1.75 but since there is no rigorous motivation for such a choice, we will regard K_{pq} as a free parameter. In the result section we will show how an estimate of K_{pq} can be obtained from an application to diatomic molecules. I_p is normally taken to be dependent on the charge present in the orbital so that

$$I_p(Q) = I_p^0 + \gamma_p (Q_p - Q_p^0) \tag{7}$$

where Q_p is the actual amount of charge in orbital p and Q_p^0 is the corresponding amount of charge in the atomic limit.

$$\gamma_p = (A - I_p^0) \tag{8}$$

where A_p denotes the affinity of level p. This form of $I_p(Q)$ then approximates the intra atomic correlation effects with a linear relation between the affinity and the ionisation potential. The charge Q is determined from a Mulliken charge population analysis. The equations (3) - (7) need to be solved self-consistently in the charge transfer and the procedure is sometimes refered to as "self consistent EHT". By populating the lowest orbitals with the available electrons and adding up their energies one arrives at an energy E_{EHT}.

$$E_{EHT}(R) = \min \sum_{p=1}^{N} \varepsilon_p(R) \tag{9}$$

In order to get the total energy one must add an electrostatic term containing the interaction energies of the nuclei.

$$E_{TOT}(R) = E_N(R) + E_{EHT}(R) \tag{10}$$

It has been shown[13] that for diatomic molecules, the nuclear repulsion term takes the form

$$E_N(R) = Z_A\left[\frac{Z_B}{R_{AB}} - \int \frac{\rho_B(r)}{|R_A - r|}\,dr\right] \tag{11}$$

(that is electrostatic energy for the interaction of nucleus A with neutral atom B.)
For ionic systems, this term usually gives a small repulsive contribution to the energy.

In order to get accurate potential energy surfaces it is important to include the repusive closed shell interaction between the inner shells of the atoms. This effect can conveniently be treated within the EHT by including inner shell orbitals.[18] Such a procedure leads to strong repulsive forces at small distances. This repulsion is usually much larger than E_N.

The above method does not include *electrostatic forces* on the electrons. In ionic molecules such Madelung fields can be large. The primary effect of the inclusion of these electrostatic forces is that the total energy of the system will be lowered. Another effect is that the Madelung energy will increase the amount of charge transfer in a molecule. A simple and straightforward way of incorporating such electrostatic forces on the electrons is by adding the Madelung fields to the effective ionisation potentials. This procedure can be justified since the electrons taken from the less

electronegative constituent not will be placed at infinity but at a neighbouring atom. Therefore, the ionisation potentials must be reduced. Similar methods have previously been suggested.[14,19] The Madelung fields can be calculated from the wavefunctions. If a point charge model is assumed for the electrons, the ionisation potential for an orbital p centered on atom A thus take the form

$$I_p(Q) = I_p^0 + \gamma_p(Q_p - Q_p^0) + \frac{1}{2}(Q_p - Q_p^0)\frac{Q_B - Q_B^0}{|R_A - R_B|} \qquad (12)$$

where $(Q_B - Q_B{}^0)$ is the actual ionic charge on atom B. The above equation can be straightforwardly generalized to clusters of atoms.

In the application to large NaCl clusters, a central property of interest is the total density of states (TDOS) and the local density of states (LDOS). These functions can be obtained from the solutions to eq. (3) and the following expression

$$D(E) = \frac{1}{\sqrt{\pi}\,\sigma}\sum_i\sum_p\sum_q C_{i,p}C_{i,q}S_{pq}\exp(-(\frac{E-\varepsilon_i}{\sigma})^2) \qquad (13)$$

For the TDOS the summation is over all orbitals p and q. For the LDOS the summation over p is restricted to the orbitals centered on the particlular atom. The σ is a small damping factor that is added in order to get a smoother curve. In the present calculation σ=0.25 eV.

This simple approximation of electrostatic energies preserve the extreme simplicity of the EHT scheme and incorporates the desired physical effect. The effects of the Madelung potential can be incorporated into the self-consistency scheme at no extra computational expense. In the next section we will give examples of the importance of including this term.

3.1 Results for diatomic molecules

In this section we will apply EHT to alkali halide molecules. The reason for this is twofold. The potential energy curves and the equilibrium properties for these molecules are relatively well known. It is thus possible to test the quality of our calculation by comparing quantities such as

bond lengths, binding energies and vibration frequencies. We also want to determine the parameters K_{pq} defined in eq. (6) above. In principle the form of eq. (6) allows the use of as many parameter as there are orbitals. In order to reduce the number of parameters we make the basic assumption that the parameters K_{pq} only depend on the types of atom that are involved. Thus, for an alkali halide AH, we need three parameters, K_{AA}, K_{AH} and K_{HH} . During the calculations for alkali halides we have, however, observed that it is only the parameter K_{AH} that influences the results, so for simplicity we will assume that $K_{AA} = K_{HH} = K_{AH} = K$. These assumptions leave us with only one parameter, K.

In fig. 1, we show how the potential energy varies with internuclear separation. We also show the contribution from the different factors that enter the total energy. The full curve is the total energy for a NaCl molecule including the Madelung corrections and the core repusion from the inner shells. The dash-dotted curve is the result if the Madelung corrections are omitted as was done in ref. 13. The dashed curve shows the contribution from the E_{EHT} term as defined by eq. (9). We note that the bare EHT term does not provide any repulsion for small intramolecular distances and that in the region of typical bond distances it varies almost *linearly* with distance. The core repulsion provides a sharp repulsive wall *and can be parametrized in an exponential form,*[18] $E_C(R) = Ce^{-kR}$ *(For NaCl we have found that* $C=4.4*10^4$ *eV and* $k=2.78$ *a.u.*$^{-1}$ *accurately describes the core repulsion.)*. The effect of the Madelung potential is to lower the total energy and to provide an extra barrier preventing large internuclear separations. It can be seen in the fig. 2 that the dashed curve slowly approaches the solid line for large distances. The difference between the two curves decreases inversely with distance as can be expected from pure electrostatics.

The calculated equilibrium properties depend on the parameter K. In order to illustrate how K can be determined for the alkali halides, we list in table 2 the calculated equilibrium properties for some different values of K. The bond distance is simply chosen as the separation for which the potential energy is minimum. The binding energy is simply taken as the energy at this position (the zero point energy is neglected). The vibration frequencies have been obtained by numerically

integrating the Scrodinger equation for the relevant ions. The potential energy curves are anharmonic and we also give the anharmonic corrections. The experimental values are also indicated in the table.

It can be seen that, in particular, the vibration frequency is very sensitive to K. In order to understand the dependence of the calculated equilibrium properties on K we recall that the binding of the molecule basically is due to three different physical effects. There is a repulsive part that comes from the core repulsion. This energy contribution varies strongly (exponentially) with intramolecular separation. The E_{EHT} term is due to the covalent interaction between the two atoms in the molecule. This term varies almost linearly with distance in the region around a typical bond distance. Finally the electrostatic contribution to the energy is attractive and varies inversely proportional to the atomic separation. This energy contribution depends on the charge of the ions in the molecule and varies quadratically with the charge transfer. It can be seen from table 2 that an increase in K leads to a decrease in the charge transfer in the molecule. For small K, this decrease in the ionicity reduces the attractive electrostatic contribution to the total energy resulting in a longer bond length and smaller binding energy. The vibration frequency of the molecule mainly depends on the curvature of the potential energy around the equilibrium position. The increase in bond length means that both the curvature of the inner repulsive wall due to the core repulsion and the curvature of the potential due to the electrostatic potential at distances larger than the equilibrium point will be smaller. This is why the molecular vibration frequency decreases with K. As K becomes larger, due to the lower ionicity, the Madelung contribution to the energy is reduced, and the change of the potential energy is determined by a balance between the core repulsion and the EHT term. The core repulsion is roughly proportional to K, but the magnitude of the E_{EHT} term increases slightly *faster than* linear. This means that the binding energy will start to increase and the bond length saturates or starts to decrease with K.

Our procedure for choosing K is to obtain as good binding energy as possible. It can be seen from table 2, that we are able to reproduce all the experimental binding energies, vibration

frequencies and bond lengths. The accuracy is within 2% for NaCl. In view of the extreme simplicity of the method this is a very encouraging result.

In the above applications it has been important to include the Madelung potential. As can be seen from table 2, the charge transfers are large and the Madelung potential therefore plays a significant role. In order to illustrate the effects of the electrostatic potential we have also calculated the equilibrium properties for a NaCl without the Madelung potential. The results are shown in table 3 for some different K. For K=1.8 we see that the charge transfer in the molecule is considerably smaller. The charge left on the Na is 0.21 instead of 0.13. We also observe that the bond length is larger due to the absence of the ionic attraction. The binding energy and the vibration frequency are also smaller as we pointed out in the discussion of ωR fig.1. In order to get reasonable equilibrium properties without the electrostatic force, a rather large K must be chosen. For K=2.10 the calculated equilibrium properties lie within 10% of the experimental values. Such a large K does, however, imply a binding of covalent nature. The overlap charge is 0.47 and only 0.57 electrons is transferred from Na to Cl. Such a small charge transfer seems unrealistic. We have found no experimental information about the charge densities of NaCl molecules but there are experimental results for the charge density distribution of bulk NaCl.[20-21] These results suggest a much larger charge transfer and will be commented upon in the next section.

3.2 Results for NaCl clusters

The previous section showed that we were able to determine the parameters K that enter the EHT scheme. Using the obtained parameters we can now study alkali halide clusters.

For simplicity and computational ease we have only considered perfectly cubic clusters. The crystal facets are thus <100> planes. The smallest cluster we have used contains 2x2x2 atoms . These atoms are all equivalent and there are of course no difference between bulk or surface effects. The second cluster we have used contains 4x4x4 atoms and here we can distinguish both bulk and surface atoms. The largest cluster we have used contain 6x6x6 atoms and here both the bulk and

the surface atoms can be well defined. The 8 atoms in the center of the cluster are considered as bulk atoms and the 4 atoms at the center of the surface are considered as surface atoms. The Madelung fields in a crystal are long range, and for finite cluster sizes it is impossible to reproduce the true Madelung potential. The calculations do however show a convergence in the Madelung potential with increasing cluster size. For our largest cluster (216 atoms), the Madelung potential at the position of a bulk or surface atom lies within 90% of what would have been the case if the cluster would have been infinite using the same charge transfers as for the bulk and surface atoms. This cluster thus gives a good description of both the bulk and the surface Madelung fields.

Even for the largest clusters that we consider, most of the atoms lies in the surface region. The calculated TDOS therefore tend to underestimate the bulk features and should not be taken as the TDOS of a macrocopic NaCl crystal. By also calculating the LDOS for bulk and surface atoms it is however possible to determine the origin and the relative importance of the spectral peaks.

In the fig. 2-4, we show the TDOS and LDOS from bulk Na, bulk Cl, surface Na and surface Cl for the different clusters. The calculated TDOS for our different clusters basically contains three different features. At around -25 eV the Cl(3s) levels form a very narrow band. At an energy around -12 eV there is a large peak which derives from the Cl(3p) levels. This is the valence band of NaCl. The Cl(3s) band and Cl(3p) band are separate. This is because there is a large difference in the ionization potentials for these states, so that there is only small hybridization. The conduction band starts at an energy of -5 eV. This band is essentially formed from the atomic Na(3s) and Na(3p) levels which hybridize strongly. The lower energy part of the conduction band is formed by surface states. This can be seen by comparing the calculated LDOS for Na in the bulk and the surface position. The bulk LDOS starts at around the vacuum level. The surface LDOS starts at -5 eV. An analysis of wave function shows that the surface states are predominantly derived from the Na(3s) states.

By comparing the LDOS from bulk Cl atom and surface Cl atom, it can be seen that the surface valence band lies about 0.25 eV higher in energy. This shift arises because the Madelung potential

is slightly smaller at the surface and because the surface atoms have smaller ionicity. From a comparison of figs. 2-4, it can be seen the basic features of the calculated density of states show relatively small changes as the cluster size is increased. For instance, the bulk bandgap in fig. 3 lies around 9 eV and for the 6x6x6 cluster it has the value 10.3 eV. The width of the valence band is around 2.0 eV for all three clusters. These values are in good agreement with experimental results and will be discussed below. We also find a band of surface states starting at around -5 eV below the vacuum level. There are also experimental indications of such surface states in the bandgap.[10] There are, of course, several properties that depend strongly on the cluster. In particular, the electronic structure of the conduction band above the vacuum level is very sensitive to the size of the cluster. This makes any detailed comparison with experimental data meaningless. For the two largest clusters however, there is a relatively sharp peak at an energy of 3.5 eV above the vacuum level. This feature comes from the bulk, as can be seen from the bulk LDOS and would, therefore, be much more pronounced for an infinite crystal. There are some experimental indications of such a state.[7]

In table 4 we compare the calculated values for the band gap and valence band widths with experimental data and other theoretical calculations. It can be seen that the present calculation give results that agree very well with both other theoretical methods and with experiments. We emphasize that the parameter K that we have used was determined independently from the application to an isolated NaCl molecule.

In table 5 we present results of a calculations without the Madelung effects for the largest cluster. Here we must chose K=2.1 in order to reproduce the equilibrium properties for the NaCl molecule. Such a large K implies a larger conduction band witdh, 3.0 eV instead of 2.0 eV, and a slighly larger bandgap, 11.5 rather than the 10.3 obtained when Madelung corrections were included. These numbers agree less well with the experimental values. A more serious deficiency of the EHT without the electrostatic corrections is the calculated charge transfers are small. It can be seen from the table that the omission of the Madelung potential, decreases the charge transfer from

0.74 to 0.42 electrons and increases the overlap charge from 0.08 to 0.16 electrons. Experimental x-ray diffraction results do however indicate that the charge transfers is larger than about 0.65 and overlap charge is smaller than 0.10 electrons.[20-21] These values are totally inconsistent with the results for the EHT method without the Madelung corrections and show the importance of including this term.

4. Discussion and Conclusions

By using the calculated results for the electronic structure of NaCl crystal, we can qualitatively explain some experimental results from low energy ESD experiments for neutral ground state Na^0 and excited state Na^*.[22]

The experiments show that Na^0 desorb with a thermal velocity distribution. The desorption threshold is very low and there are very few pronounced features in the yield versus incident photon energy. The absence of core excitation thresholds have been taken as an indication that the primary desorption mechanism is a valence excitation. Our calculated TDOS shows that this is a reasonable interpretation. The valence band is derived from Cl(3p) states. The lower part of the conduction band and the surface states derive primarily from Na(3s) states. A valence excitation removes an electron from a Cl ion and places it at a Na(3s) state. The Na atom formed is thus neutral and could in principle desorb with a low (thermal) velocity. Since the surface states fill at least the upper part of the bandgap we would expect a very small threshold for this excitation.

The desorption of Na^* show a completely different behaviour than the ground state Na. The velocity distribution is *hyperthermal* and there are pronounced thresholds at the Na(2s) and Na(2p) core level energies. The fact that Na^* desorb with high velocities and that the thresholds correlate with Na core excitations has been taken as evidence for the desorption mechanism for excited atoms is through a core-hole Auger decay.[22,23] The present calculations show that the Na atoms are almost ionic. The core excitation will thus create a doubly ionized Na. The core-hole can decay with the emission of an Auger electron from a neighbouring Cl atom. This process creates a Na^+

and a Cl^+ ions at neighbouring positions on the surface. The Na^+ may be ejected by electrostatic repulsion. As this ion passes through the surface region it can be easily neutralised either by electrons from occupied surface states or by possible curve crossing transitions in the vicinity of a Cl^- ions.[22]

We have presented an simple procedure to include the effect of the electrostatic potential into the extended Huckel scheme. We have shown that molecular, bulk and surface properties can be obtained and that they compare well with experimental results. This agreement would have been impossible without the inclusion of the Madelung potential in the calculation. The proposed procedure is very simple and can be incorporated into the EHT self-consistent scheme without any extra computational effort.

ACKNOWLEDGEMENT

We are greatly indebted to Prof. K. M. Zhang and Prof. L. Ye for providing the basic extended Huchel program. The authors also acknowledge Prof. M. H. Mendenhall for various help with graphics preparation.

This work was funded by the AFOSR University Research Initiative Contract No. F49620-86-C-0125DEF, by the Air Force Office of Scientific Research under Contract No. AFOSR-86-0150 and by the Office of Naval Research under Contract No. N00014-86-K-0735.

References

1. A comprehensive review of this field is given in the following books: Desorption induced by electronic transitions I, eds. N. H. Tolk, M. M. Traum, J. C. Tully and T. E. Madey, (Springer, Berlin, New York , 1983); Desorption induced by electronic transitions II, eds. W. Brenig and D. Menzel, (Springer, Berlin, 1985)
2. N. O. Lipari and A. B. Kunz, Phys. Rev. B3 (1971) 491
3. R. T. Poole, J. Liesegang, R. C. G. Leckey and J. G. Lenkin, Phys. Rev. B11 (1975) 5190, and references therein.
4. A. B. Kunz, Phys. Rev. B26 (1982) 2056, and references therein.
5. M. R. Norman and J. P. Perdew, Phys. Rev. B28 (1983) 2135
6. D. M. Roessler and W. C. Walker, Phys. Rev. 166 (1968) 599
7. W. Pong and J. A. Smith, Phys. Rev. B9 (1974) 2674
8. R. T. Poole, J. G. Jenkin, J. Liesegang and R. C. G. Leckey, Phys. Rev. B11 (1975) 5179
9. F. J. Himpsel and W. Steinmann, Phys. Rev. B17 (1978) 2537
10. G. Singh and T. E. Galllon, Solid State Commun. 51 (1983) 281; L. Ernst, Solid State Commun. 19 (1976) 311; Nuovo Cimento 398 (1917) 797; Surf.Sci. 176 (1986) L825
11. T. A. Green, G. M. Loubriel, P. M. Richards, N. H. Tolk and R. F. Haglund Jr., Phys. Rev. B35 (1986) 781
12. R. Hoffmann, J. Chem. Phys. 39 (1963) 1397
13. A. B. Anderson and R. Hoffmann, J. Chem. Phys. 609 (1974) 4271
14. K. B. Hathaway and J. A. Krumhansl, J. Chem. Phys. 63 (1975) 4313
15. G. Blyholder and C. A. Coulson, Teoret. Chim. Acta (Berl:) 10 (1968) 316
16. M. Nishida, Surf. Sci. 72 (1978) 589
17. M. Wolfsberg and L. Helmholz, J. Chem. Phys. 20 (1952) 837
18. K. B. Hathaway and J. A. Krumhansl, J. Chem. Phys. 63 (1975) 4308

References

19. S. Larsson and P. Pyykko, Chem. Phys. 101 (1986) 355

20. G. Schoknecht, Z. Naturforschung 12 (1957) 983

21. H. Witte and E. Wolfel, Rev. Mod. Phys. 30 (1958) 51

22. T. R. Pian, N. H. Tolk, J. Kraus, M. M.Traum, J. Tully and W. E. Collins, J. Vac. Sci. Technol. 20 (1982) 555; R. F. Haglund Jr., R. G. Albridge, D. W. Cherry, R. K. Cole, M. M. Mendenhall, W. B. Peatman, N. H. Tolk, D. Niles, G. Margaritondao, N. G. Stoffel and E. Taglauer, Nucl. Inst. Meth. Phys. Res. B13 (1986) 525

23. P. J. Feibelman and M. L. Knotek , Surf. Sci. 90 (1979) 78

Figure captions

Figure 1. Potential energy as function of distance for NaCl. The solid line is the total potential energy with the proposed Madelung corrections. The dashed line is contribution from only the E_{EHT} term. The dash-dotted line is the potential if only the E_{EHT} term and the core repulsions are used (No Madelung). The horizontal axis is the intra-molecular separation measured in a.u. and the vertical axis is the energy in eV.

Figure 2. Calculated TDOS and LDOS for the 2x2x2 cluster illustrated in the upper left corner. The horizontal scale is the energy measured from the vacuum level. The vertical scale is omitted since only the relative peak heights are of interest.

Figure 3. Calculated TDOS and LDOS for the 4x4x4 cluster indicated in the upper left corner. The horizontal axis is the energy in eV measured from the vacuum level and the vertical axis is in arbitrary units and different in the different situations. Note that the valence and core peaks in the TDOS inset have been scaled down by a factor of 5.

Figure 4. Calculated TDOS and LDOS for the 6x6x6 cluster indicated in the upper left corner. The horizontal and vertical axis are defined as in fig. 3.

Note that the valence and core peaks in the TDOS inset have been scaled down by a factor of 5.

Table 1. Atomic wavefunctions and orbital energy parameters.

Element	Orbital	STO ξ [a]	I_p^0(eV) [b]	γ_p [c]
Li	1 S	2.6906	59.84	0
	2 S	0.6396	5.392	4.774
	2 P	0.6012	3.542	3.542
Na	2 S	3.2857	64.26	0
	2 P	3.4009	36.30	0
	3 S	0.8358	5.139	4.591
	3 P	0.8253	3.036	3.036
K	3 S	2.8933	40.17	0
	3 P	2.5752	23.58	0
	4 S	0.8738	4.341	3.840
	4 P	0.7701	2.731	2.731
F	2 S	2.5638	35.850	0
	2 P	2.5500	17.423	14.023
Cl	3 S	2.3561	24.64	0
	3 P	2.0387	12.968	9.348

[a] From E.Clementi , C.Roetti , At.Data Nucl. Data Tables 14,177 (1974).

[b] From A.A.Radzig , B.m.Smirnov , Reference Data on Atoms,Molecules, and Ions, 1985 by Springer-Verlag Berlin Heidelberg and F.Herman , S.Skillman , Atomic Structure Calculations , 1963 by Prentice-Hall ,Inc. Englewood Cliffs New Jersey.

[c] Affinity Potential . A_p are from [b] .

$\gamma_p = 0$ is for the orbital without charge transfer .

$A_p = 0$ for unoccurpied P orbitals .

Table 2. The calculated equilibrium properties for different K.

	K	R_e(a.u.)	E_d(eV)	ω(cm^{-1})	$\chi\omega$(cm^{-1})*	Q(alkali)	Q(halide)	Q(overlap)
NaCl	**1.70**	**4.10**	**6.62**	**443**	**3.5**	**0.06**	**0.94**	0.058
	1.80	4.30	6.41	375	2.9	0.13	0.87	0.17
	1.90	4.40	6.46	345	2.6	0.19	0.81	0.26
	Exp+	4.46	5.72	366	2.1			
KCl	1.80	5.10	5.17	298	2.3	0.05	0.95	0.055
	1.90	5.20	5.10	269	1.8	0.090	0.91	0.12
	2.00	5.30	5.14	255	1.7	0.12	0.88	0.17
	Exp+	5.04	5.02	281	1.3			
LiF	2.00	2.85	8.29	1172	17.5	0.10	0.90	0.15
	2.10	2.90	8.17	1117	15.3	0.14	0.86	0.20
	2.20	2.95	8.20	1107	16.3	0.17	0.83	0.25
	Exp+	2.96	7.91	910	7.9			

* $\chi\omega$ is obtained from fitting $E = \omega(n + 1/2) - \chi\omega(n + 1/2)^2$ to the lowest vibrational levels.

+ From reference [b] in table 1.

Table 3. A comparison of calculations with and without the Madelung correction.

	K	R_e(a.u.)	E_d(eV)	ω(cm^{-1})	Q(Na)	Q(Cl)	Q(overlap)
with Madelung correction	1.80	4.30	6.41	375	0.13	0.87	0.17
no Madelung correction	1.80	4.80	3.75	208	0.21	0.79	0.21
	1.90	4.50	4.31	246	0.28	0.72	0.30
	2.10	4.15	5.81	386	0.43	0.57	0.47
Exp*		4.46	5.72	366			

* From reference [b] in table 1.

Table 4. A comparison of calculated properties of NaCl crystal with other methods..

	Expt.	Theoretical method						
		EHT	LDA[a]	HF[b]	APW[c]	OPW[c]	MB[c]	EMP[c]
Band gap	9.0[d]	10.3	5.6	10.0	8.4	7.4	9.96	(8.97)
Width	2.2 ± 0.2[e] 2.4 ± 0.2[f] 3.1 ± 0.3[g]	2.0	1.77	3.0	1.63	1.35	4.38	1.5

a LDA - local density approximation, Ref.8.

b HFC - Hartree-Fock with correlation correction, Ref.7.

c APW - augmented plane wave, Ref.6.
OPW - orthogonalized-plane wave, Ref.6.
MB - nonrelativistic mixed-basis, Ref.6 . .
EMP - empirical pseudopotential, Ref.6 (8.97) is obtained by fitting expt. data.

d Ref.2.

e Ref.4.

f Ref.5.

g Ref.3.

Table 5. A comparison of calculations with and without the Madelung correction for 6x6x6 cluster.

	K	bulk (6x6x6)				
		Q(Na)	Q(Cl)	Q(overlap)	E_g	E_w
with Madelung correction	1.80	0.26	7.74	0.08	2.0	10.3
no Madelung correction	2.10	0.58	7.42	0.16	3.0	11.5

	K	Surface (6x6x6)		
		Q(Na)	Q(Cl)	Q(overlap)
with Madelung correction	1.80	0.28	7.72	0.10
no Madelung correction	2.10	0.59	7.41	0.18

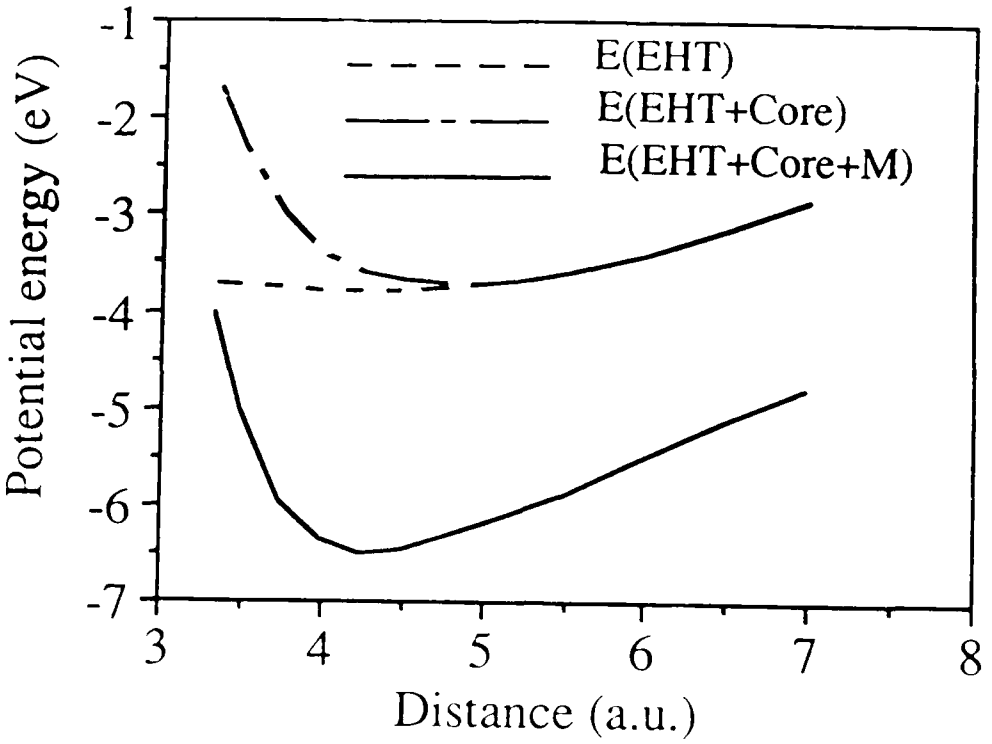
E(EHT)
E(EHT+Core)
E(EHT+Core+M)
Potential energy (eV)
-1
-2
-3
-4
-5
-6
-7
3
4
5
6
7
8
Distance (a.u.)

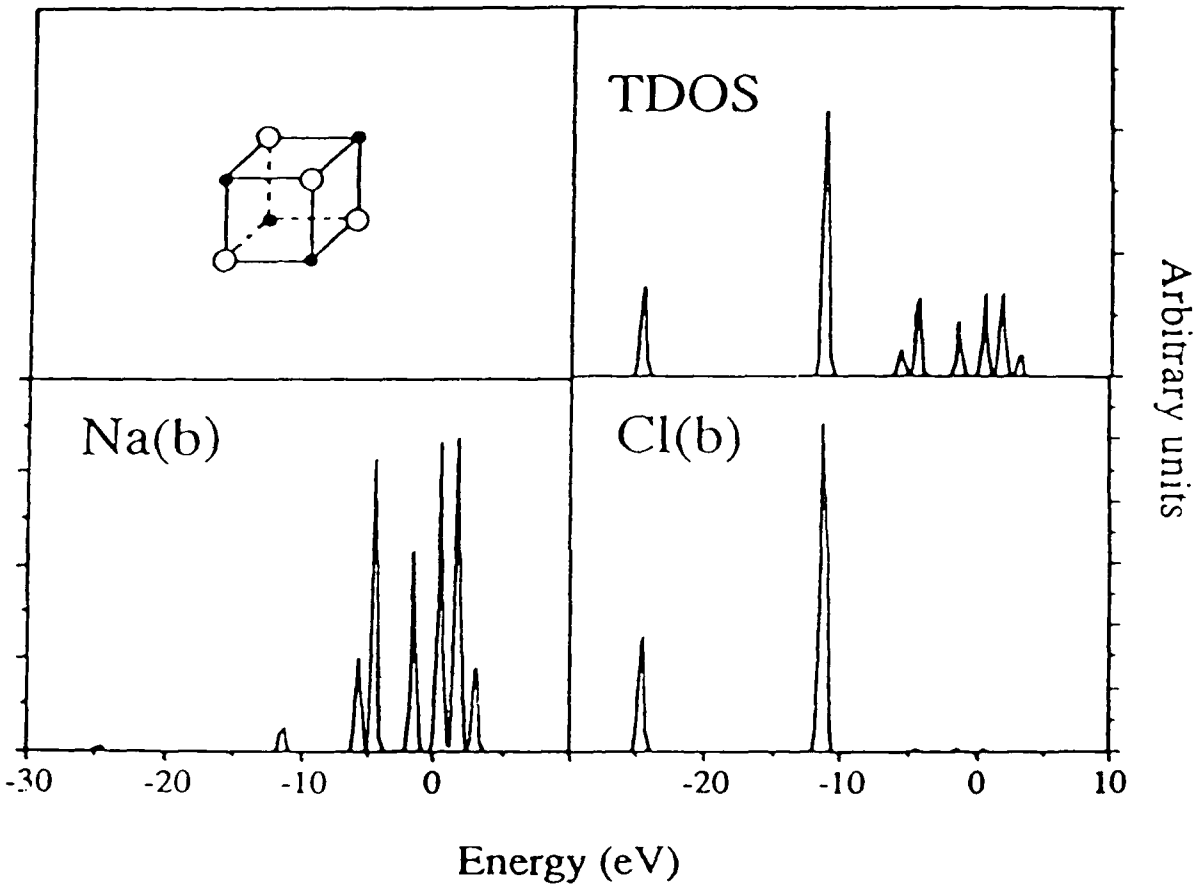
TDOS
Na(b)
Cl(b)
Arbitrary units
-30
-20
-10
0
-20
-10
0
10
Energy (eV)

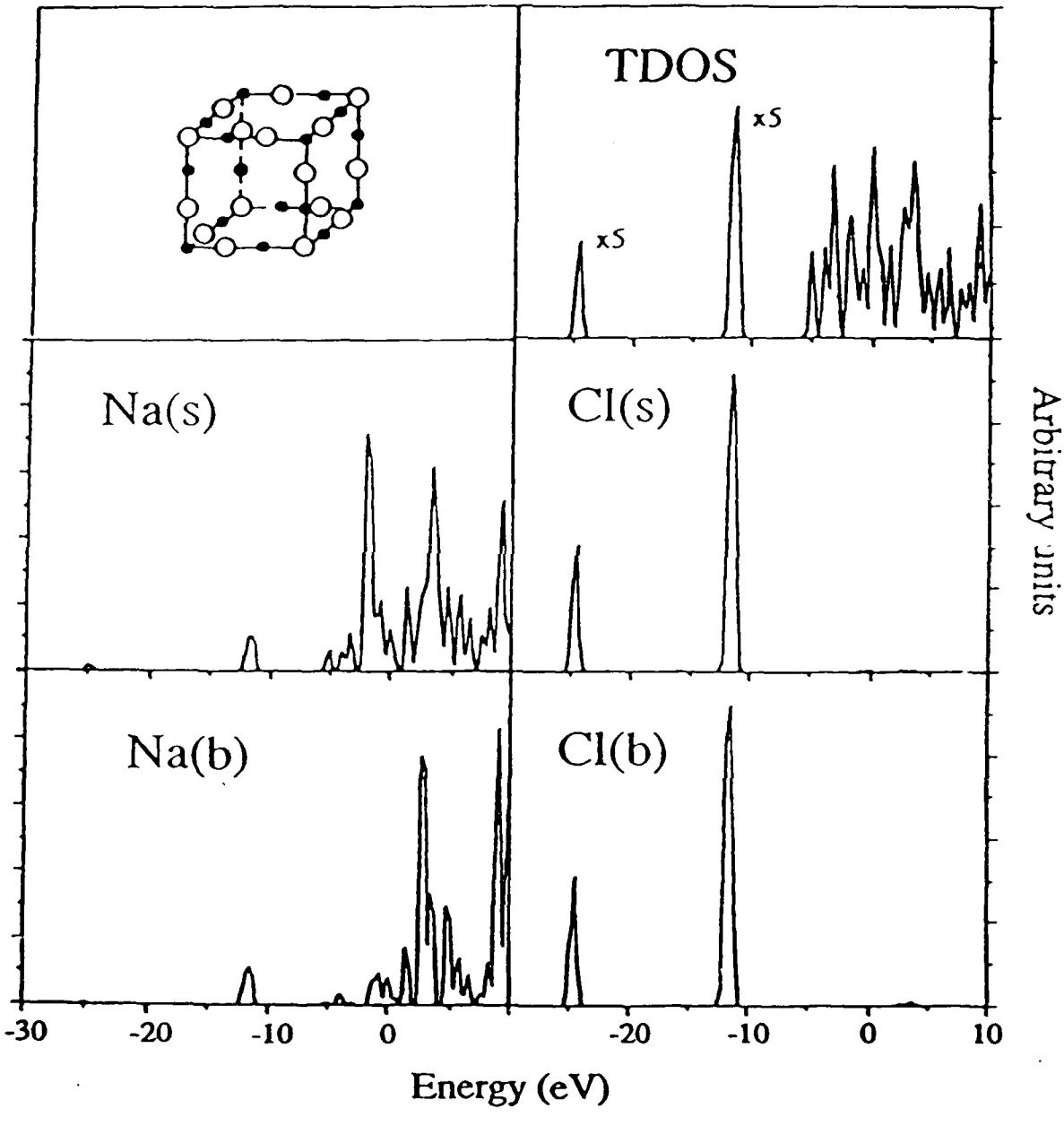
TDOS
x5
x5
Na(s)
Cl(s)
Na(b)
Cl(b)
-30
-20
-10
0
-20
-10
0
10
Energy (eV)
Arbitrary units

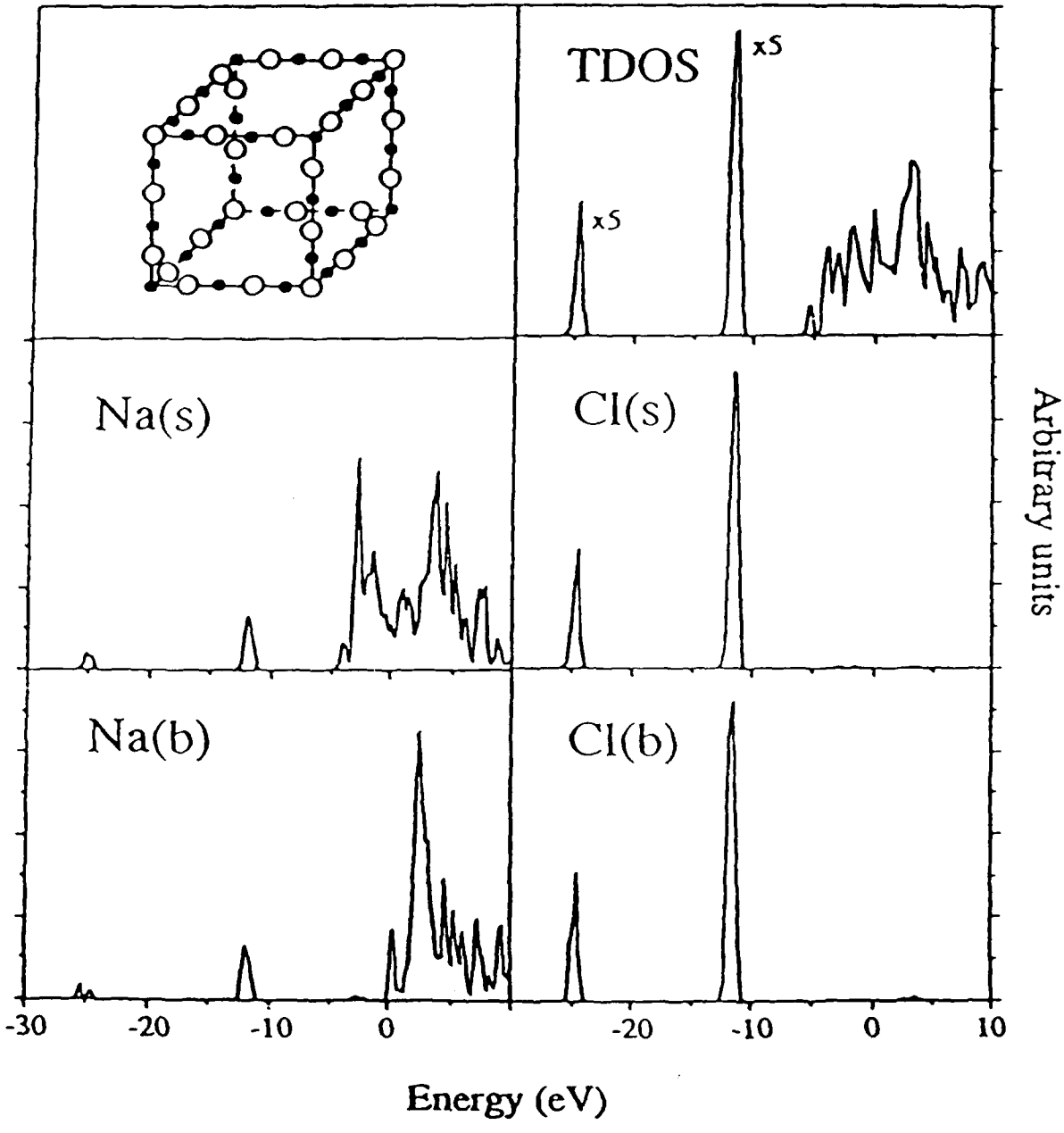
TDOS
x5
x5
Na(s)
Cl(s)
Na(b)
Cl(b)
-30
-20
-10
0
-20
-10
0
10
Energy (eV)
Arbitrary units

New Squeezed ... APS. 55

PSD of Excited Hydrogen from KCl

L.T. Hudson, A. V. Barnes, N. J. Halas, R. F. Haglund, M. H. Mendenhall, P. Nordlander, N. H. Tolk, and Y. Wang

Center for Atomic and Molecular Physics at Surfaces
Department of Physics and Astronomy, Vanderbilt University
Nashville, TN 37235, USA

R. A. Rosenberg

Synchrotron Radiation Center, U. of Wisconsin-Madison
3731 Schneider Dr., Stoughton, WI 53589

1. Introduction

The electronic interaction of hydrogen with surfaces is of fundamental interest in the study of DIET processes. The hydrogen-surface model system provides important information on bond-breaking mechanisms at surfaces which lead to excitation and charge transfer processes and desorption. The ejection of protons from surfaces has been studied previously [1-3]. We present first measurements of fluorescence radiation from excited hydrogen neutrals desorbed from KCl under photon bombardment. The observed temperature and time dependences of the Balmer alpha (H_α) radiation cast light upon the nature and strength of the hydrogen bond on alkali halide surfaces. In addition, the introduction of hydrogen is also seen to dramatically affect the desorption yield of excited-state substrate potassium atoms. This work is an extension of and complementary to that presented in DIET II [4] on the *electron* stimulated desorption of hydrogen neutrals from alkali halide substrates.

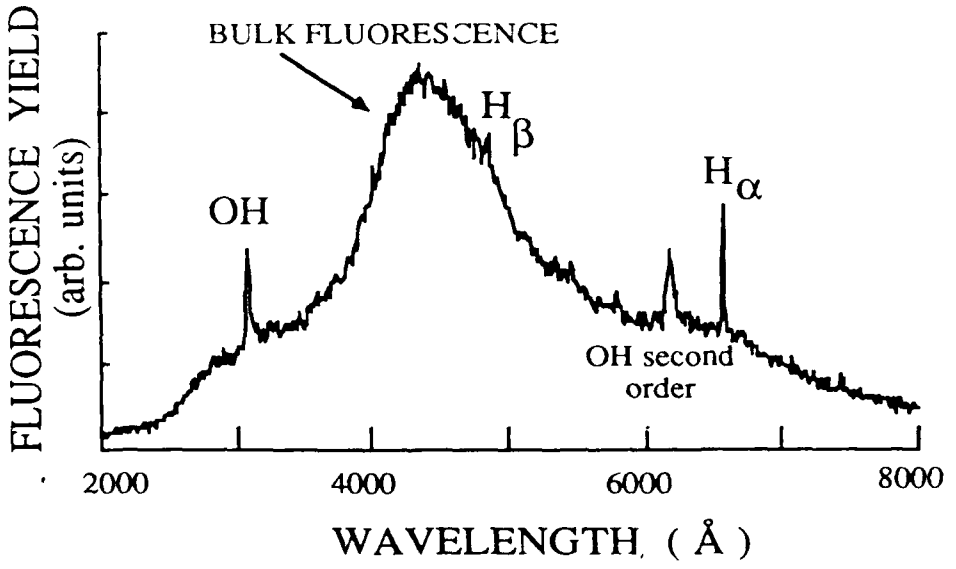

Fig. 1 Fluorescence spectrum upon photon bombardment of KCl dosed with H_2

2. Balmer Radiation from Photon-Stimulated Desorption of Excited Hydrogen

These experiments were performed at the University of Wisconsin's Synchrotron Radiation Center on a beamline equipped with a grazing incidence Brown-Lien-Pruett grating monochromator (20-1200 eV). The photon beam was

incident along the normal of a single crystal KCl sample which had been cleaved in air and baked in vacuum at 400 °C. Fluorescence radiation was collected 90° from the surface normal. The ambient pressure was less than 3 x 10^{-10} Torr throughout these experiments.

Before H_2 was introduced, a spectral scan with incident zero order (undispersed) light showed KCl bulk fluorescence [5], but no hydrogen or potassium line radiation. The sample was then dosed continuously at room temperature at 2.4 x 10^{-7} Torr hydrogen partial pressure. To eliminate scattered light in the 2000 Å - 8000 Å region of detection, an aluminum filter was placed in the zero order beam, thereby passing only photons in the range of ≅ 16 - 70 eV. The fluorescence spectrum is shown in Fig. 1. Our ESD spectra taken under the same conditions exhibit similar features: bulk fluorescence, the Balmer lines of hydrogen, and emission from the hydroxyl radical OH. The precursor surface state of desorbed excited state hydrogen continues to be the subject of ongoing investigations. Apparently some incident H_2 dissociates on the surface to form OH. Other possibilities include HCl, KH, H and H_2 diffusing from the bulk, and hydrogen at defect sites.

The first order (monochromatic) photon "current" through the monochromator was less than 0.1 μA. Using dispersed wavelengths, we detected no hydrogen Balmer radiation. This is consistent with our ESD studies of hydrogen; the H_α signal decreases with electron current and is barely above background at 0.1 μA.

3. Temperature Studies and the Supression of Excited Potassium

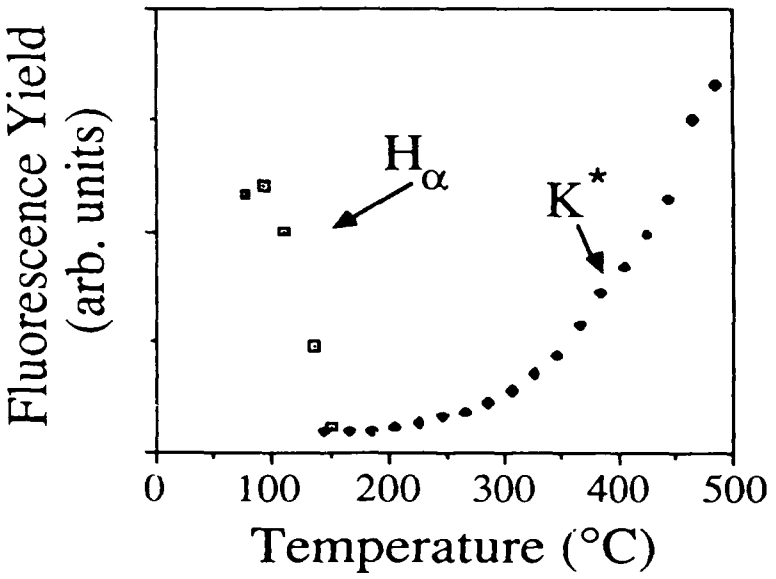

Fig. 2 Comparison of H_α and excited potassium PSD yields vs. temperature.

Figure 2 compares the temperature dependences of the Balmer alpha and excited potassium yields. In each case off-line background was subtracted and then the signal normalized to synchrotron beam flux. The two signals do not share a common absolute ordinate axis, but each signal was pursued until barely above background. The intensity of the H_α line decreases rapidly with temperature and at temperatures over 200°C it was not discernible under these experimental condition We interpret this behavior as an effect of hydrogen coverage. Hydrogen is expected

to bind very weakly to the surface and therefore at elevated temperatures can be entirely removed. The K^* line, however, increases with temperature exhibiting an Arrhenius type behavior. We note that the potassium line only appears after the disappearance of the hydrogen signal. Our ESD studies have further suggested that K^* may be quenched by hydrogen coverage at low temperatures. This is seen in the two spectra of Fig. 3, taken only five minutes apart. The front spectrum resulted from 22 μA of electrons incident on clean KCl at 34° C. The potassium doublet at 7665/7699 Å is clearly visible. Hydrogen was introduced at 2.0×10^{-8} Torr, and, as the rear spectrum reflects, K^* was quenched. Both spectra are plotted with the same ordinate scaling.

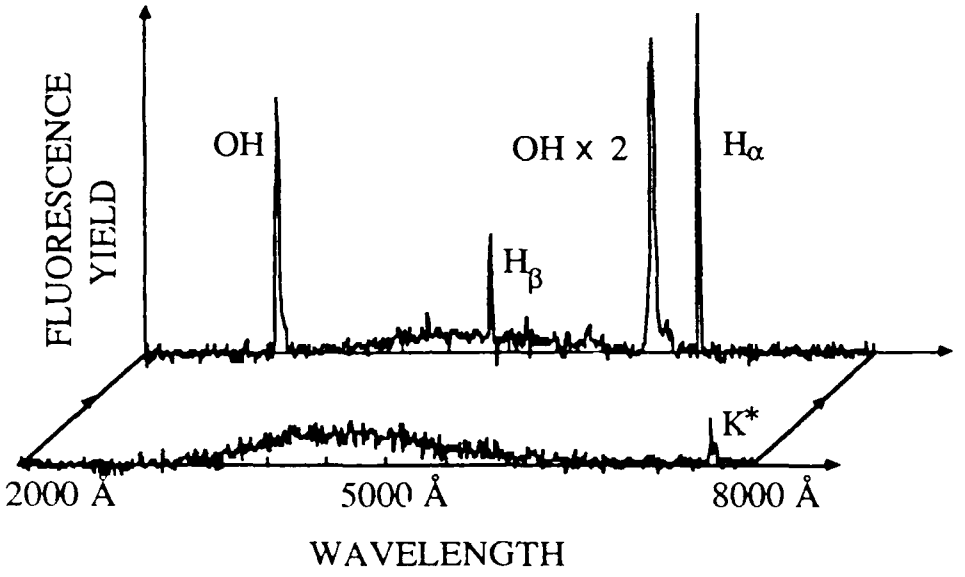

Fig. 3 ESD spectra from KCl before (front) and after (back) dosing with hydrogen. The electron beam was chopped at 100 Hz. On-counts minus off-counts are plotted.

4. Timing Studies

When photons or electrons are first incident on a hydrogen dosed alkali halide sample, we observe a turn-on transient of the Balmer hydrogen fluorescence signal. An example is shown in Fig. 4. It shows the yield of H_α as incident synchrotron radiation is opened to and blocked from the sample. In measurements of this type, the signal generally decays to some nonzero constant value. This corresponds to a steady state between all sources and sinks of hydrogen, the level of which is a sensitive function of H_2 dosing pressure and incident photon flux. The absence of a marked turn-on at T=78 s in Fig. 4 is due to the brief time between the second and third exposures of the sample to synchrotron radiation. These measurements indicate that the equilibration of H_2 on the surface is a slow process ($\geq$ 2s).

5. Summary and Future Work

We present first measurements of fluorescence spectra, temperature and timing dependences of excited hydrogen desorbed from an alkali halide surface. H^* was not detected with the low fluxes of first order light. We also found hydrogen coverage to supress K^* emission at room temperature. Each of the PSD results agrees with our earlier ESD work. This suggests the involvement of common electronic desorption mechanisms. One primary concern is the precursor state of the

desorbing hydrogen. To this end, future studies shall include the dependence of excited and ground state hydrogen yields upon incident photon and electron energies and from substrates with different electronic structure.

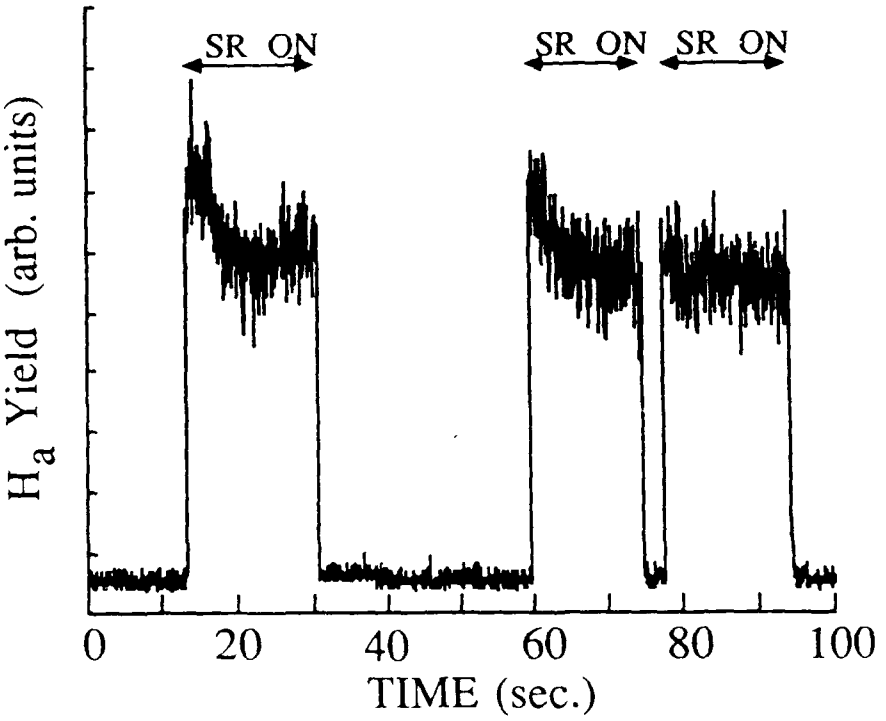

Fig. 4 Turn on transient of H_a. SR = synchrotron radiation.

References

1. M. L. Knotek, V. O. Jones and V. Rehn, Phys. Rev. Lett. 43 (1979) 300

2. T. R. Pian, M. M. Traum, J. S. Kraus, N. H. Tolk, N. G. Stoffel and G. Margaritondo, Surf. Sci. 128 (1983) 31

3. C. C. Parks, D. A. Shirley and G. Loubriel, Phys. Rev. B 29 (1984) 4709

4. N. H. Tolk, R. F. Haglund, Jr., M. H. Mendenhall, E. Taglauer and N. G. Stoffel: in Desorption Induced by Electronic Transitions DIET II, ed. by W. Brenig and D. Menzel (Springer, Heidelberg, 1985) 152

5. A. I. Bazhin, E. O. Rausch, and E. W. Thomas, Phys. Rev. B 14 (1976) 2583

Optical Radiation from Electron, Photon and Heavy Particle Bombardment of Lithium Fluoride and Lithium-dosed Surfaces

N. H. Tolk, R. G. Albridge, A. V. Barnes, R. F. Haglund Jr., L. T. Hudson,
M. H. Mendenhall, D. P. Russell, J. Sarnthein, P. M. Savundararaj and P. W. Wang

Department of Physics and Astronomy
Center for Atomic and Molecular Physics at Surfaces
Vanderbilt University, Nashville, TN 37235, USA.

1. Introduction

Comparative studies of electron, photon and ion bombardment of the same sample surface probe the various channels through which incident particle energy is dissipated, often leading to desorption. Electron or photon irradiation of alkali halides results in the swift ejection of halide atoms, leaving behind an enriched alkali metal surface from which the alkali atoms thermally desorb. Ion bombardment involves momentum transfer as well as electronic mechanisms, which results in a different surface stoichiometry at the time of desorption. This study explores how the degree of surface metallization influences the choice of the final excitation state of the desorbing particle. An important way to study the desorption products is to monitor the characteristic spectral radiation from the de-excitation of ejected species [1]. In this paper we report recent results of this type. Measurements were made to compare the desorption of excited state neutral lithium from lithium fluoride by electron, photon and ion bombardment and from lithium-dosed tungsten and lithium-dosed glass by electron and photon bombardment.

2. Experimental Results

A. PSD of Li* from Lithium Fluoride

Photon irradiation studies were performed at the University of Wisconsin's Synchrotron Radiation Center at Stoughton, Wisconsin. Zero order visible and ultraviolet photons from the two meter grazing incidence Brown-Lien-Pruett monochromator (20 - 1200 eV) were incident along the surface normal upon a LiF crystal which was previously cleaved in air and baked under UHV conditions at 600°C.

The photon detection system included a 0.3 meter McPherson 218 monochromator which has a resolution of 26.5 Å at 1 mm slit width, a photo-multiplier in a cooled housing, and a multi-channel analyzer or CAMAC crate for data acquisition. We scanned the spectral region of 2000-7000 Å using a 1200 lines/mm grating blazed at 5000 Å. Fluorescence radiation was measured at 90° to the surface normal. The base pressure in the experimental chamber was less than 3×10^{-10} Torr throughout these experiments.

The spectrum obtained from irradiation of lithium fluoride (Fig.1) at room temperature shows the first resonance line of lithium at 6708 Å and two broad continua centered at about 3200 Å and 5600 Å. These continua are due to bulk luminescence and scattered light from the irradiating zero order photon beam. No other line radiation was detected above the background noise. We estimate that other spectral lines have maximum intensities that are at least a factor of 100 less intense than the intensity of the observed resonance line.

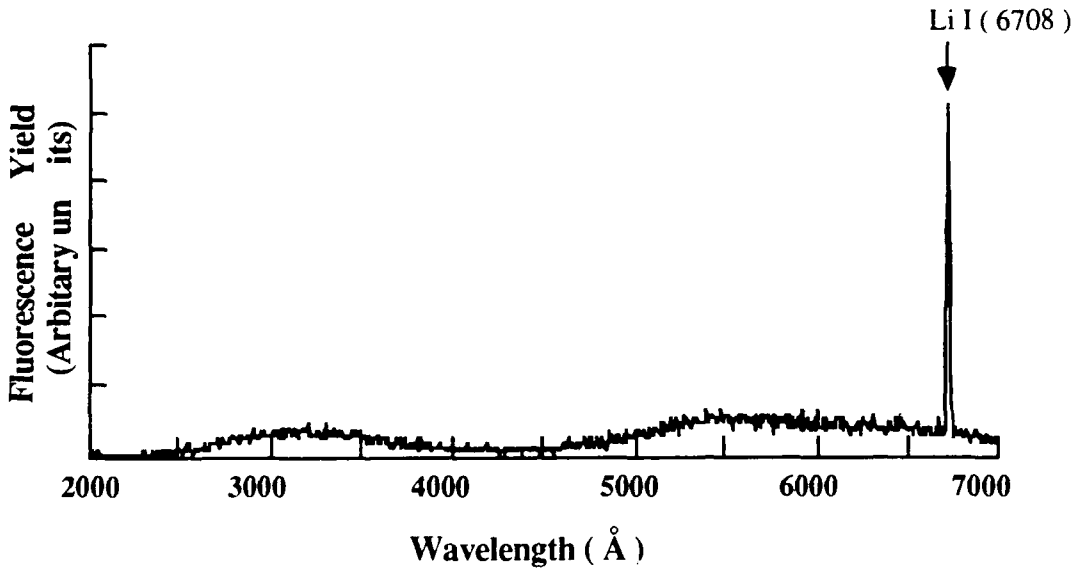

Fig.1 Fluorescence spectrum from photon irradiation of lithium fluoride

B. Ion Bombardment of Lithium Fluoride

In further studies, we irradiated a similarly prepared lithium fluoride sample with a 9 keV H_2^+ beam from a Colutron ion source. The de-excitation of the desorbed species from the surface and the bulk luminescence were monitored by the signal detection scheme discussed in part A. The ion bombardment was performed at room temperature. Note that in addition to the first resonance line of lithium 6708 Å (2p-2s) there are lithium lines at 3233 Å (3p-2s), 4603 Å (4d-2p) and 6104 Å (3d-2p). The relative intensities of the excitations originating at $n \geq 3$ after correcting for detection system efficency are greatly enhanced compared to arc discharge data. This indicates a preferential population of these higher excited states via some unknown mechanism.

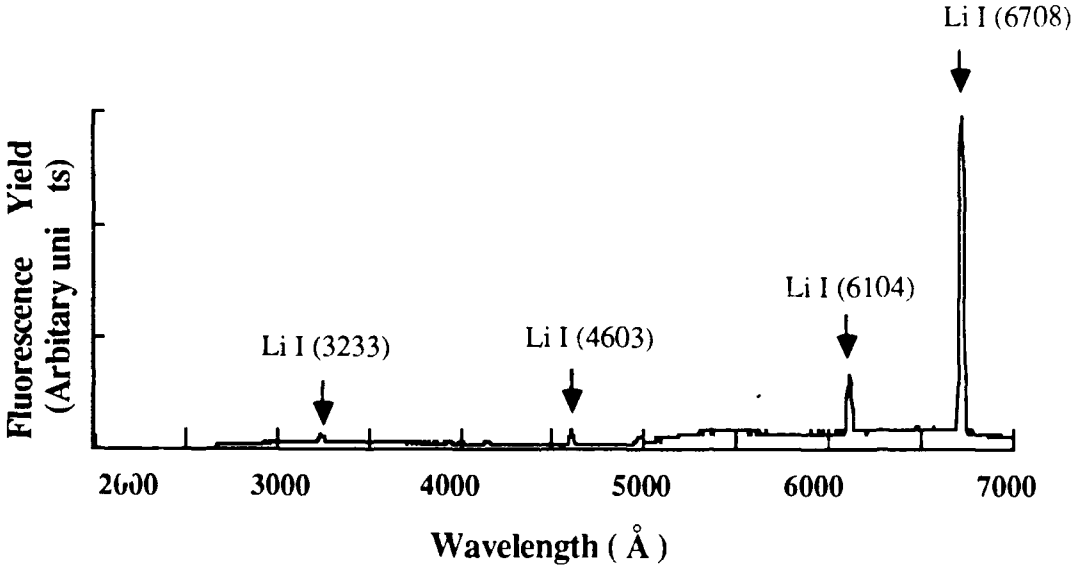

Fig 2. Fluorescence spectrum from 9 keV H_2^+ bombardment of lithium fluoride

C. ESD of Li* from Lithium Fluoride

It is well known that electron bombardment of alkali halides can desorb generous amounts of excited alkali atoms [2]. A typical optical spectrum taken at room temperature is shown in Fig. 3. Here, a 300 eV electron beam was incident along the surface normal on a single crystal LiF sample which had been cleaved in air and baked under UHV conditions at 600°C. Fluorescence radiation was collected at 90° from the surface normal; the ambient pressure was less than 10^{-9} Torr. The 6708 Å lithium resonance line is clearly visible as well as a trace signal of hydrogen Balmer alpha at 6563 Å. As in the photon irradiation studies, no other excited lithium lines were observed above the background noise and would have to be at least a factor of 100 weaker than the observed line.

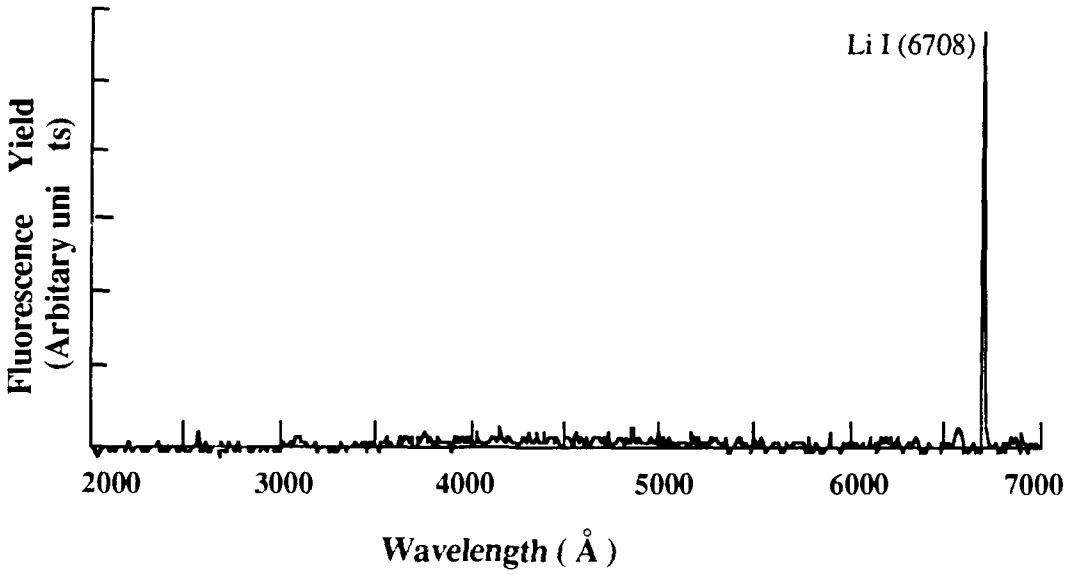

Fig 3. Fluorescence spectrum of LiF bombarded with 300 eV electrons

D. Lithium Metal Studies

We have observed energetic electron and photon induced desorption of excited lithium neutrals from a thickly dosed lithium film, which was possibly contaminated with oxygen. The experimental setup was similar to that described above. In vacuum we dosed a soda-lime glass plate by means of a SAES lithium getter. Since the dosed film was opaque (it appeared shiny gray), we conclude from the attenuation length of light in lithium that it had a thickness of at least 1000 Å. At a pressure of 10^{-9} Torr we observed electron stimulated desorption of Li* (6708 Å) within 5 minutes of deposition. The electron beam current was 80 μA and energy 300 eV. Figure 4 shows a fluorescence spectrum taken with the sample at room temperature. The spectrum represents 200 signal integrations over five minutes at 1 mm slit width. Previously observed bulk fluorescence of the glass plate had vanished; the plate is viewed as a mechanical support only. The power density of the electron beam was 10 mW/mm^2 which does not cause appreciable heating or thermal evaporation of the lithium layer.

In another study, we used a tungsten substrate. The base pressure was 10^{-11} Torr, thus the environment was much "cleaner" than that for the study described above. The lithium resonance line was not seen until several hours after the dosing. Subsequently, zero order Synchrotron radiation was used to desorb Li*. The results show exactly the same

characteristics as those for electrons.

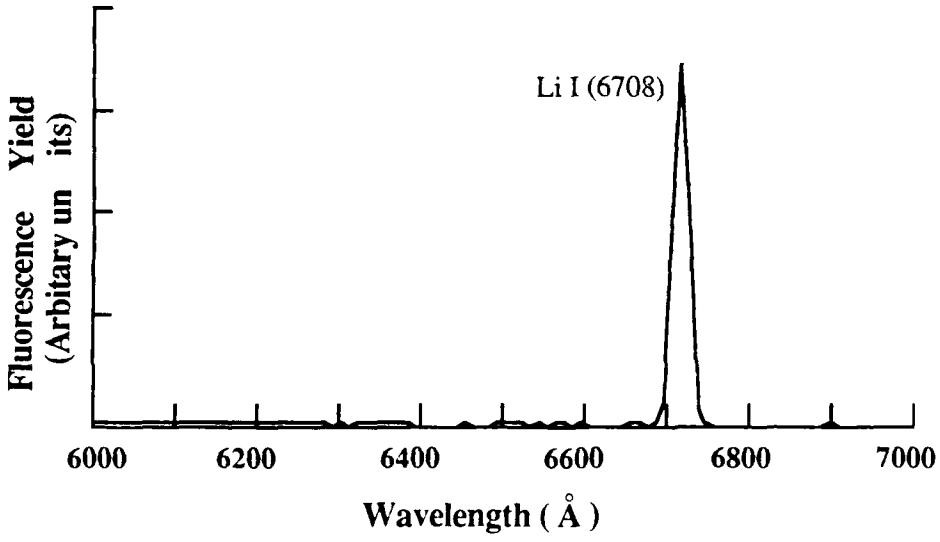

Fig 4. ESD of Li* from a lithium layer dosed on glass

3. Discussion

In the DIET experiments (Figs. 1, 3 and 4), we observe only the first lithium resonance line. These contrast with the ion sputtering results of Fig. 2, where emissions from higher excited states are observed. We therefore propose the following picture.

It has been well established that the surface does not remain stoichiometric during electron or photon induced desorption of alkali halides at room temperature. The halide atoms desorb much faster leaving behind an alkali enriched surface [3]. In our ESD and PSD studies of LiF, we thus expect to have excited lithium atoms desorbing from a surface enriched with lithium metal by a previously discussed mechanism [4]. In the desorption studies of dosed lithium, excited lithium is also desorbing in the presence of a metallic lithium surface. In this case, contamination provides centers of localization for the electronic energy deposited by the incoming electrons or photons leading to desorption of lithium.

We now account for the fact that only the 2p-2s transition is observed in the DIET experiments: as Li* leaves the surface it interacts with the band structure of lithium metal surrounding the desorption site (Fig. 5). Electrons in the 2p level cannot resonantly tunnel to the filled levels of the metal below the Fermi energy. Excitations of Li* to the $n \geq 3$ levels may resonantly ionize (10^{-15}s) faster than de-excitation (10^{-9}s). Hence, higher transitions are supressed and we observe only the single 2p-2s line in our spectra.

In contrast to this, we do see higher excited states of lithium upon ion bombardment of LiF. Ion sputtering is much more violent than desorption induced by electronic transitions and proceeds through momentum exchange processes. Under ion bombardment, the surface is more rugose and a lithium metal band structure will be much less developed. The desorbing Li* departs with a higher velocity and resonant de-excitation of higher excited states by interaction with the band structure is less probable. Consequently, we are able to observe radiative transitions from the higher excited states of lithium.

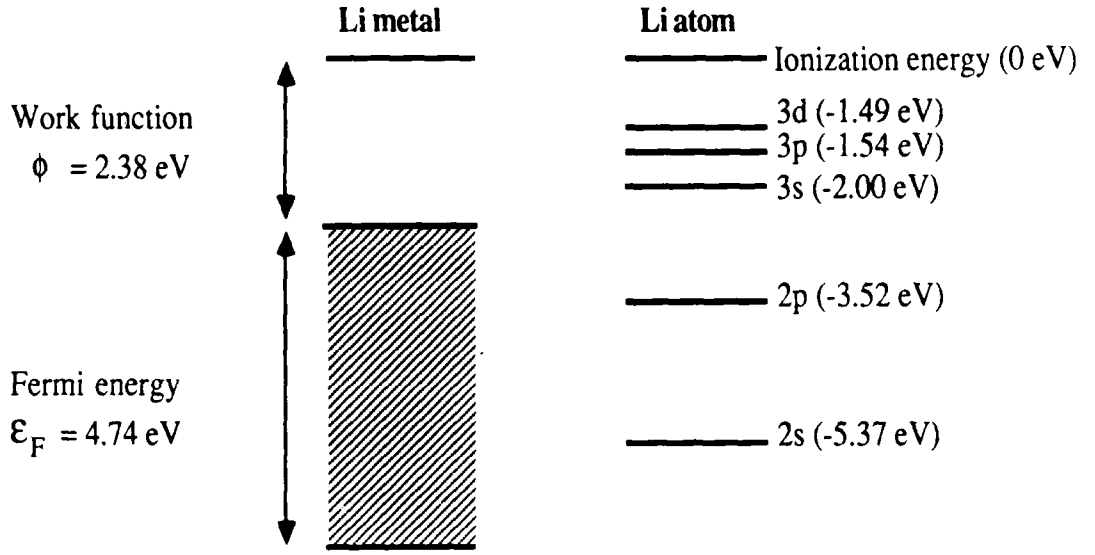

Fig. 5. Schematic energy level diagram of a lithium atom near lithium metal.

4. Conclusions

In conclusion, it is clear that desorption induced by electrons and photons proceeds by different mechanisms than does desorption induced by ion bombardment. For the ESD and PSD processes occuring at LiF and lithium-dosed surfaces at room temperature, the presence of a metallic rich surface provides a channel for de-excitation of excited lithium states which are above the lithium metal Fermi energy. This quenching of the higher excited lithium lines is less likely when the sample is excited by ions. Further studies will include careful surface analysis of the stoichiometry of lithium fluoride during ion, electron and photon irradiation. The ultimate aim of these studies is to characterize the final states of all the desorption products and the extent to which they are influenced by the surface, exciting beam and secondary processes.

This work was supported in part by the Office of Naval Research under contract no. N00014-86-K-0735, by the Air Force Office of Scientific Research under contract no. AFOSR-86-0150 and by an AFOSR University Research Initiative contract no. F49620-86-C-0125DEF.

References

[1] N.H. Tolk, I.S.T. Tsong, and C.W. White, Analytical Chemistry, 49, 16 (1977)

[2] N. H. Tolk, L. C. Feldman, J. S. Kraus, R. J. Morris, T. R. Pian, M. M. Traum and J. C. Tully: in Inelastic Particle-Surface Collisions, ed. by E. Taglauer and W. Heiland (Springer-Verlag, Heidelberg, 1981) p. 112

[3] P. D. Townsend, R. Browning, D. J. Garlant, J. C. Kelly, A. Mahjoobi, A. J. Michael and M. Saidoh, Radiation Effects, 30, 55 (1976)

[4] T. R. Pian, N. H. Tolk, M. M. Traum, J. Kraus and W. E. Collins, Surf. Sci., 129, 573 (1983)

product techniques dealing in vector-matrix-vector multiplication and triple matrix multiplication. A microcomputer-based optical processing system for digital-optical computation is utilized. Programmable magnetooptic spatial light modulators (MOSLMs) are used to generate the time sequence input signals and the bilinear systolic engagement matrix. A CCD detector is in the output plane as a time integrator for the systolic processing. The proposed hybrid optical architectures offer high-data-rate and high-accuracy processing capabilities.

Experimental demonstrations for the bilinear transformations and multiple matrix multiplication are also given. **(12 min)**

THI4 Optical phase conjugation-based ultrafast digital computation

YAO LI, GEORGE EICHMANN, ROGER DORSINVILLE, ROBERT R. ALFANO, CUNY-City College, Department of Electrical Engineering, New York, NY 10031

An ultrafast parallel optical phase conjugation (OPC) effect for the use of optical digital computation is described. Using spatially encoded logic values, symbols, optical binary, multiple-varied logic, symbolic, as well as interconnect operations are performed. The proposed processors are experimentally verified with a 32-ps pulse Nd^{3+}:YAG laser. Based on these elemental processors, an OPC-based optical digital computer architecture is proposed. Using this architecture, iterative arithmetic and symbolic computation examples are presented. Some of the OPC computer performance factors, such as real-time encoding, signal amplification, etc. are also discussed. **(12 min)**

THI5 Noise in optical matrix-vector multipliers: experiments

S. G. BATSELL, T. L. JONG, JOHN F. WALKUP, THOMAS F. KRILE, Texas Tech U., Department of Electrical Engineering, Lubbock, TX 79409

Considerable interest has been expressed in the use of optical matrix-vector multipliers. The accuracy of these processors is limited by sources of deterministic and random error. We measure both the component and system noise levels associated with various implementations. These are compared with earlier theoretical calculations. We then use these results to determine the accuracy limits of the processors. **(12 min)**

1. T. L. Jong, J. F. Walkup, T. F. Krile, and I. Suzuki, "Noise Effects in Optical Linear Algebra Processors," in *Technical Digest, Optical Society of America Annual Meeting*, (Optical Society of America, Washington, DC, 1986), paper MU3.

THI6 Programmable logic array design using polarization-encoded optical shadow-casting

M. A. KARIM, A. A. S. AWWAL, U. Dayton, Electrical Engineering Department, Dayton, OH 45469-0001

An efficient optical computing system may involve the use of a programmable logic array (PLA) where only ON outputs are stored in locations addressable by the inputs. The lensless optical shadow-casting (OSC) system[1] using LEDs provides an easier and reliable means to generate logic operations. This scheme has been recently extended[2,3] to include polarized sources, masks, and encoding codes, thus increasing the design flexibility. In an OSC, each LED produces a shadow of the input overlap pattern, which along with the other similarly produced shadows give an output overlap pattern which is subsequently decoded by means of decoding masks. The original[1] and polarization-encoded[2,3] optical shadow-casting systems explored so far are designed to generate only one output at a time. We report the design of a polarization-encoded PLA device where multiple outputs are generated simultaneously for all the input pixels without switching either LEDs or mask. The proposed algorithm is thereafter employed to design an optimal multiple-output binary multiplication unit. **(12 min)**

1. J. Tanida and Y. Ichioka, J. Opt. Soc. Am. **73**, 800 (1983).
2. Y. Li, G. Eichmann, and R. R. Alfano, Appl. Opt. **25**, 2636 (1986).
3. M. A. Karim, A. K. Cherri, A. A. S. Awwal, and A. Basit, Appl. Opt. **26**, 2446 (1987).

Thursday **MORNING**
22 October 1987 **THJ**
BOULEVARD

10:00 Symposium on Laser-Induced Desorption

Norman H. Tolk, Vanderbilt University, Presider

THJ1 Molecular dynamics of laser-induced desorption

JOHN C. TULLY, AT&T Bell Laboratories, Murray Hill, NJ 07974

Molecular dynamics techniques have been developed to simulate accurately laser-induced chemistry at surfaces with the full complexity of multidimensional interactions. Equations of motion are integrated explicitly for a slab of about fifty atoms with additional adsorbate molecules. Stochastic boundary conditions incorporate energy flow to the remaining bulk atoms and permit transient heating effects to be included correctly. Infrared laser excitation is described by an applied oscillatory external force that drives the dipole moment of the system. The simultations reveal directly the extent of disequilibrium achieved by short-pulse laser excitation. Predictions are made of situations where selective (nonthermal) desorption may be possible.
(invited paper, 25 min)

THJ2 Effect of near-surface gas-phase collisions on desorption measurements

ROGER KELLY, R. W. DREYFUS, IBM T. J. Watson Research Center, Yorktown Heights, NY 10598.

If desorbed particles have a sufficiently low number density they disperse collisionlessly. This means that if, for example, the mechanism is thermally activated, a time-of-flight spectrum yields the surface temperature through the relation $kT = \bar{E}/2$, $\bar{E}$ being the most probable kinetic energy, and the signal is proportional to $\cos\theta$. If, on the other hand, the number density is high enough for a few (estimates range from 3 to 20) collisions to occur, a so-called Knudsen layer is formed. We first show how this problem can be solved analytically and then explore its consequences to thermally activated desorption. In particular, when there is a Knudsen layer, (1) 18–24% of the desorbed particles are found to recondense, (2) the temperature falls to 70–90% of the value at the surface, but this is more than compensated by a center-of-mass velocity, (3) the relation between kT and $\bar{E}$ changes significantly, and (4) the angular distribution becomes strongly forward peaked ($\sim\cos^3\theta$). We finally consider the effect of a Knudsen layer on an electronic desorption process, especially on the energy spectrum and on the angular distribution. **(invited paper, 25 min)**

THJ3 Electronic transitions in photon-stimulated desorption

R. F. HAGLUND, JR., A. V. BARNES, N. HALAS, M. H. MENDENHALL, NORMAN H. TOLK, Vanderbilt U., Department of Physics & Astronomy, Nashville, TN 37235

The discovery that neutral excited-state atoms were desorbed by UV photons with orders of magnitude greater efficiency than ions from alkali-halide surfaces has wrought a fundamental change in our approach to the study of photon–surface interactions, both with synchrotron and laser light sources. In particular, laser–surface interactions in general and laser-induced material damage in particular—once considered primarily due to the absorption of thermal energy from the incident photons—now appear to be linked to electronic interactions both at the surface and in the near-surface bulk, even for photon energies below the bulk band gap. Thus it is appropriate to consider even laser–surface interactions as generically related to the process of desorption induced by electronic transitions (DIETs), a class of energy–surface interactions triggered in exemplary fashion by photons and electrons.

In recent DIET experiments, we focused our attention on the mechanisms through which incident electronic energy is absorbed, localized, and ultimately transformed into kinetic energy of the desorbing atoms or molecules. While specific electronic defect-formation channels can be identified as the precursors of efficient photon-stimulated desorption of ground-state neutral atoms from alkali halides, the desorption of excited-state atoms appears to be correlated with specific core-level excitations of the desorbing species. Similar mechanisms, characterized by the creation of excitons which relax to form permanent, mobile electronic defects, appear to be operative in virtually all wide-band-gap optical dielectrics. In many semiconductors, on the other hand, the smaller band gap allows for the creation of a dense electron–hole plasma under UV photon or laser irradiation, and a different class of energy localization mechanism due to electron–electron correlations must be invoked to account for photon-induced desorption. **(invited paper, 25 min)**

THJ4 Creating a total flux scale from the spectral irradiance standard

YOSHIHIRO ONO, Matsushita Electric Industry Co., Ltd., Lighting Research Laboratory, 3-15 Yakumonakamachi, Moriguchi, Osaka 570, Japan; DONALD A. McSPARRON, U.S. National Bureau of Standards, Radiometric Physics Division, Gaithersburg, MD 20760.

As an alternate method of creating a total flux scale, a method using an integrating sphere with an opening and two baffles and the spectral irradiance standard placed outside the sphere is proposed. Theoretical analysis was made by computer simulation on several models of the above-mentioned integrating sphere whose geometry was not axially symmetric. The window illuminance was analyzed for varying conditions of sphere geometry such as size and location of the baffles, internal source, and wall reflectance, and an optimum geometry was predicted. Based on the results of the theoretical analysis, an integrating sphere of 20-in. diameter was actually built, and measurements were made in varied conditions, and the experimental results were compared with the results of